République Algérienne Démocratique et populaire

Ministère de l'Enseignement Supérieur et de la Recherche Scientifique

Université M'HAMED BOUGARA BOUMERDES

Institut National de Génie Electrique et Electronique

Department of Electrotechnics and Automatics

Report

Presented in partial fulfilment of the requirements of the degree of

MAGISTER DEGREE

In Electrical Engineering

Maximum Power Point Tracking (MPPT) For Photovoltaic System

Submitted By: Malki Sihem Option: Electric Drives and Control

In front of the Examiners board:

Mr. Benazzouz Djamal, Professeur, UMBB, Président

Mr. Bentarzi Hamid, MCA, UMBB, Examinateur

Mr. Zerroug Hocine, Professeur, USTHB, Examinateur

Mr. Refoufi Larbi, Professeur, UMBB, Rapporteur

Boumerdes: 2011

TABLE OF CONTENTS:

Acknowledgements

I wish to express my sincere gratitude to Prof. **Refoufi Larbi** for his excellent supervision, interest and encouragement throughout this work.

I am thankful to all the department staff for the facilities provided and valuable suggestions in improving this work.

Finally, I thank my family and friends for their valuable support and encouragement.

ABSTRACT

This thesis presents a theoretical study of maximum power point tracking (MPPT) for photovoltaic (PV) system. The study includes discussion of various MPPT algorithms and perform comparative tests of the two popular MPPT algorithms (the Perturbation and Observation algorithm and the Incremental and Conductance algorithm) using actual irradiance data. Some important applications of the MPPT for different loads are described; first the PV system with resistive load is discussed, the modeling and the simulation of the PV generator and the DC/DC converter is carried out using MATLAB software. After that a .study of PV water pumping system has been undertaken using DC motor and AC motor. A comparison between the performance of those systems with and without MPPT in terms of PV total energy produced and total volume of water pumped per day is carried out.

Results show that MPPT can very significantly improve the performance of PV pumping system.

Résumé

Cette thèse présente une étude théorique suivie de point de puissance maximale (MPPT) pour le system photovoltaïque (PV). L'étude présente une analyse des différents algorithmes MPPT et effectue des tests comparatifs des deux algorithmes MPPT les plus utiliser (l'algorithme de Perturbation et l'Observation et l'algorithme Incrémental et Conductance) en utilisant des données réelles de radiation solaire. Certaines applications importantes de la technique MPPT pour différentes charges sont décrites: d'abord le système photovoltaïque avec charge résistive est discuté, la modélisation et la simulation du générateur photovoltaïque et du convertisseur DC / DC était faite en utilisant le logiciel MATLAB. Une étude du system de pompage d'eau photovoltaïque a été entreprise par moteur à courant continu et moteur à courant alternatif. Une comparaison entre les performances de ces systèmes avec et sans MPPT en termes de PV énergie totale produite et le volume total d'eau pompée par jour était effectuée. Les résultats montrent que la technique MPPT peut substantiellement améliorer la performance du système de pompage photovoltaïque.

ملخص

هذه المذكرة تقدم دراسة نظرية لتعقب القدرة الأعظمية (MPPT) للنظام الكهروضوئي وتناقش بعض أهم استعمالاته. الدراسة تتضمن مناقشة عدة أنواع من خوارزميات التعقب للقدرة الأعظمية, و مقارنة بين اثنين من الخوارزميات الأكثر انتشارا (IncCond) و P&O باستعمال معطيات واقعية للإشعاعات الشمسية تم محاكاتها باستعمال برمجة MATLAB. بعض أهم استعمالات التعقب للقدرة الأعظمية لمختلف الحمولات تم وصفها. أولا ستتم مناقشة النظام الكهروضوئى وهو يغذي مقاومة, حيت يتم نمذجة و محاكاة المولد الكهروضوئى والمحول تيار مستمر/تيار مستمر. بعد ذلك سيتم دراسة نظام الضخ الكهروضوئي باستعمال محرك دائم المغنطة و محرك حثي, مقارنة بين كفاءة هذه الأنظمة باستعمال التعقب للقدرة الأعظمية و بدونه استنادا للطاقة المنتجة و كمية المياه المضخة يوميا يتم انجازها في هذه المذكرة. النتائج تبين أن تعقب القدرة الأعظمية يستطيع بصفة كبيرة جدا تحسين كفاءة و فعالية النظام الكهروضوئي.

LIST OF FIGURE:

LIST OF TABLES:

NOMENCLATURE :

PV: Photovoltaic,

I: Cell current (the same as the module current) (A),

I_{sc}: Short-circuit current that is equal to the photon generated current (A),

I_o: Reverse saturation current of diode (A), ,

V: Cell voltage = {module voltage} ÷ {# of cells in series}(V),

T: Temperature (^{o}c),

R_s: Series resister (Ω),

R_p: Parallel resistance (Ω),

n: Diode quality factor,

T_{ref}: Reference temperature of PV cell in Kelvin (K), usually 298 K (25^{o}c),

a: Temperature coefficient of I_{sc} in percent change per degree temperature,

G: Irradiance (KW/m^2),

G_o: Nominal value of irradiance, which is normally 1 KW/m^2,

I_o: Reverse saturation current of diode at the reference temperature (T_{ref}) (A),

q: Electronic charge (1.6022 10-^{19} C),

k : Boltzman's constant (13,807 10^{-23} Jk^{-1}),

V_{oc} : Open-circuit voltage of the PV module (V),

P_{max}: Maximum power (W),

V_{mp}: Voltage at P_{max} (V),

I_{mp}: Current at P_{max} (A),

MPPT: Maximum Power Point Tracker,

I_L: Load current (A),

V_L: Load voltage (V),

R_{load} : Impedance load (Ω),

R_{op} : Optimal load for PV (Ω),

V_o : Output voltage of the converter (V),

V_s : Input voltage of the converter (V),

D: Duty cycle of chopper,

I_o: Output current of the converter (A),

I_s: Input current of the converter (A),

R_{in}: Input impedance of the converter (Ω),

t_{on}, t_1: Time when the chopper is closed (s),

t_{off}, t_2: Time when the chopper is opened (s),

f: Chopping frequency (Hz),

C_L: The converter capacitor (F),

L: The converter inductance (H),

P: PV cell power (W),

M_V: Voltage factor,

VMPPT: Voltage-Based Maximum Power Point Tracking,

V_{ref}: Reference voltage of the PV panel (V),

E: Electric potential (V),

w: Angular speed of the rotor (rd/s),

R_a: Armature resistance (Ω),

a_1, a_2 and a_3: Geometric parameters characterizing the pump,

Q: Flow rate of the pump (m^3/h),

H: Total height (m),

R_s: Per phase resistance of the stator winding of induction motor (Ω),

X_s: Per phase leakage reactance of the stator winding (Ω),

R'_r: Rotor resistance referred to the stator (Ω),

X'_r: Rotor reactance referred to the stator (Ω),

R_m: Resistance for excitation (or core) loss (Ω),

X_m: Magnetizing reactance (Ω),

Z_s: Stator impedance (Ω),

Z_{RF}: Equivalent per phase impedance seen by the stator across the motor gap (Ω),

P_g: Gap power of the induction motor (W),

P_d: Developed power of the induction motor (W),

s: Slip,

f_{ca}, f_{cb} and f_{cc}: PWM control signals,

v_{as}, v_{bs}, v_{cs}: Stator voltage of the induction motor (V),

η: Efficiency.

Chapter 1: General Introduction.

The development of renewable energy has been an increasingly critical topic in the 21st century with the growing problem of global warming and other environmental issues. With greater research, alternative renewable sources such as wind, water, geothermal and solar energy have become increasingly important for electric power generation. Although photovoltaic cells are certainly nothing new, their use has become more common, practical, and useful for people worldwide.

The most important aspect of a solar cell is that it generates electrical energy directly from solar energy through the solar photovoltaic module, made up of silicon cells. Although each cell outputs a relatively low voltage, if many are connected in series, a solar photovoltaic module is formed. In a typical module, there can be up to 36 solar cells, producing an open circuit voltage of about 20V. Although the price for such cells is decreasing, making use of a solar cell module still requires substantial financial investment. Thus, to make a PV module useful, it is necessary to extract as much energy as possible from such a system.

At a given temperature and insolation level, PV cells supply maximum power at one particular operation point called the maximum power point (MPP). Unlike conventional energy sources, it is desirable to operate PV systems at its MPP. However, the MPP locus varies over a wide range, depending on PV array temperature and insolation intensity.
Instantaneous shading conditions and ageing of PV cells also affect the MPP locus. In addition, the load electrical characteristics may also vary. Thus, to achieve operation at the MPP, a time varying matching network is required that interfaces the varying source and possibly the varying load. The role of this matching network, called the maximum power point tracking network (MPPT) is to ensure operation of the PV array at its MPP, regardless of atmospheric conditions and load variations. MPPT circuits are realized by means of switched mode DC–DC converters.

Many algorithms have been proposed for MPP tracking, the most widely used ones are the ‘Perturb and Observe’ (P&O) and the Incremental Conductance algorithms. The duty cycle of the converter will be controlled, so that the source will send maximum power to the load.

Solar energy is used for deferent applications, it is used to charge a battery, to feed the grid network and also it is used for a standalone PV pumping system.

Water resources are essential for satisfying human needs, protecting health, and ensuring food production, energy and the restoration of ecosystems, as well as for social and economic development and for sustainable development. However, it has been estimated that two billion people are affected by water shortages in over forty countries, and 1.1 billion do not have sufficient drinking water. There is a great and urgent need to supply drinking water. Remote water pumping systems are a key component in meeting this need where no grid system is available, PV generator will be very promising solution.

Water pumps are driven by various types of motors. AC induction motors are cheaper and widely available worldwide. The system, however, needs an inverter to convert DC output power from PV to AC power, which is usually expensive. In general, DC motors are used because they are highly efficient and can be directly coupled with a PV module or array.

Background and scope of this thesis:

Numerous studies have been done in PV systems, a significant number of them in Europe, Japan, Australia and the United Sates. In Algeria there is a growing interest in PV system; Achour Betka from university of Biskra [2] gives an important study for photovoltaic pumping development in the south without given great attention to the MPPT, he was focus in motors operations and optimization of PV pumping system. L. Barazane, C. Larbès from Polytechnic National School and S. Kharzi, A. Malek from Center of Development of Renewable Energies, Algeria were interested on the control of the asynchronous motor supplied by photovoltaic solar energy. Dr. A. Moussi, A. Saadi, A. Betka from university of Biskra [29], [28] study the deferent elements of PV pumping system. M. Arrouf*, N. Bouguechal from University of Batna [35] focused on Vector control of an induction motor fed by a photovoltaic generator. B. Bouzidi from Center of Development of Renewable Energies, and M. Haddadi [b], O. Belmokhtar from Polytechnic National School [42] were attracted to the economical aspect of PV system. In this thesis we try to study deeply the maximum power point tracking (MPPT) and it's used in PV system.

The thesis consists of five chapters, chapter one provide general introduction of the thesis.

Chapter two will describe the solar cell, module, and panel and analyses its characteristics. Also the modeling of the PV module is described and simulated using MATLAB software.

In chapter three, the maximum power point tracking (MPPT) problematic is defined and the mechanism of the transfer of maximum power from the non linear source to the load using DC/DC converter as an interface between them is described.

In chapter four two important MPPT algorithms which are the 'Perturb and Observe' (P&O) and the Incremental Conductance algorithms are described and simulated using MATLAB. Also a comparison between the performances of the two algorithms is carried out using actual radiation data for sunny and cloudy days.

Chapter five deals with MPPT application for the PV pumping system. Pumping system with DC motor-pump load is described and simulated, following by an AC pumping system with induction motor-pump load. To see the performance of the MPPT, a comparison between direct coupled systems and systems with MPPT is undertaken.

Finally we will end up with general conclusion.

Chapter 2: Photovoltaic System Modeling.

2.1- INTRODUCTION:

RENEWABLE energy technologies are playing an increasingly important role in supplying the world's electricity demands. In particular, the photovoltaic (PV) generation system, a promising source of energy for the future, is evolving rapidly and showing an industrial growth of approximately 40% per year worldwide [1].

Solar energy which is free and abundant in most parts of the world has proven to be an economical source of energy in many applications. The energy the earth receives from the sun is so enormous and so lasting that the total energy consumed annually by the entire world is supplied in as short a time as a half hour. On a clear day the sun's radiation on the earth can be 3000 watts per square meter depending on the location. The sun is a clean and renewable energy source, which produces neither green-house effect gas nor noxious waste through its utilization [2].

The photovoltaic process is completely solid state and self contained. There are no moving parts and no materials are consumed or emitted. Consider the advantages that photovoltaic systems have over competing power options:

- They are non-polluting with no detectable emissions or odours.
- They can be stand-alone systems that reliably operate unattended for long periods.
- They require no connection to an existing power source or fuel supply.
- They may be combined with other power sources to increase system reliability.
- They can withstand severe weather conditions including snow and ice.
- They consume no fossil fuels - their fuel is abundant and free.
- They can be installed and upgraded as modular building blocks - as power demand increases; more photovoltaic modules may be added [2].

The history of PV dates back to 1839 when a French physicist, Edmund Becquerel, discovered the first photovoltaic effect when he illuminated a metal electrode in an electrolytic solution. Thirty-seven years later British physicist, William Adams, with his student, Richard Day, discovered a photovoltaic material, selenium, and made solid cells with 1~2% efficiency which were soon widely adopted in the exposure meters of camera. In 1954

the first generation of semiconductor silicon-based PV cells was born, with efficiency of 6%, and adopted in space applications. Today, the production of PV cells is following an exponential growth curve since technological advancement of late ‘80s that has started to rapidly improve efficiency and reduce cost [3].

2.2- SOLAR CELL, MODULE AND PANEL:

A solar cell consists of a p-n junction similar to semiconductor based diodes, as depicted in Figure 2-1:

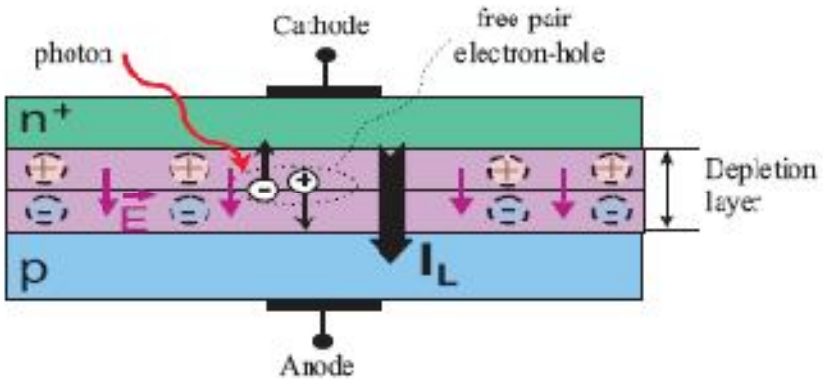

Figure 2-1: Structure of a PV cell.

When a solar cell is exposed to light, the semiconductor material will absorb the photons that have a higher energy than the band gap energy of the semiconductor material. This absorption of a photon shoots out an electron from the crystal lattice. The cycling movement of the electrons forms movable pair electron-hole. The electric field of the depletion region forces those excess carriers according to their charge to drift through the semiconductor material. The absorption of suitable photons and therefore the creation of excess carriers increase with the magnitude of the solar irradiation. The drifting of the carriers produces a continuous photocurrent. Since the number of free carriers increases proportional to the incident radiation, the current also increases proportional to the irradiation [4].

In order to have higher production, solar cells are connected into larger units using either parallel or series connection. A series connection of PV cells benefits from a higher voltage but the current through all cells is defined by its weakest cell, this current result a reduction of the maximum available power. A parallel connection of PV cells produces a higher current but the output voltage is lower. There are configurations where cells are parallel and serial

connected in one single module. Usually, around 36 to 72 PV cells connected in series form a module and the peak power rating of such an assembly ranges from 10W up to 200W. Connected solar modules form a PV panel. The relation of PV cell, module, panel and array is shown in Figure 2-2 [4].

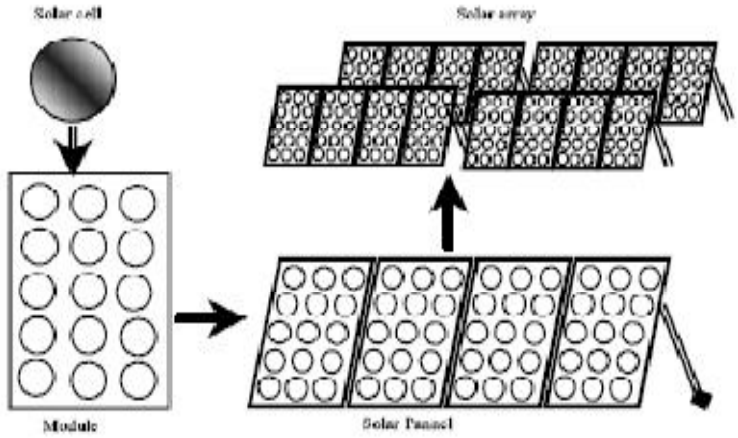

Figure 2-2: Relation of a PV cell, module, panel and array.

2.3- SOLAR ARRAYS CHARACTERISTIC ANALYSIS:

The solar array is a nonlinear device and its electric power fluctuates depending on the solar radiation value and temperature [5]. The I-V characteristic and the power curve of solar array are represented in Figure 2-3 and Figure 2-4.

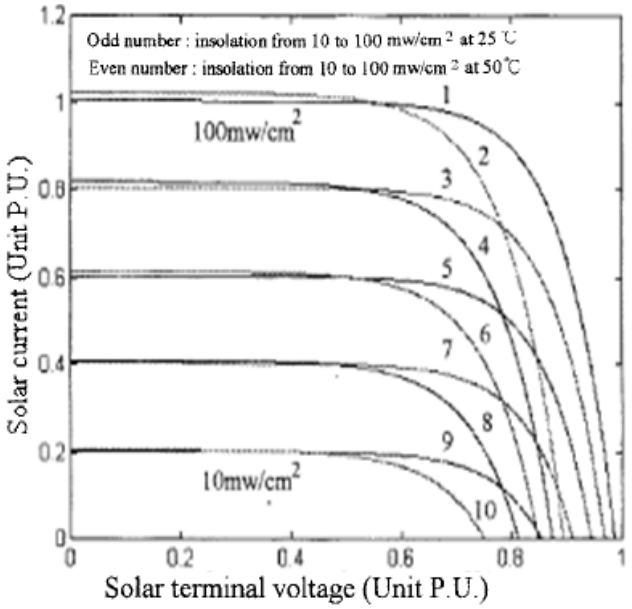

Figure 2-3: Current–voltage curves.

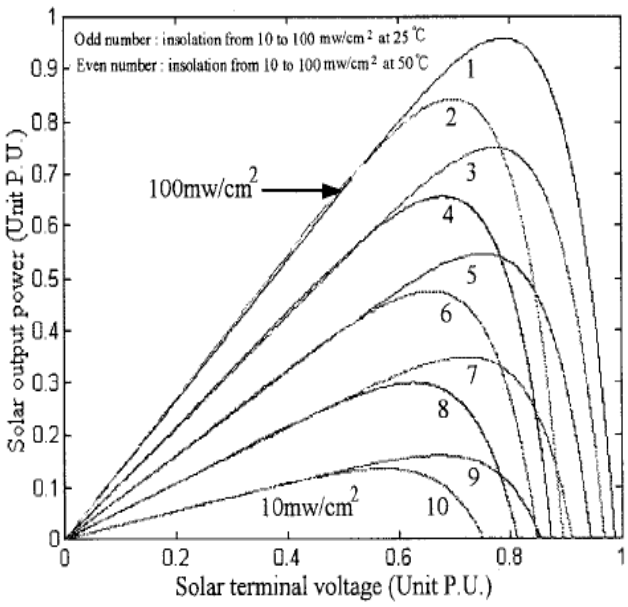

Figure 2-4: Power–voltage curves.

Thus the simplest equivalent circuit of a solar cell is a current source in parallel with a diode. The output of the current source is directly proportional to the light falling on the cell. The diode determines the I-V characteristics of the cell [6].

Increasing sophistication, accuracy and complexity can be introduced to the model by adding in turn:

- Temperature dependence of the diode saturation current I_{sat}.
- Temperature dependence of the photo current I_L.
- Series Resistance:

  In a practical PV cell, there is a series of resistance in a current path through semiconductor material, the metal grid, contacts, and current collecting bus. These resistive losses are lumped together as a series resister (R_s). Its effect becomes very conspicuous in a PV module that consists of many series-connected cells, and the value resistance is multiplied by the number of cells [3].

- Parallel Resistance:

  This is also called shunt resistance. It is a loss associated with a small leakage of current through a resistive path in parallel with the intrinsic device. This can be represented by a parallel resister (R_p). Its effect is much less conspicuous in a PV module compared to the series resistance, and it will only become noticeable when a number of PV modules are connected in parallel for a larger system.

- Recombination:

  Recombination in the depletion region of PV cells provides non-ohmic current paths in parallel with the intrinsic PV cell [3], this allowing the diode quality factor n to become a variable parameter (instead of being fixed at either 1 or 2) or introducing two parallel diodes (one with n = 1, one with n = 2) with independently set saturation currents [6].

The equivalent circuit of the solar cell will be represented in figure 2-5:

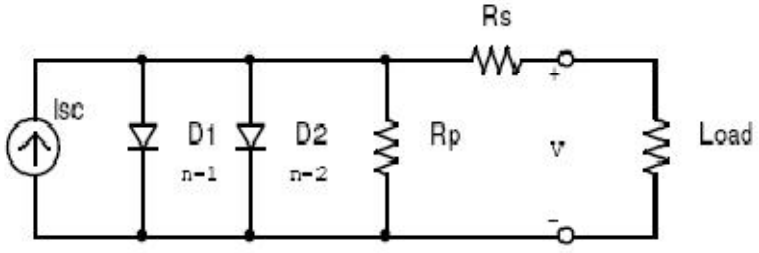

Figure 2-5: More accurate equivalent circuit of PV cell.

2.4- MODELING OF A PV MODULE:

The electric model with moderate complexity shown in Figure 2-6 used for the modelling of the PV cell [6]. It provides fairly accurate results. The model consists of a current source (I_{sc}), a diode (D), and a series resistance (R_s). The effect of parallel resistance (R_p) is very small in a single module, thus the model does not include it. To make a better model, it also includes temperature effects on the short-circuit current (I_{sc}) and the reverse saturation current of diode (I_o). It uses a single diode with the diode ideality factor (n) set to achieve the best I-V curve match.

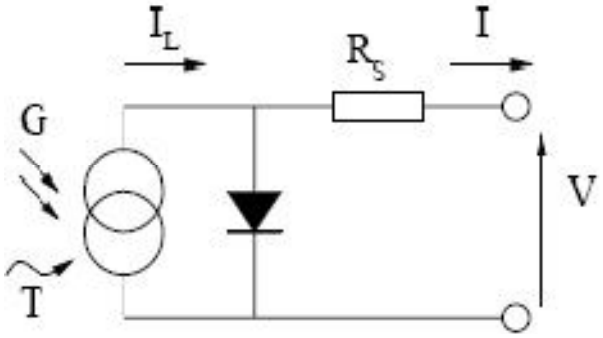

Figure 2-6: The circuit diagram of the PV model.

This model is a simplified version of the two diode model. The equation which describes the I-V characteristics of the cell is [4]:

$$I = I_{sc} - I_0 \left[e^{q\left(V + I.R_s \,/\, nkT\right)} - 1 \right] \qquad (2.1)$$

Where: I is the cell current (the same as the module current),

I_{sc} is the short-circuit current that is equal to the photon generated current,

I_o is the reverse saturation current of diode,

V is the cell voltage = {module voltage} ÷ {# of cells in series},

T is the cell temperature, q is the electronic charge (1.6022 10-^{19} C), k is Boltzman's constant (13,807 10^{-23} Jk^{-1}).

First, calculate the short-circuit current (I_{sc}) at a given cell temperature (T):

$$I_{sc}\Big|_T = I_{sc}\Big|_{T_{ref}} .\left[1 + a\left(T - T_{ref}\right)\right] \qquad (2.2)$$

Where: I_{sc} at T_{ref} is given in the datasheet (measured under irradiance of 1000 W/m^2),

T_{ref} is the reference temperature of PV cell in Kelvin (K), usually 298 K (25^{o}c),

a is the temperature coefficient of I_{sc} in percent change per degree temperature also given in the datasheet.

The short-circuit current (I_{sc}) is proportional to the intensity of irradiance, thus I_{sc} at a given irradiance (G) is:

$$I_{sc}\Big|_{G} = \left(\frac{G}{G_{o}}\right) I_{sc}\Big|_{G_{o}} \tag{2.3}$$

Where: G_o is the nominal value of irradiance, which is normally 1 KW/m^2.

The reverse saturation current of diode (I_o) at the reference temperature (T_{ref}) is:

$$I_{o} = \frac{I_{sc}}{\left(e^{qV_{OC}/nkT} - 1\right)} \tag{2.4}$$

The reverse saturation current (I_o) is temperature dependant and the I_o at a given temperature (T) is calculated by the following equation [3]:

$$I_{o}\Big|_{T} = I_{o}\Big|_{T_{ref}} \left(\frac{T}{T_{ref}}\right)^{\frac{3}{n}} .e^{\frac{-qE_g}{nk}\left(\frac{1}{T}-\frac{1}{T_{ref}}\right)} \tag{2.5}$$

The diode ideality factor (n) is unknown and must be estimated. It takes a value between one and two; the value of n=1 (for the ideal diode) is, however, used until the more accurate value is estimated later by curve fitting [6]. Figure 2-7 shows the effect of the varying ideality factor.

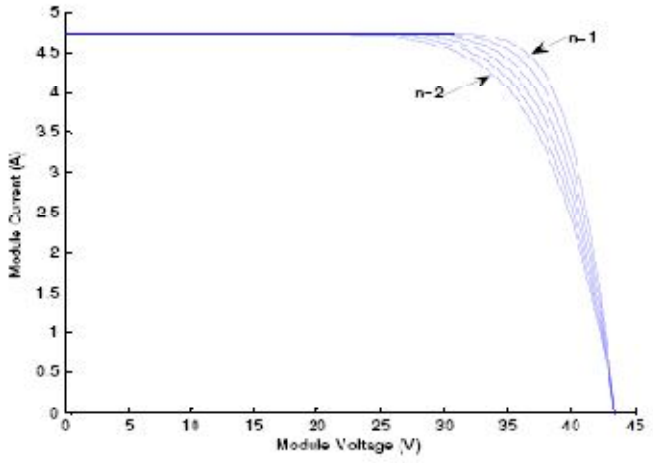

Figure 2-7: effect of diode ideality factors.

The series resistance (R_s) of the PV module has a large impact on the slope of the I-V curve near the open-circuit voltage (V_{oc}), as shown in Figure 2-8; hence the value of R_s is calculated by evaluating the slope dI/dV of the I-V curve at the V_{oc} [6]. The equation for R_s is derived by differentiating the equation (2.1) and then rearranging it in terms of R_s.

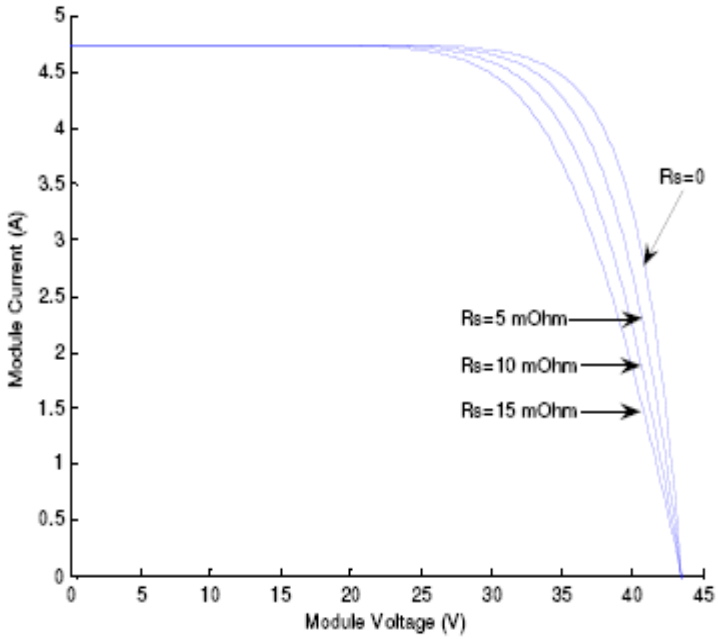

Figure 2-8: Effect of series resistances

$$I = I_{sc} - I_0\left[e^{q\left(\frac{V+I.R_S}{nKT}\right)} - 1\right] \tag{2.6}$$

$$dI = 0 - I_0.q\left(\frac{dV + R_s.dI}{nKT}\right).e^{q\left(\frac{V+I.R_s}{nKT}\right)} \tag{2.7}$$

$$R_s = -\frac{dI}{dV} - \frac{nKT\ /\ q}{I_0.e^{q\left(\frac{V+I.R_s}{nKT}\right)}} \tag{2.8}$$

Then, evaluate the equation (2.8) at the open circuit voltage that is V=Voc (also let I=0).

$$R_s = -\frac{dV}{dI}\Big|_{V_{OC}} - \frac{nKT\ /\ q}{I_0.e^{\frac{qV_{OC}}{nKT}}} \tag{2.9}$$

Where: $\frac{dV}{dI}\Big|_{V_{OC}}$ is the slope of the I-V curve at the Voc, Voc is the open-circuit voltage of cell (found by dividing Voc in the datasheet by the number of cells in series).

The calculation using the slope measurement of the I-V curve published on the BP SX 150 datasheet gives a value of the series resistance per cell, Rs = 5.1mΩ [3].

Finally, it is possible to solve the equation of I-V characteristics (2.1). It is, however, complex because the solution of current is recursive by inclusion of a series resistance in the model. Although it may be possible to find the answer by simple iterations, the Newton's method is chosen for rapid convergence of the answer [6]. The Newton's method is described as:

$$x_{n+1} = x_n - \frac{f(x_n)}{f'(x_n)} \qquad (2.10)$$

Where: f □(x) is the derivative of the function, f (x_0) □0, x_n is a present value, and x_{n+1} is a next value.

Rewriting the equation (2.1) gives the following function:

$$f(I) = I_{sc} - I - I_0\left[e^{q\left(\frac{V+I.R_s}{nKT}\right)} - 1\right] = 0 \qquad (2.11)$$

Plugging this into the equation (2.10) gives a following recursive equation, and the output current (I) is computed iteratively.

$$I_{n+1} = I_n - \frac{I_{sc} - I_n - I_0\left[e^{q\left(\frac{V+I_n.R_S}{nKT}\right)} - 1\right]}{-1 - I_0\left(\frac{q.R_s}{nKT}\right)e^{q\left(\frac{V+I_n.R_s}{nKT}\right)}} \qquad (2.12)$$

The MATLAB function written in this thesis performs the calculation five times iteratively to ensure convergence of the results.

2.5- MATLAB SIMULATION:

BP Solar BP SX 150S PV module is chosen for a MATLAB simulation model. The module is made of 72 multi-crystalline silicon solar cells in series and provides 150W of nominal maximum power. Table 2-1 shows its electrical specification.

Electrical Characteristics	
Maximum Power (P_{max})	150W
Voltage at P_{max} (V_{mp})	34.5V
Current at P_{max} (I_{mp})	4.35A
Open-circuit voltage (V_{oc})	43.5V
Short-circuit current (I_{sc})	4.75A
Temperature coefficient of I_{sc}	0.065 ± 0.015 %/ °C
Temperature coefficient of V_{oc}	-160 ± 20 mV/ °C
Temperature coefficient of power	-0.5 ± 0.05 %/ °C
NOCT	47 ± 2°C

Table 2-1: Electrical characteristics data of PV module taken from the datasheet [9].

After some trials with various diode ideality factors, the MATLAB model chooses the value of n = 1.62 that attains the best match with the I-V curve on the datasheet. The figures show good correspondence between the data points and the simulated I-V curves.

- Figure 2-9 shows the plots of I-V characteristics at various module temperatures simulated with the MATLAB model for BP SX 150S PV module.

- Figure 2-10 shows the plot of I-V characteristics at various sun irradiations simulated with the MATLAB model for BP SX 150S PV module.

- Figure 2-11 shows the plot of power at various module temperatures simulated with the MATLAB model for BP SX 150S PV module.

- Figure 2-12 shows the plot of power at various sun irradiations simulated with the MATLAB model for BP SX 150S PV module.

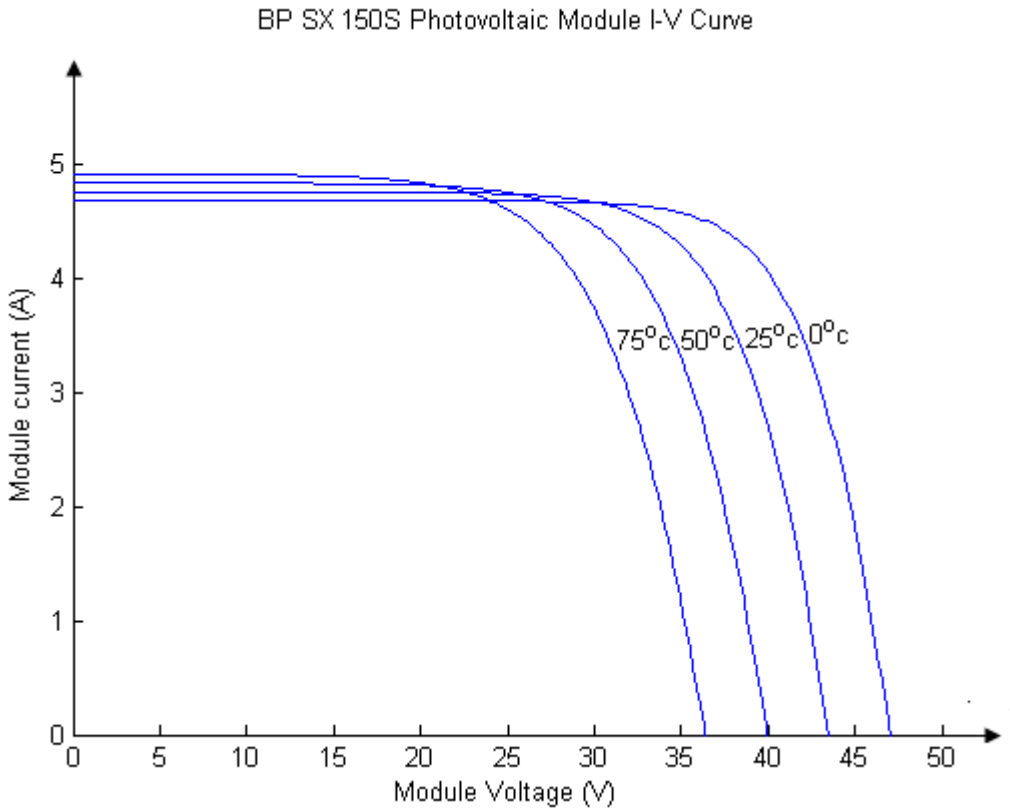

Figure 2-9: I-V curves of BP SX 150S PV module at various temperatures

Simulated with the MATLAB model.

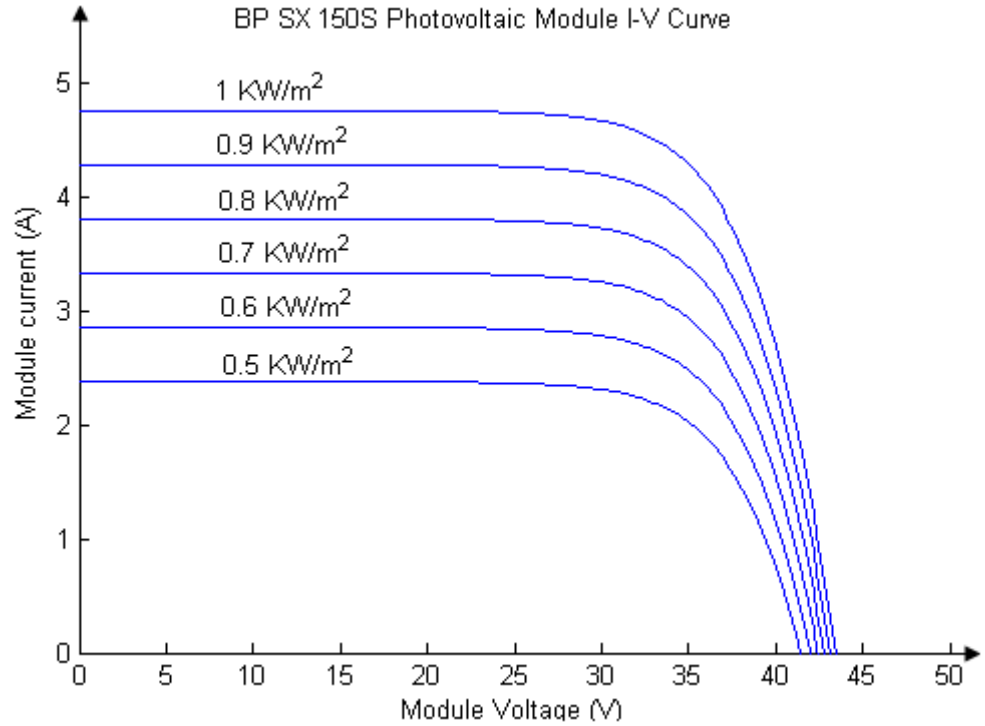

Figure 2-10: I-V curves of BP SX 150S PV module at various sun radiations simulated with MATLAB model

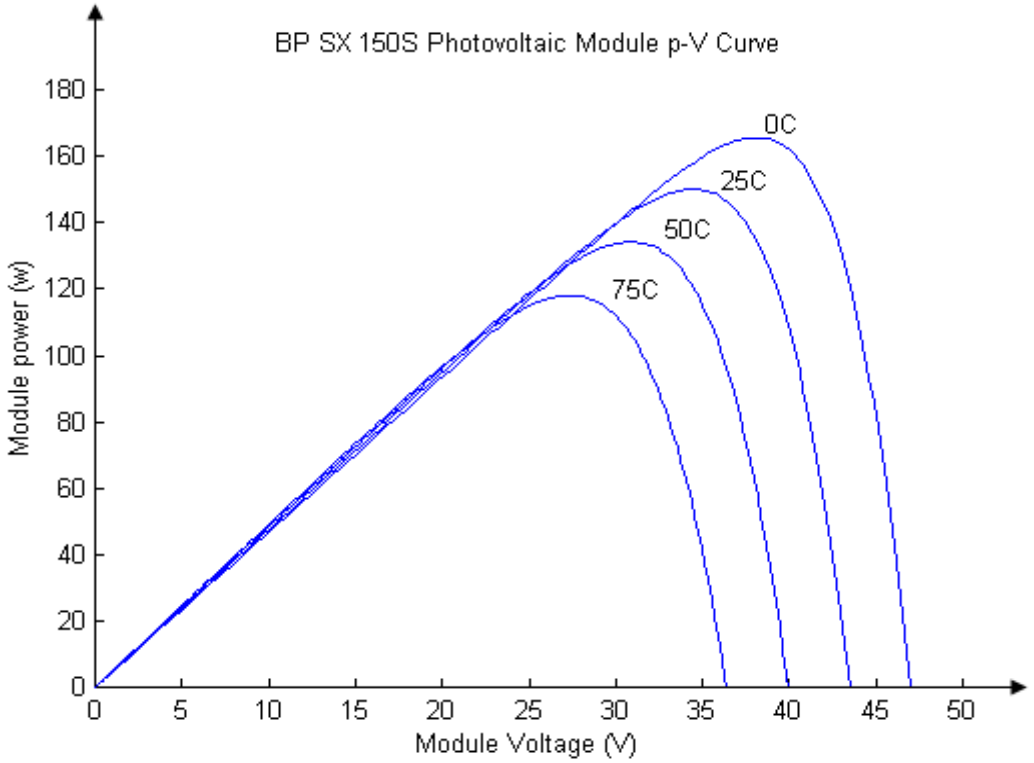

Figure 2-11: power curves of BP SX 150S PV module at various temperatures

Simulated with the MATLAB model.

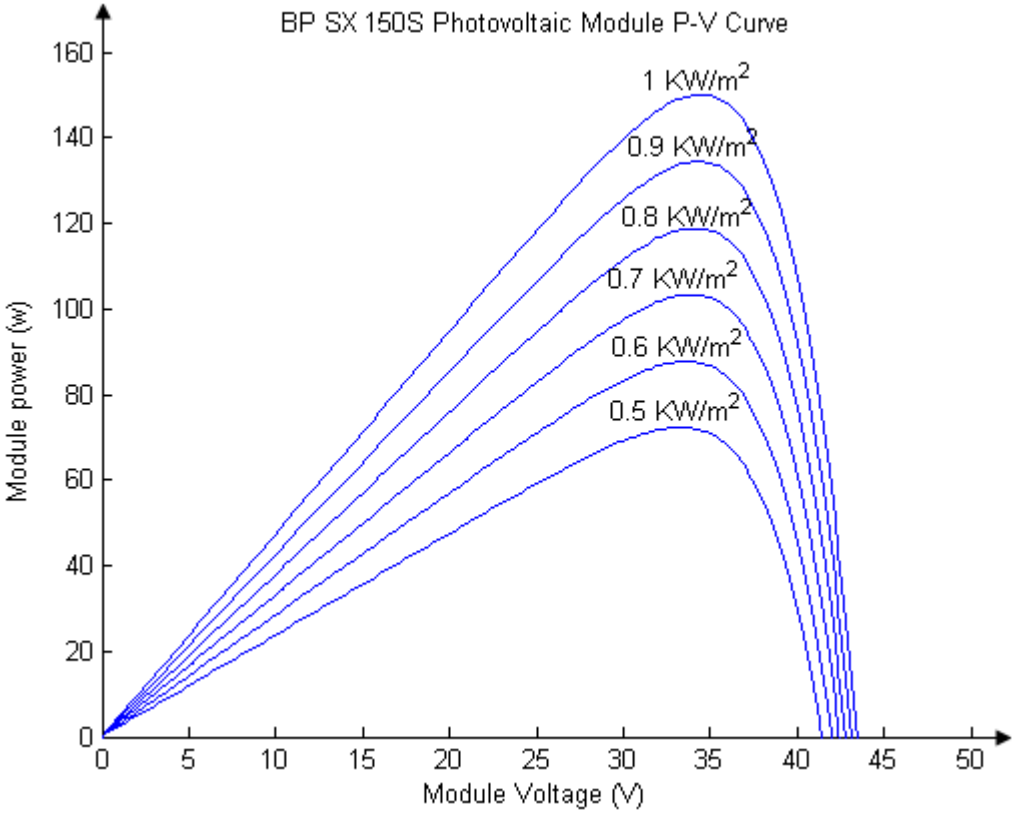

Figure 2-12: power curves of BP SX 150S PV module at various temperatures

Simulated with the MATLAB model.

2.6- COMMENTS:

The simulation results show that the modelling of the PV module using the equivalent circuit in moderate complexity gives an accurate matching with the data sheet information. For example, in the data sheet, the maximum power of the BP SX 150S PV module at 25^{o}c and 1 KW/m^2 of temperature and radiation is 150 W and the simulated value is about 149.985 W, so the accuracy of the modelling is about 99.99 %. However, for the large PV system it is preferred to use the most accurate equivalent circuit to have good results.

2.6.1- Effect of temperature:

A PV module's temperature has a great effect on its performance. It is observed in figure 2-9 that the temperature mainly affects the terminal voltage, it increases with decreasing temperature. This is somewhat surprising as one would typically expect the solar panel to operate more efficiently as temperature increases. However, one of the reasons the solar panel operates more efficiently with decreasing temperature is due to the electron and hole mobility of the semiconductor material [7]. As temperature increases, the electron and hole mobility in the semiconductor material decreases significantly.

The band gap energy of semiconductor materials also varies with temperature. An increase in temperature will cause the band gap energy of the material to increase. With higher band gap energy, the electrons in the valence band will require more energy from the photons to move to the conduction band. This means that a lot more photons will not have sufficient energy to be absorbed by the electrons in the valence band resulting in fewer electrons making it to the conduction band and a less efficient solar cell.

At high temperatures, a PV module's power output is reduced. The temperature of a PV module also affects its efficiency. In general, a crystalline silicon PV module's efficiency will be reduced about 0.5 percent for every degree °c increase in temperature. The effect of varying temperature does not have a very large effect on the current developed [8].

2.6.2- Effect of Irradiance:

Solar panels are only as effective as the amount of energy they can produce. Because solar panels rely on conditions that are never constant, the amount of power extracted from a PV module can be very inconsistent. Irradiance is an important changing factor for a solar

array performance. It is a characteristic that describes the density of radiation incident on a given surface. In terms of PV modules, irradiance describes the amount of solar energy that is absorbed by the array over its area. Irradiance is expressed typically in watts per square meter (W/m^2). Given ideal conditions, a solar panel should obtain an irradiance of 100 mW/cm^2, or 1000 W/ m^2). Unfortunately, this value that is obtained from a solar panel will vary greatly depending on geographic location, angle of the sun… [8].

As can be observed from figure 2-12 and figure 2-10, the output power is directly proportional to the irradiance. As such, a smaller irradiance will result in reduced power output from the solar panel. However, it is also observed that only the output current is affected by the irradiance. This makes sense since by the principle of operation of the solar cell the generated current is proportional to the flux of photons. When the irradiance or light intensity is low, the flux of photon is less than when the sun is bright and the light intensity is high [7], thus more current is generated as the light intensity increases. The change in voltage is minimal with varying irradiance and for most practical application, the change is considered negligible.

2.7- THE I-V CURVE AND MAXIMUM POWER POINT:

It should be noted that there are various voltage-versus-current curves and different power-versus-current curves according to the combinations of temperature and radiation. In addition, there exist other factors that strongly affect the electrical characteristics, i.e., shades on the PV panel and surface contamination. Therefore, the number of the characteristic curves is actually innumerable, depending on the possible combinations of environmental factors [5]. Each curve has a unique point near the knee, called a maximum power point (MPP), at which the module operates with the maximum efficiency and produces the maximum output power. It is possible to visualize the location of the maximum power point (MPP), by fitting the largest possible rectangle inside of the I-V curve, and its area equal to the output power which is a product of voltage and current [3].

As we said that the amount of power produced by the PV module varies greatly depending on its operating conditions (temperature and irradiation). Hence, there is a need to constantly track the power curve and keep the solar panel operating voltage at the point where the most power is extracted; we called this process the maximum power point tracker [7].

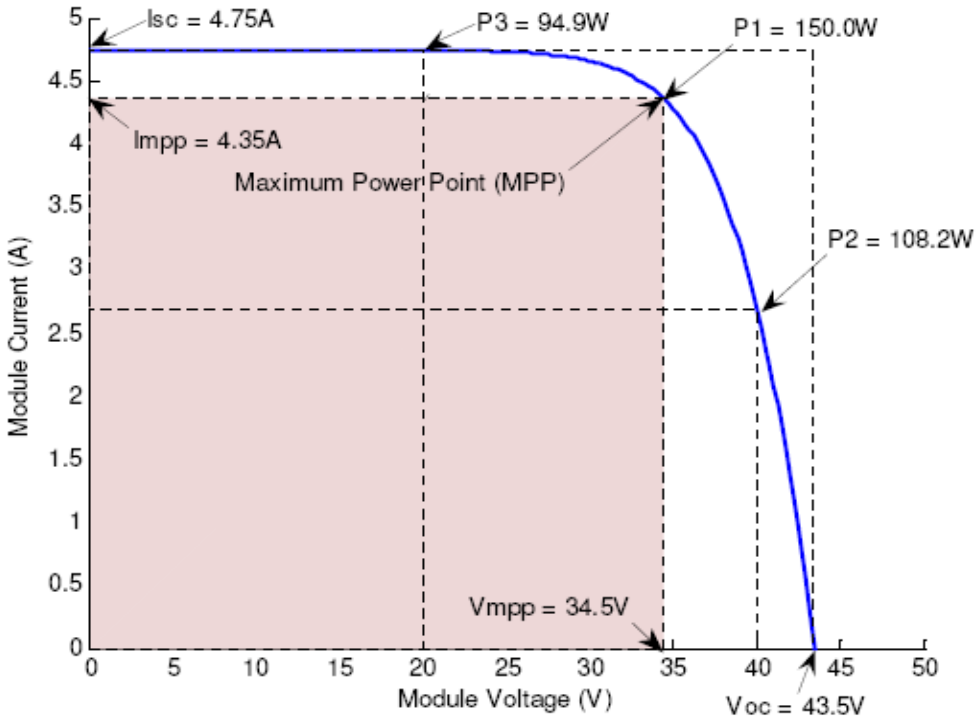

Figure 2-13: I-V curve of BP SX 150S PV module and the max power point.

2.8- CONCLUSION:

In this chapter we have seen the modelling of the PV module using the equivalent circuit in moderate complexity since we are working in low and medium size of PV generator. The results show good matching with the data sheet.

The I-V characteristic curve of the PV module is nonlinear and the amount of power extracted varies greatly depending on the temperature and radiation. The power produced from the PV panel is directly proportional to the irradiance and inversely proportional to the temperature.

For each value of radiation and temperature we have a maximum power operating point. This MPP is tracked on a permanent basis for a given radiation and temperature that will be the object of the next chapter.

Chapter 3: MPPT Problematic.

3.1- INTRODUCTION:

PHOTOVOLTAIC (PV) systems find increased use in electric power technologies. The main drawbacks of PV systems are high fabrication cost and low energy-conversion efficiency, which is partly caused by their nonlinear and temperature-dependent V–I and P–I characteristics. To overcome these drawbacks, three essential approaches can be followed:

1) Improving manufacturing processes of solar arrays: many research efforts have been performed with respect to materials and manufacturing of PV arrays.

2) Controlling the insulation input to PV arrays: the input solar energy is maximized using sun-tracking solar collectors or rearranging the solar-cell configurations of PV arrays with respect to changes in environmental conditions [10].

3) Using maximum power point tracking (MPPT).

A change in the solar irradiation or the temperature results in a shift of the MPP over a wide range, Instantaneous shading conditions and ageing of PV cells also affect the MPP locus. In addition, the load electrical characteristics may also vary [11].

As previously mentioned, the MPPT is the technique that ensures that the PV panel under any change in irradiance and cell temperature conditions gives the maximum available power. In other words, there is a need to track the MPP to maximize the power drawn off from the PV panel under any circumstance that can possibly cause the system to lose regulation [4].

3.2- NEED FOR MAXIMUM POWER POINT TRACKER:

As seen in the PV (power vs. voltage) curve of the module in the first chapter, there exists a peak power corresponding to a particular voltage and current. Since the PV module efficiency is low (13%), it is desirable to operate the module at the peak power point so that the maximum power can be delivered to the load under varying temperature and insulation conditions. Hence maximization of power improves the utilization of the solar PV module. A maximum power point tracker (MPPT) is used for this reason. A dc/dc converter (step up/step

down) serves the purpose of transferring maximum power from the solar PV module to the load. A dc/dc converter acts as an interface between the load and the module figure 3-1 [12].

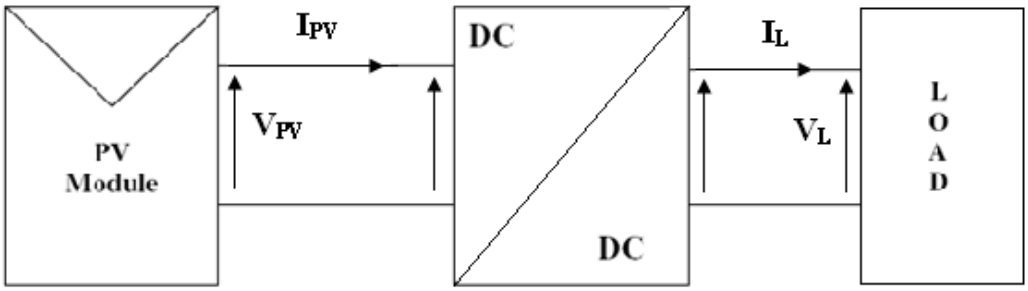

Figure 3-1: Block diagram of a typical MPPT system.

3.3- THE MAXIMUM POWER POINT TRACKING PROCESS:

Figure 3-2 illustrates the electrical characteristics of the solar array under a given insulation. The internal impedance of the solar array is low on the right side of the curve and high on the left side. The maximum power point of the solar array is located at the knee of the curve. According to the maximum power transfer theory, the power delivered to the load is maximum when the source internal impedance matches the load impedance. Thus, the impedance seen from the converter side (which can be adjusted by controlling the duty cycle) needs to match the internal impedance of the solar array if the system is required to operate close to the MPP's of the solar array. Most traditional dc/dc converters have an inherent negative impedance characteristic, as their current increases when the voltage decreases. This behavior is due to the constant input power and the adjustable output voltage of the power supply. If the system operates on the high-impedance (namely, low-voltage) side of the solar array characteristic curve, the solar array terminal voltage will collapse. Therefore; the solar array is required to operate on the right side of the curve to perform the tracking process. Otherwise, the converter will operate with the maximum duty cycle, and the solar array voltage will only change with the insulation. Thus, the system cannot achieve maximum power tracking and might even mistake the present operating point for the MPP [5].

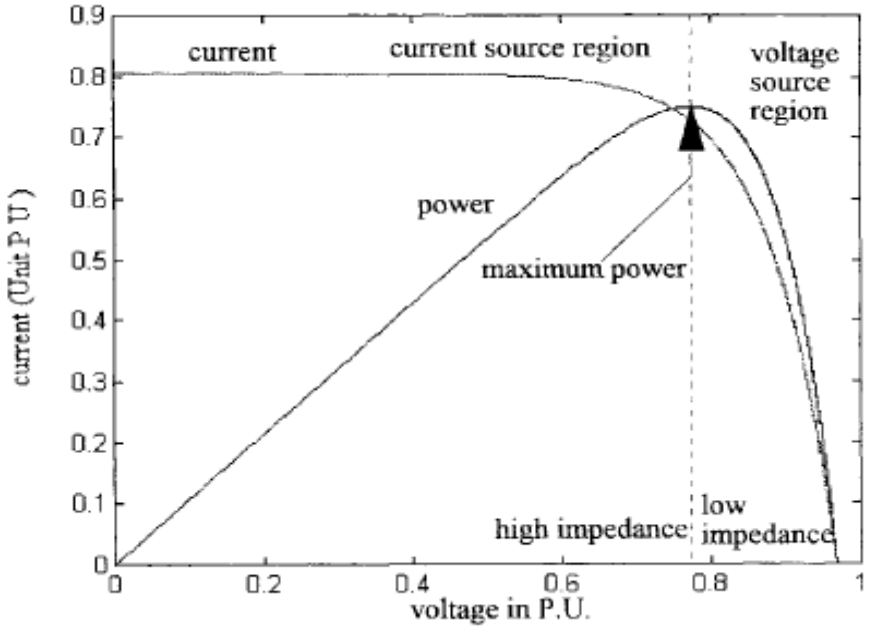

Figure 3-2: Solar array characteristic curves.

3.4- LOAD MATCHING MECHANISM TO ACHIEVE THE MAXIMUM POWER POINT:

When a PV module is directly coupled to a load, the PV module's operating point will be at the intersection of its I–V curve and the load line which is the I-V relationship of the load. For example in figure 3-3 (a), a resistive load has a straight line with a slope of 1/Rload as shown in figure 3-3 (b). In general, this operating point is seldom at the PV module's MPP, thus it is not producing the maximum power. A study shows that a direct-coupled system utilizes approximately 31% of the PV capacity [4].

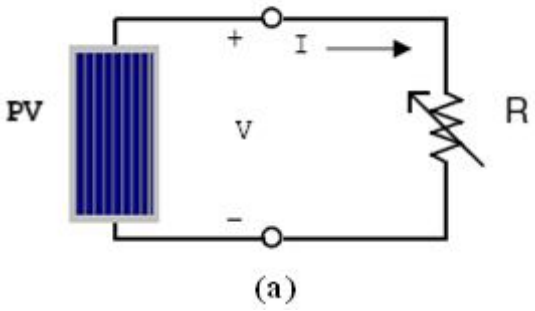

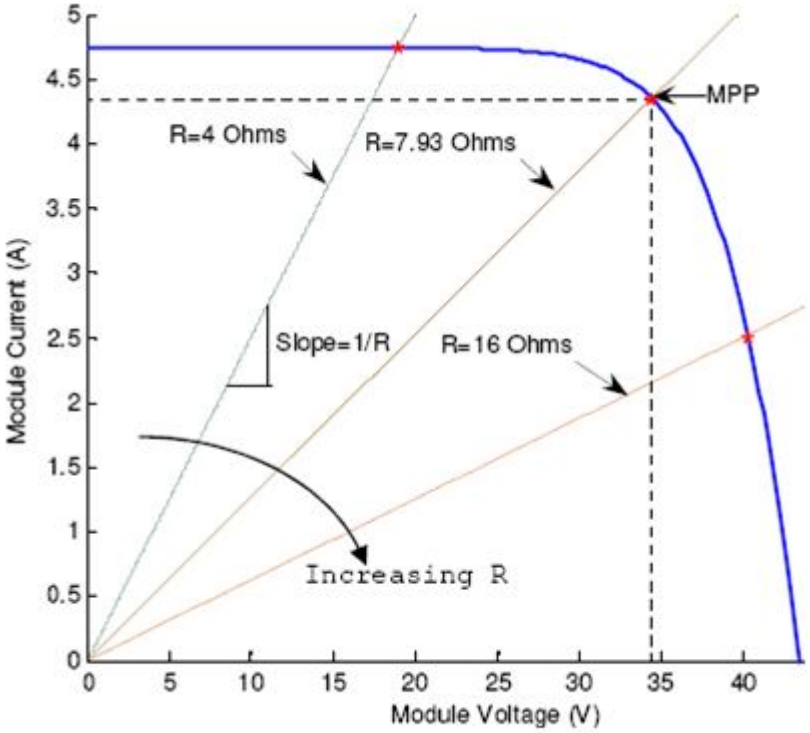

(b)

Figure 3-3: a) direct coupled system with resistive load. **b)** I-V curves of BP SX 150S PV module and various resistive loads Simulated with the MATLAB model (1KW/m^2, 25°c).

To increase the efficiency of the PV system, a DC-to-DC converter is used as an interface between the PV module and the load to perform the MPPT process and the load matching $(R_{load} = R_{op})$, where R_{load} is the impedance load; R_{op} is the optimal load for PV.

By changing the duty cycle of the converter the peak power point is obtained.

Considering a step up converter is used, its average output voltage is:

$$V_o = \frac{1}{1-D} V_s \qquad (3.1).$$

Where: D is the duty cycle of chopper given by the relationship between the ON time and the OFF time of the switch:

$$D = \frac{\text{ON time}}{\text{ON time} + \text{OFF time}}$$

V_o is the output voltage of the converter.

V_s is the input voltage of the converter.

Assuming power constancy we can write:

$$\frac{I_o}{I_s} = \frac{V_s}{V_o} = 1 - D \qquad (3.2).$$

Where: I_o is the output current of the converter.

I_s is the input current of the converter.

From equations (3.1) and (3.2), the input impedance of the converter is then:

$$R_{in} = \frac{V_s}{I_s} = (1-D)^2 \frac{V_o}{I_o} = (1-D)^2 R_{load} \qquad (3.3)$$

The impedance seen by PV is the input impedance of the converter (R_{in}). By changing the duty cycle (D), the value of R_{in} can be matched with that of R_{op} [12]. Therefore, the impedance of the load can take any value as long as the duty cycle is adjusted accordingly.

3.5- DC-DC CONVERTERS:

The heart of MPPT hardware is a switch-mode DC-to-DC converter that converts a DC input voltage into a DC output voltage of lower or higher amplitude. In addition, DC-to-DC converters are used to provide noise isolation, power bus regulation…etc [13].

There are a number of different topologies for DC-DC converters. The most important are: boost converter (step-up converter), buck converter (step-down converter), buck- boost converter.

3.5.1- The step-up converter (Boost converter):

Figure 3-4 (a) shows the basic boost converter. This circuit is used when a higher output voltage than the input is required. It is made up of an inductor that is followed by a power switch, a diode and output capacitance as shown in figure 3-4 (a).

The circuit operation can be divided into two modes, figure 3-4 (b). Mode 1 begins when switch SW (chopper) is closed for time t_1 (t_{on}), the inductor current rises and energy is stored in the inductor L. Mode 2 begins when the switch is opened for time t_2 (t_{off}), the energy stored in the inductor is transferred to load through the diode D_1 and the inductor current falls. Assuming a continuous current flow (continuous conduction mode), the wave forms for the switch state, voltage, and current are shown in figure 3-4 (c) [14].

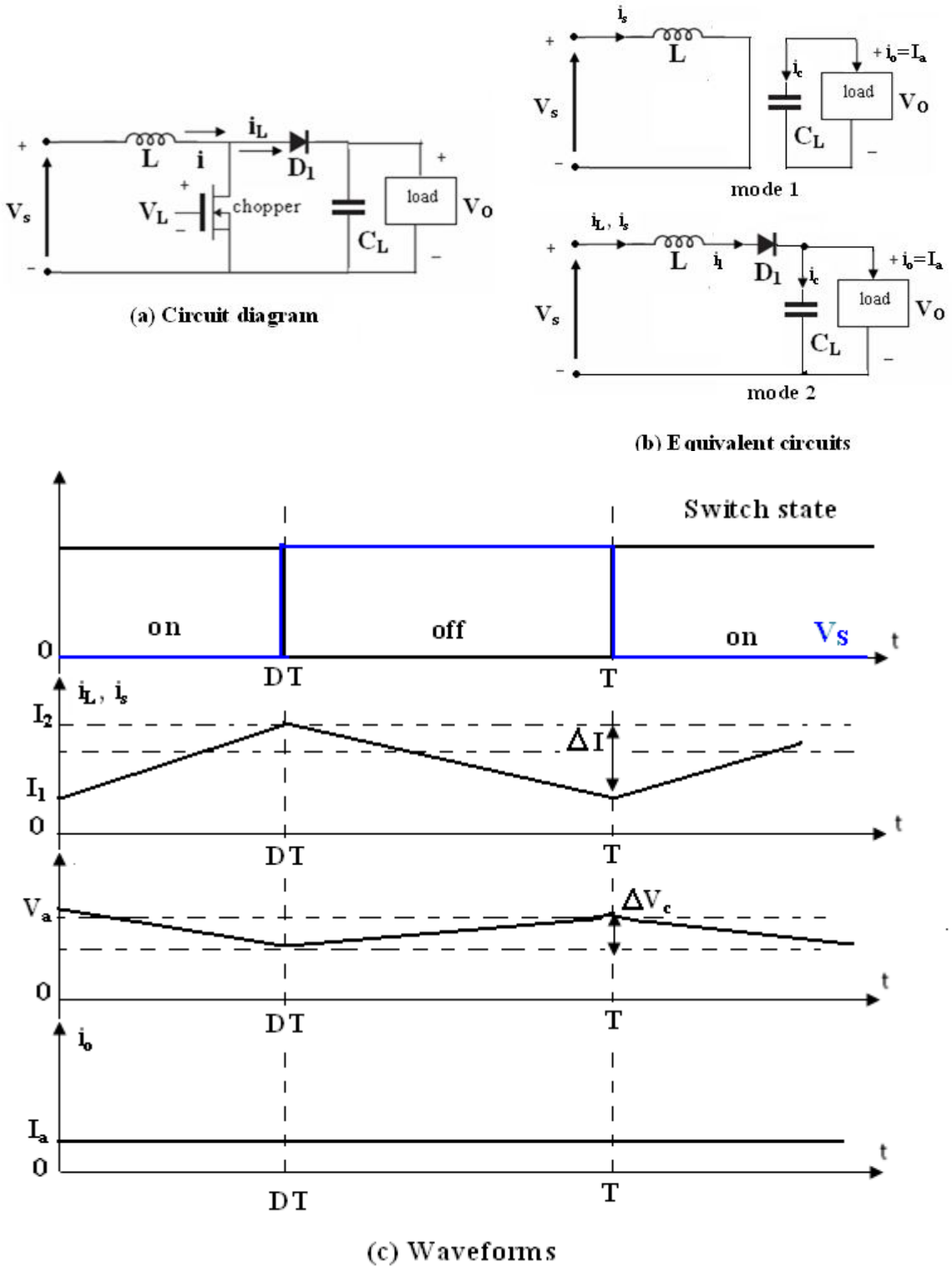

Figure 3-4: boost converter under continuous conduction mode of current.

When the converter is turned on, the voltage across the inductor is:

$$v_L = L \frac{di}{dt} \tag{3.4}$$

And this gives the peak-to-peak ripple current in the inductor as:

$$\Delta I = \frac{V_s}{L} t_1 \qquad (3.5)$$

The average output voltage is:

$$V_o = V_s + L\frac{\Delta I}{t_2} = V_s\left(1+\frac{t_1}{t_2}\right) = V_s\frac{1}{1-D} \qquad (3.6)$$

Where: $D = \frac{t_1}{T} = t_1 * f$ is the duty cycle of chopper.

T: is the chopping period.

f: is the chopping frequency.

Because the large capacitor C_L is connected across the load, the output voltage is greatly switched and v_o becomes the average value V_a. We can notice from equation (3.6) that the voltage across the load can be stepped up by varying the duty cycle D and the minimum output voltage is V_S when D=0, however, the converter cannot be switched on continuously such that D=1, for value of D tending to unity, the output voltage becomes very large and very sensitive to changes in D as shown in figure 3-5. There is a maximum duty cycle which has to be calculated for the protection of the system, V_O/V_S cannot increase indefinitely. The maximum duty cycle is related to the load characteristics.

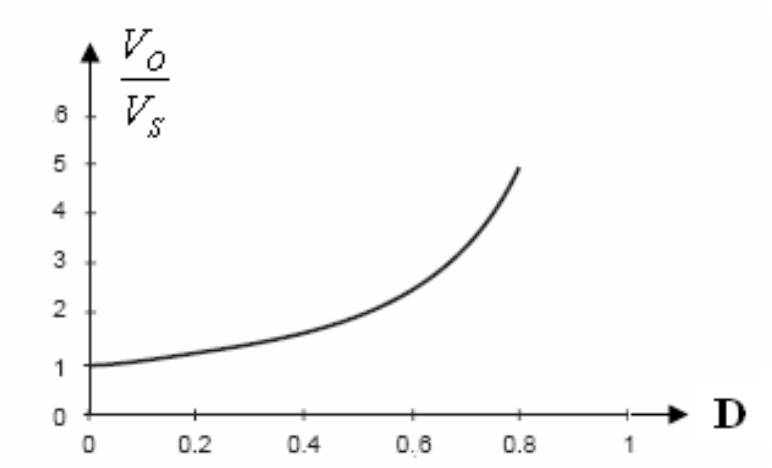

Figure 3-5: output voltage dependency on duty cycle D for the boost converter.

3.5.2- Step down converter (buck converter):

A basic buck converter as shown in figure 3-6(a) is used to step down the input voltage when the load requires a lower voltage.

When SW is turned on, current begins flowing through SW and L, and then into C_L and the load. The magnetic field in L therefore builds up, storing energy in the inductor with the voltage drop across L opposing or (bucking) part of the input voltage. Then when SW is turned off, the inductor opposes any drop in current, and now supplies current to the load itself via D_1 [15]. The wave forms for the switch state, voltage, and current are shown in figure 3-6 (c).

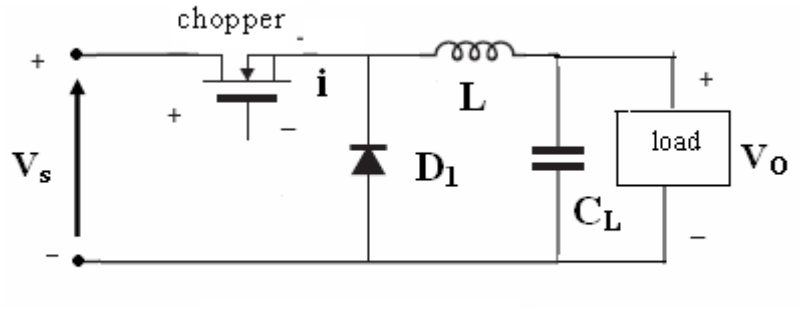

(a) Circuit diagram

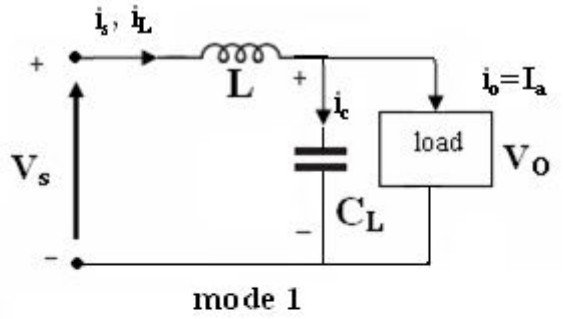

mode 1

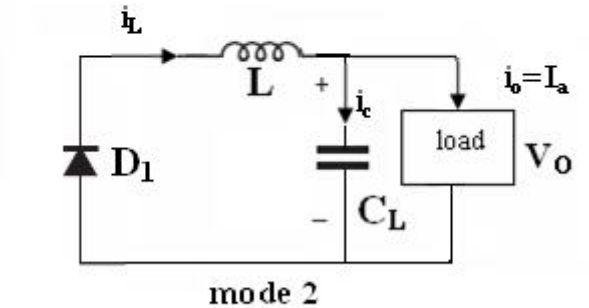

mode 2

(b) Equivalent circuits

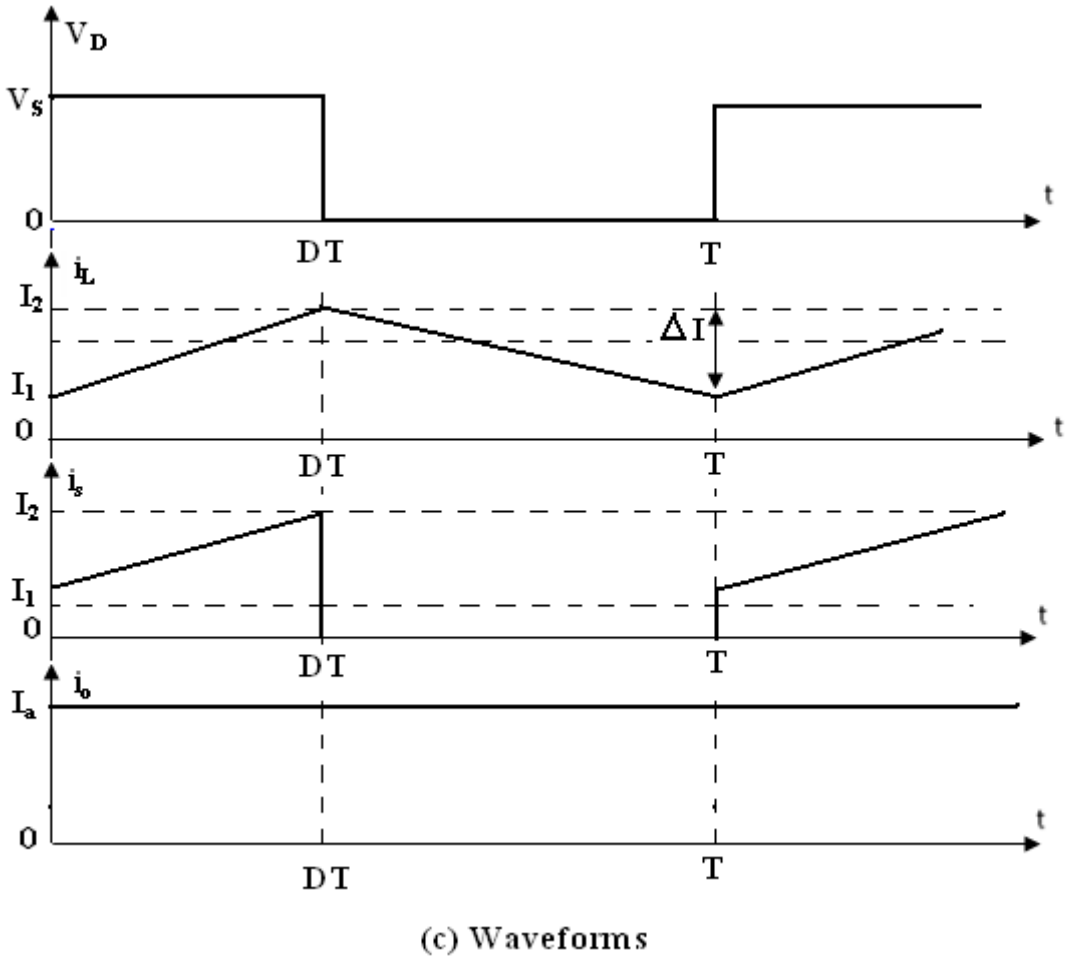

(c) Waveforms

Figure 3-6: buck converter under continuous conduction mode of current.

The average output voltage is given by:

$$V_o = \frac{1}{T}\int_0^{t_1} v\,dt = \frac{t_1}{T}V_s = f t_1 V_s = D V_s \qquad (3.7)$$

The DC output voltage which appears across the load is a fraction of the input voltage, and this fraction turns out to be equal to the duty cycle. So we can write:

$$\frac{V_o}{V_s} = D \quad , \quad V_o = V_s * D \qquad (3.8)$$

So by varying the switching duty cycle, the buck converters output voltage can be varied as a fraction of the input voltage. A duty cycle of 50% gives a step-down ratio of 2:1, for example, as needed for a 24/12V step down converter as shown in figure 3-7.

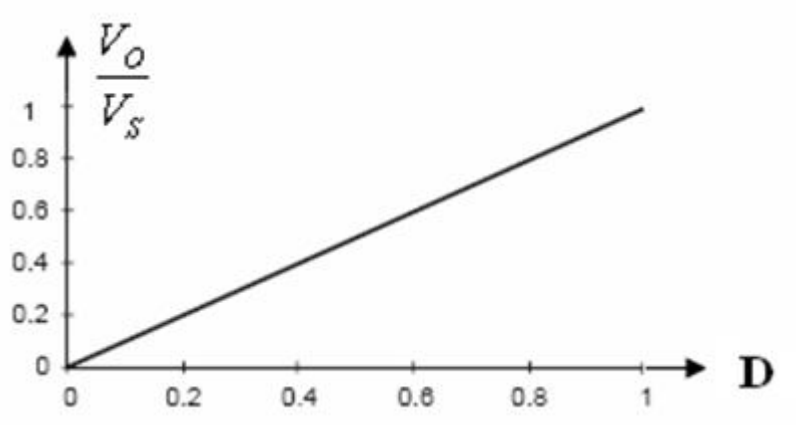

Figure 3-7: output voltage dependency on duty cycle D for the buck converter.

3.5.3- Step down-step up converter (buck-boost converter):

A buck-boost converter provides an output voltage that may be less than or greater than the input voltage; the output voltage polarity is opposite to that of the input voltage. The circuit arrangement of a buck-boost converter is shown in figure 3-8 (a) [14].

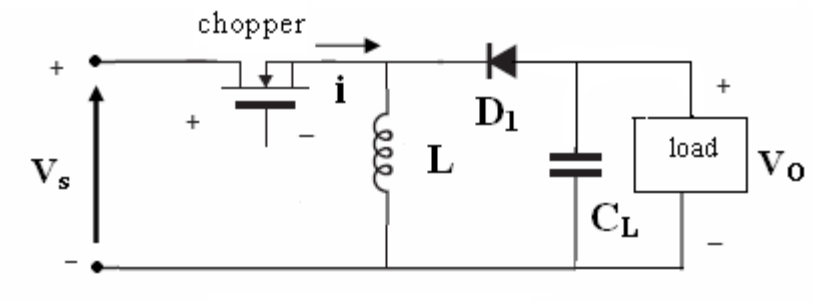

(a) Circuit diagram

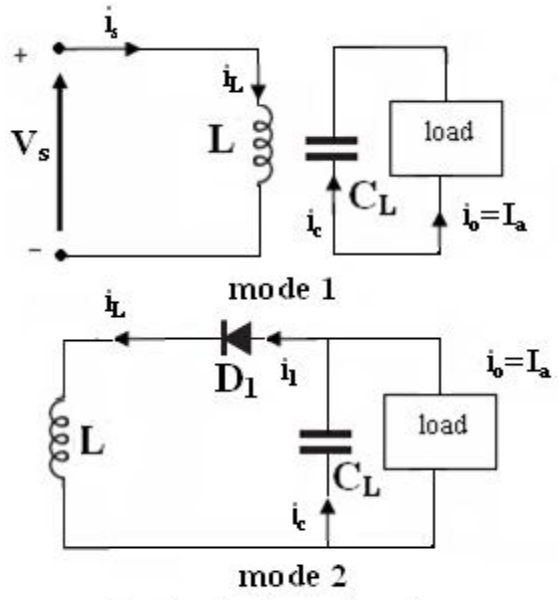

(b) Equivalent circuits

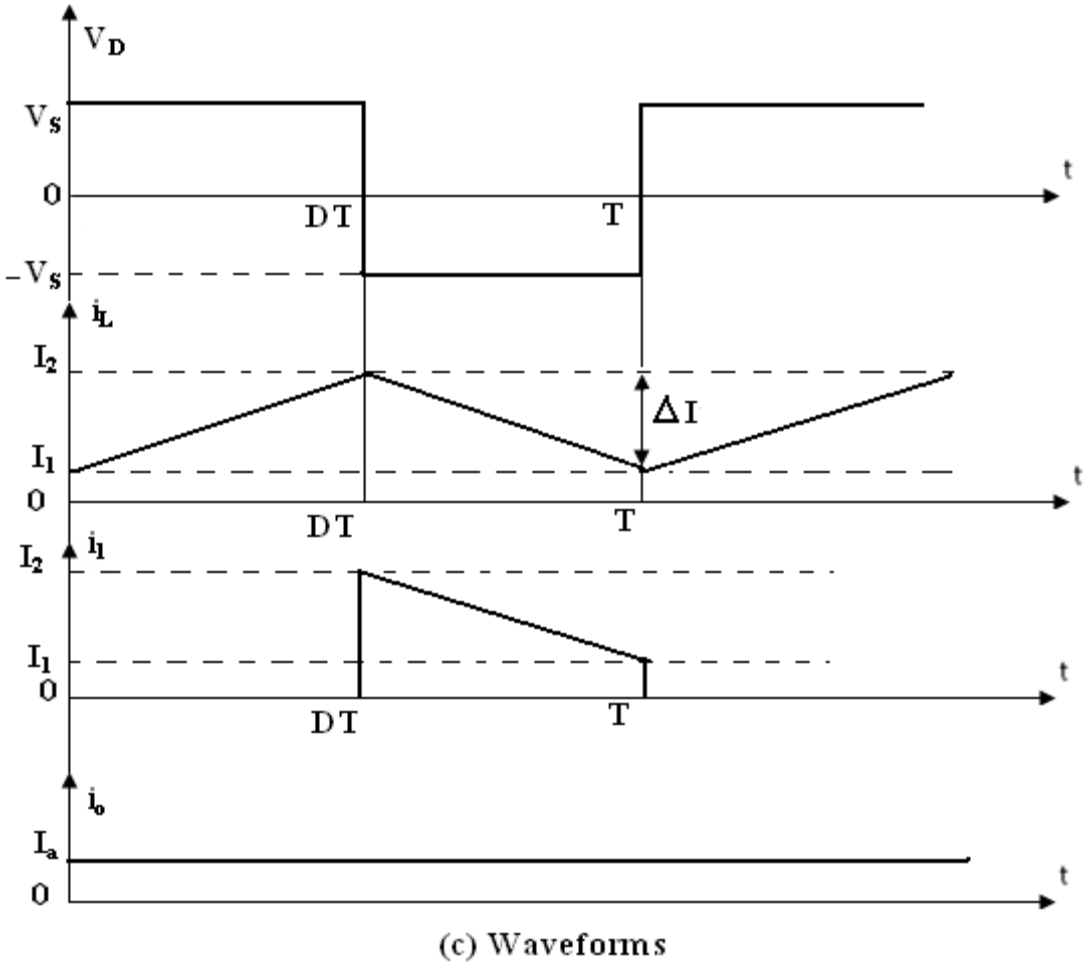

Figure 3-8: buck-boost converter under continuous conduction mode of current.

The circuit operation is divided into two modes, figure 3-8 (b). When the chopper is on and diode D_1 is reversed biased, the input current, which rises, flows through inductor L and the chopper. When the shopper is off and the current which was flowing through inductor L, would flow through L, C_L, D_1 and the load. The energy stored in inductor L would transferred to the load and the inductor current fall until chopper is switched on again in the next cycle.

With the buck-boost converter, the ratio between the output voltage and the input voltage turns out to be:

$$\frac{V_o}{V_s} = -\frac{D}{1-D} = -\frac{t_{on}}{t_{off}} \qquad (3.9)$$

So the buck-boost converter steps the voltage down when the duty cycle is less than 50% (i.e., $t_{on} < t_{off}$), and steps it up when the duty cycle is greater than 50% ($t_{on} > t_{off}$).

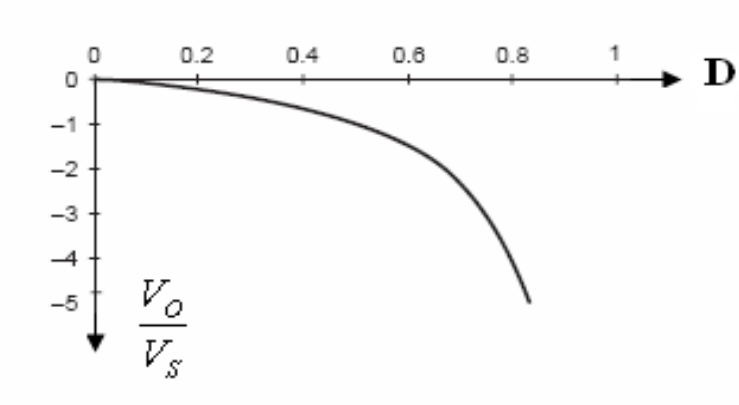

Figure 3-9: output voltage dependency on duty cycle D for the buck-boost converter.

3.5.4- DC-DC converter for PV applications:

In PV applications, the buck type converter is usually used for charging batteries and for water pumping systems because usually lower voltage than the voltage source is needed. A buck converter can operate at the MPP under most conditions, but it cannot do so when the MPP goes below the battery charging voltage under a low irradiance and high temperature condition. Thus, the additional boost capability can appreciably increase the overall efficiency [3].

The grid-tied systems use a boost type converter to step up the output voltage to the utility level before the inverter stage. The boost converter allows tracking the MPP also at a low irradiation level or at high temperatures since the low voltage of the PV module can still be boosted to the required inverter input voltage [4].

3.6-CONCLUSION:

As we have seen in this chapter, MPPT is an important process for the PV system to deliver maximum power to the load and also to increase the efficiency. A DC-DC converter is included in the system between the load and the source to achieve maximum power transfer between the source and the load. Boost converter is used when the load impedance is less than the source impedance and the buck converter is used when the load impedance is higher than the source impedance.

By changing the duty cycle of the converter for each weather condition (temperature and radiation), the impedance matching can be reached using MPPT algorithms and that will be the aim of the next chapter.

Chapter 4: MPPT Algorithms.

4.1- INTRODUCTION:

Peak power is reached with the help of a dc/dc converter between the PVG and the load by adjusting its duty cycle such that the resistance matching is obtained. Now the question arises how to vary the duty cycle and in which direction so that maximum power is attained. The automatic tracking can be performed by utilizing various algorithms [12].

Those algorithms are the heart of the MPPT controller. The algorithms are implemented in a microcontroller or a personal computer to implement maximum power tracking. The algorithm changes the duty cycle of the dc/dc converter to maximize the power output of the module and make it operate at the peak power point of the module. Algorithm that can be used is of the following types:

- Perturb and observe.
- Incremental Conductance.
- Parasitic Capacitance.
- Voltage Based Peak Power Tracking.
- Current Based peak power Tracking.

These algorithms are briefly described in the following section:

4.2- PERTURBATION AND OBSERVATION ALGORITHM:

The Perturb & Observe (P&O) algorithm, also known as the “hill climbing” method, is very popular and the most commonly used in practice because of its simple structure and the few measured parameters which are required [5]. The (P&O) algorithm is based on the constant measuring of the PV current and voltage and calculation of its power output while the operating point is moving in order to reach the maximum power.

In this algorithm the operating voltage of the PV module is perturbed by a small increment, and the resulting change of power, ΔP, is observed. As shown in figure 4-1, if the ΔP is positive, then it is supposed that it has moved the operating point closer to the MPP. Thus,

further voltage perturbations in the same direction should move the operating point toward the MPP. If the ΔP is negative, the operating point has moved away from the MPP, and the direction of perturbation should be reversed to move back toward the MPP. This algorithm has two parameters:

1) The time interval between the times when measurement is done and the time when the operating point moves from its optimal value.

2) The increment of the movement of the operating point itself.

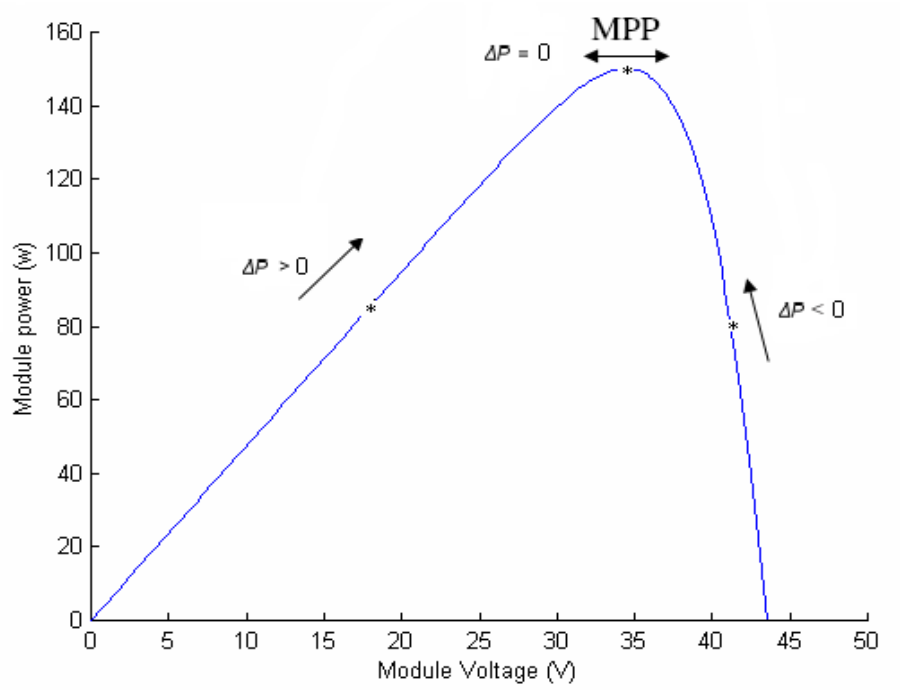

Figure 4-1: Plot of power vs. voltage for BP SX 150S PV module (1KW/m^2, 25^{o}c).

When the steady state is reached the algorithm oscillates around the peak point. In order to keep the power variation small the perturbation size is kept very small. The algorithm is developed in such a manner that it sets a reference voltage of the module corresponding to the peak voltage of the module. A PI controller then acts moving the operating point of the module to that particular voltage level. It is observed that there is some power loss due to this perturbation also the fails to track the power under fast varying atmospheric conditions. But still this algorithm is very popular and simple.

The flowchart of this algorithm is given in Figure 4-2:

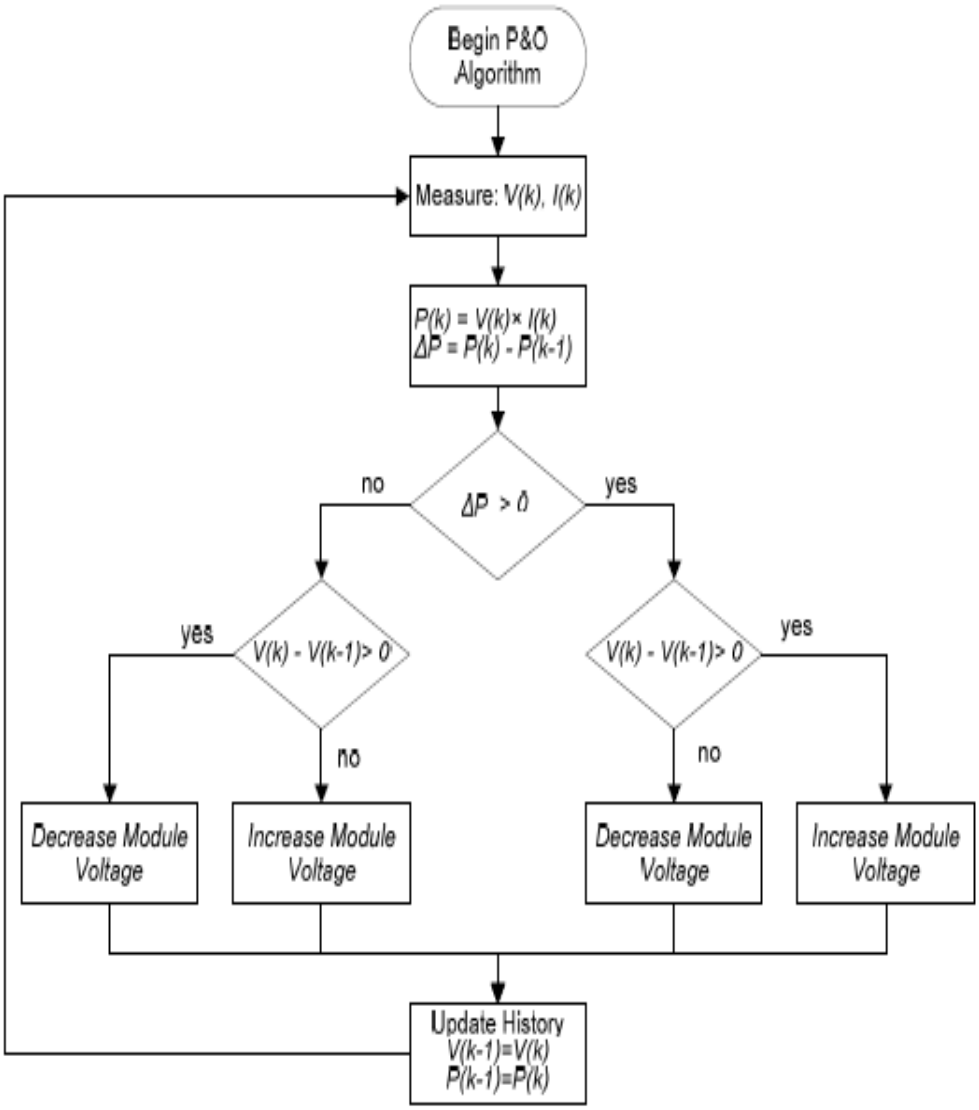

Figure 4-2: Flowchart of the P&O algorithm [4].

4.3- INCREMENTAL CONDUCTANCE ALGORITHM:

The disadvantage of the Perturb & Observe algorithm when tracking the peak power under fast varying atmospheric condition is overcome by the Incremental Conductance algorithm. The Incremental Conductance (IncCond) method is based on the fact that the slope dP/dv of the PV panel power-voltage curve is positive on the left side of the MPP, zero at the MPP and negative on the right side of the MPP as shown in figure 4-3.

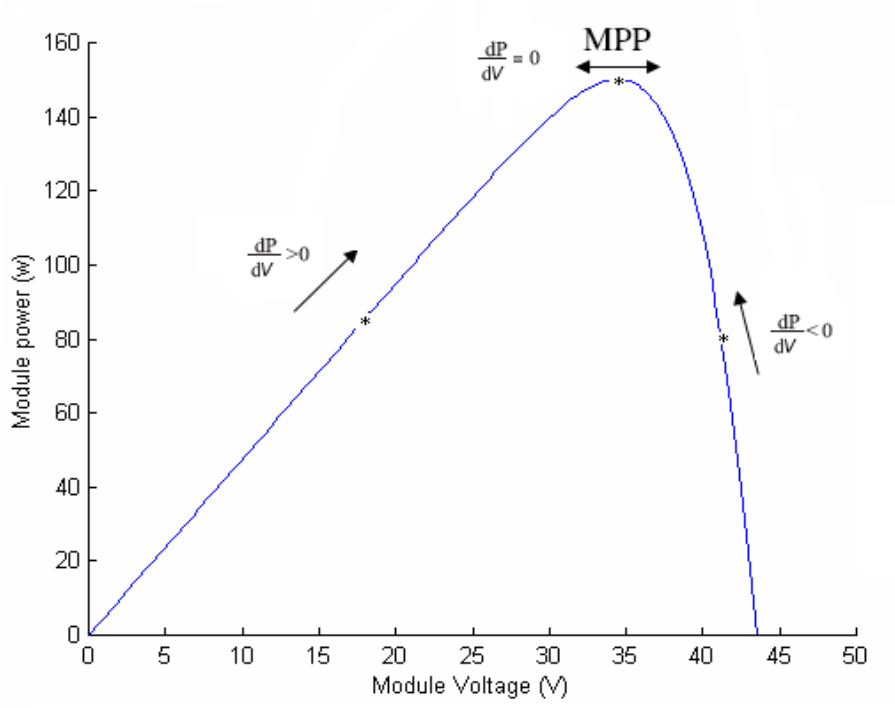

Figure 4-3: Plot of power vs. voltage for BP SX 150S PV module (1KW/m^2, 25^{o}c).

The incremental and conductance algorithm makes use of the following equations:

$$\frac{dP}{dV} = 0 \quad \text{at MPP.} \tag{4.1}$$

$$\frac{dP}{dV} > 0 \quad \text{at the left of MPP.} \tag{4.2}$$

$$\frac{dP}{dV} < 0 \quad \text{at the right of MPP.} \tag{4.3}$$

The above equations can be written in terms of voltage and current as follows:

$$\frac{dP}{dV} = \frac{d(V.I)}{dV} = I\frac{dV}{dV} + V\frac{dI}{dV} = I + V\frac{dI}{dV} \tag{4.4}$$

If the operating point is at the MPP, equation (4.4) becomes:

$$I + V\frac{dI}{dV} = 0 \Rightarrow \frac{dI}{dV} = -\frac{I}{V} \tag{4.5}$$

If the operating point is at the left side of the MPP, equation (4.4) becomes:

$$I + V\frac{dI}{dV} > 0 \Rightarrow \frac{dI}{dV} > -\frac{I}{V} \tag{4.6}$$

If the operating point is at the right side of the MPP, equation (4.4) becomes:

$$I + V\frac{dI}{dV} < 0 \Rightarrow \frac{dI}{dV} < -\frac{I}{V} \tag{4.7}$$

The flowchart shown in Figure 4-4 below describes the operation of this algorithm. It starts with measuring the present values of the PV generator voltage and current. Then, it calculates the incremental changes, dI and dV, using the present values and previous values of voltage and current. The main check is carried out using the relationships in the equations (4.5), (4.6), and (4.7). If the condition satisfies the inequality (4.6), it is assumed that the operating point is at the left side of the MPP therefore must be moved to the right by increasing the PVG voltage. Similarly, if the condition satisfies inequality (4.7), it is assumed that the operating point is at the right side of the MPP, thus must be moved to the left by decreasing the PVG voltage. When the operating point reaches the MPP, the condition satisfies the equation (4.5), and the algorithm bypasses the voltage adjustment. At the end of the cycle, it updates the history by storing the voltage and current data that will be used as previous values in the next cycle. Another important check included in this algorithm is to detect atmospheric conditions. If the MPPT is still operating at the MPP (condition: dV = 0) and the irradiation has not changed (condition: dI = 0), it takes no action. If the irradiation has increased (condition: dI > 0), it raises the MPP voltage. Then, the algorithm will increase the operating voltage to track the MPP. Similarly, in case of decreasing irradiation (condition: dI< 0), the MPP voltage will be lowered. Then, the algorithm will decrease the operating voltage .So it can be said that the incremental conductance can track rapidly increasing and decreasing irradiance conditions with higher accuracy than Perturb and Observe algorithm [13]. One disadvantage of this algorithm is the increased complexity when compared to the Perturb and Observe algorithm [12].

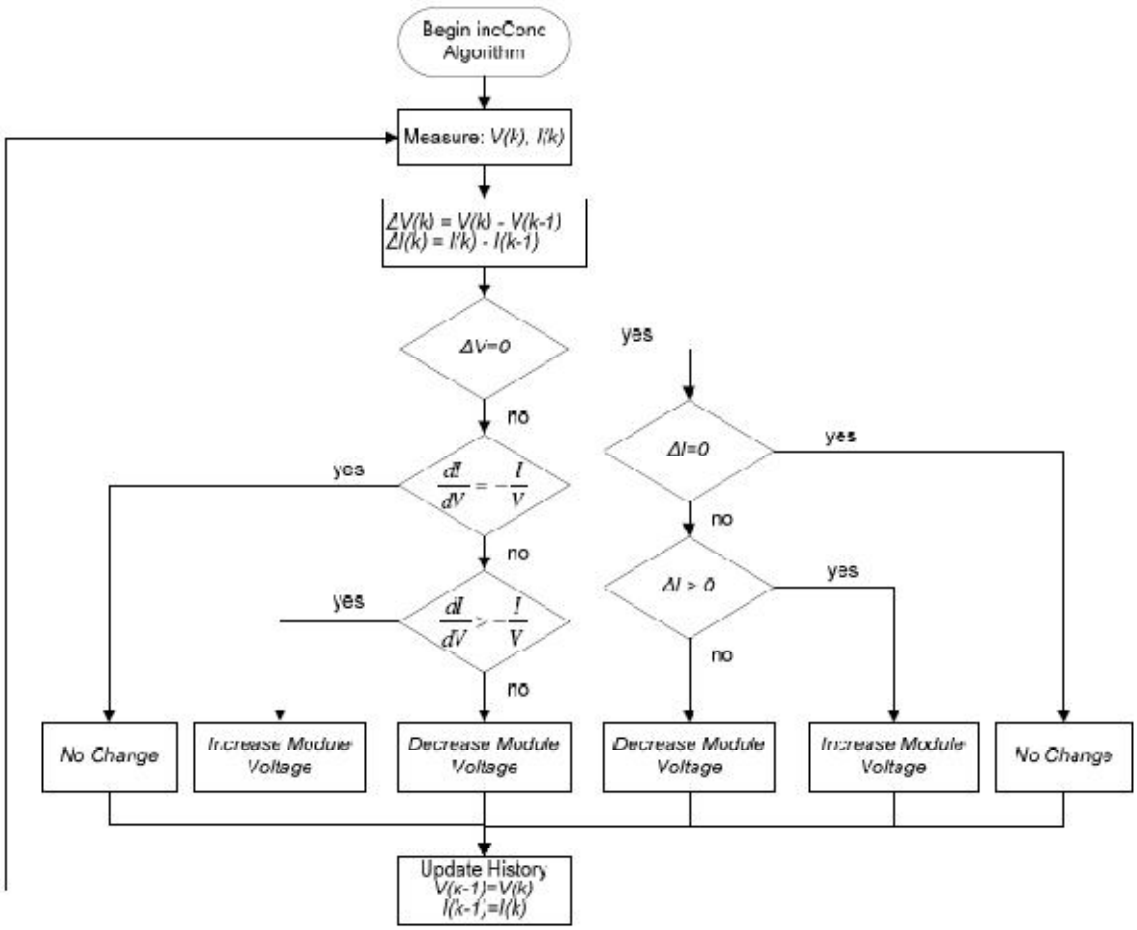

Figure 4-4: Flowchart of the IncCond algorithm [4].

4.4- PARASITIC CAPACITANCES METHOD:

The parasitic capacitance method is a refinement of the incremental conductance method that takes into account the parasitic capacitances of the solar cells in the PV array. Parasitic capacitance uses the switching ripple of the MPPT to perturb the array. To account for the parasitic capacitance, the average ripple in the array power and voltage, generated by the switching frequency, are measured using a series of filters and multipliers and then used to calculate the array conductance**.** The incremental conductance algorithm is then used to determine the direction to move the operating point of the MPPT. One disadvantage of this algorithm is that the parasitic capacitance in each module is very small, and will only come into play in large PV arrays where several module strings are connected in parallel. Also, the DC-DC converter has a sizable input capacitor used filter out small ripple in the array power. This capacitor may mask the overall effects of the parasitic capacitance of the PV array.

4.5- VOLTAGE CONTROL MAXIMUM POWER POINT TRACKER:

A linear dependency exists between “cell voltages corresponding to maximum power” and “cell open circuit voltages” [16]:

$$V_{MP} = M_V . V_{OC} \tag{4.8}$$

This equation characterizes the main idea of the Voltage-Based Maximum Power Point Tracking (VMPPT) technique. M_V is called the “voltage factor” and is equal to 0.74 [16]. Equation (4.8) is plotted in Figure 4-5 together with the computed (almost linear) dependency of V_{MP} with respect to V_{OC} (shown by “+” signs).

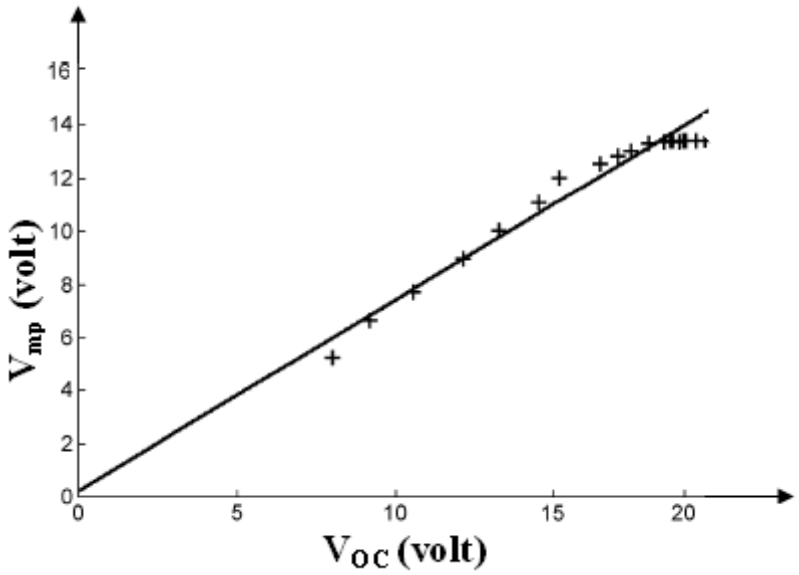

Figure 4-5: optimum voltage versus open voltage [16].

So by measuring the open circuit voltage a reference voltage can be generated and a feed forward voltage control scheme can be implemented to bring the solar PV module voltage to the point of maximum power. Though the simplicity of this technique, it presents one drawback. the open circuit voltage of the PVG varies with the temperature. So as the temperature increases the PVG open circuit voltage changes and we have to measure the open circuit voltage of the module very often. Hence the load must be disconnected from the module to measure open circuit voltage. So some PVG power will be lost [12].

4.6- CURRENT CONTROL MAXIMUM POWER POINT TRACKER:

The optimum operating current I_{op} for the maximum output power is proportional to the short current I_{sc} under various conditions of irradiance G [17]. The proportionality relationship is expressed as follows:

$$I_{op}(G) = k.I_{sc}(G) \quad (4.9)$$

Where k: is the proportional constant.

I_{sc}: is the short current of the PVG.

I_{op}: is the optimum operating current.

This equation indicates that current I_{op} can be determined instantaneously by detecting I_{sc} and that the MPPT can be achieved by giving a current command $I^* = I_{op}$ to a current-controlled power converter. However, the effect of the temperature has to be studied first by using the test PV module over a wide range of the temperature.

Figure 4-6 shows the measurement results and it can be seen that the relationship between I_{op} and I_{sc} is still proportional, despite the temperature variation from 0^oc to 60^oc [12]. From this figure, the proportional parameter k can be estimated to be approximately 0.92.

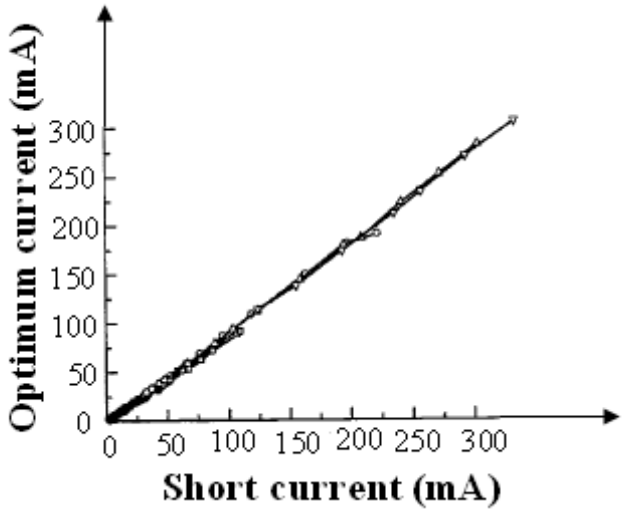

Figure 4-6: Optimum current versus short current [12].

The main drawback with this method is that a high power resistor is required which can sustain the short-circuit current.

The PVG has to be short circuited to measure the short circuit current as it goes on varying with the changes in insulation level [12].

4.7- CONTROL OF MPPT SCHEME:

As explained in the previous sections, the MPPT algorithm tells an MPPT controller how to move the operating voltage. Then, it is an MPPT controller's task to bring the voltage to a desired level and maintain it. The MPPT algorithm (Perturbation and Observation, Incremental and Conductance …etc) is implemented in a software program with a self-tuning function, which automatically adjusts the array reference voltage and voltage step size to quickly achieve the Maximum Power Tracking under rapidly changing conditions. Then, there is another control loop that is the proportional and integral (PI) controller which regulates the input voltage of the converter. The task of the PI controller is to minimize the error between (V_{ref}) and the measured voltage by adjusting the duty cycle [3]. The PI loop operates with a fast rate and provides fast response and is used to improve the system stability. The functions in the two loops can be performed by a DSP. The DSP-based controller senses the PVG current and voltage as shown in figure 4-7, and calculates the PVG output power, power slope, and (V_{ref}) to track the MPP [5] [3].

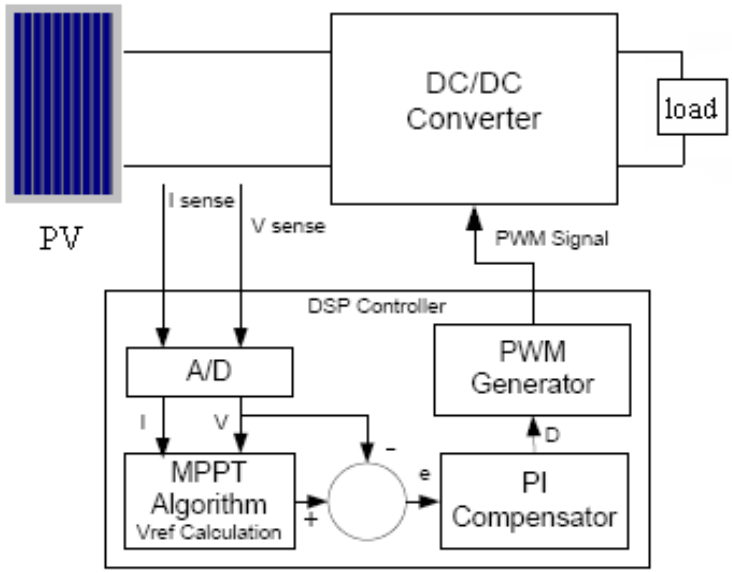

Figure 4-7: Block diagram of MPPT with the PI compensator.

4.8- SIMULATION:

In the last sections deferent MPPT algorithms have been described, in this present study the Perturb & Observe (P&O) and Incremental Conductance (IncCond) methods are chosen to be implemented and tested in MATLAB simulations.

We have chosen those algorithms because they are simple, stable, they can achieve higher efficiencies, and the main reason is that the other algorithms need monitoring system (sensors, calculators...etc) and thus increase the cost, so the Perturb & Observe (P&O) and Incremental Conductance (IncCond) methods are the usual choice for MPPT [3]-[5].

Since the purpose is to make comparisons of two algorithms, each simulation contains only the PV model and the algorithm in order to isolate any influence from a converter or load.

The algorithms are tested with variable irradiance data, the MATLAB use two sets of data: the first set of data is the measurements of a sunny day taken every 15 minutes during a typical day in April in Bechar, Algeria (709 km away, location: 31°36'28", North, 2°13'12", West) [18], where the irradiance changes slowly during the day. The second set of data is for a cloudy day in the same month in Barcelona, Spain, where the irradiance changes rapidly [3]. The irradiance values between two data points are estimated by the cubic interpolation in MATLAB functions.

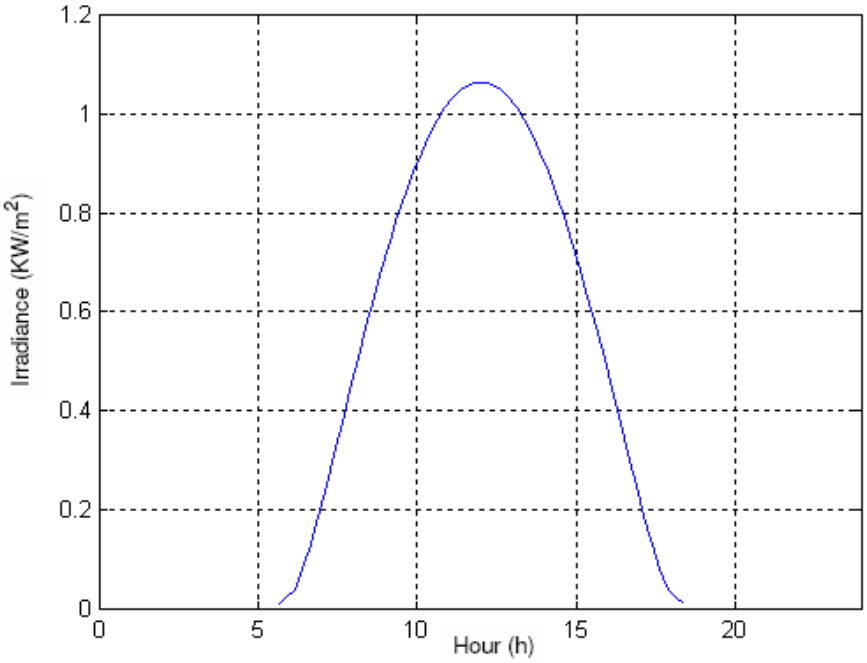

Figure 4-8: Irradiance data for a sunny day in Bechar, Algeria.

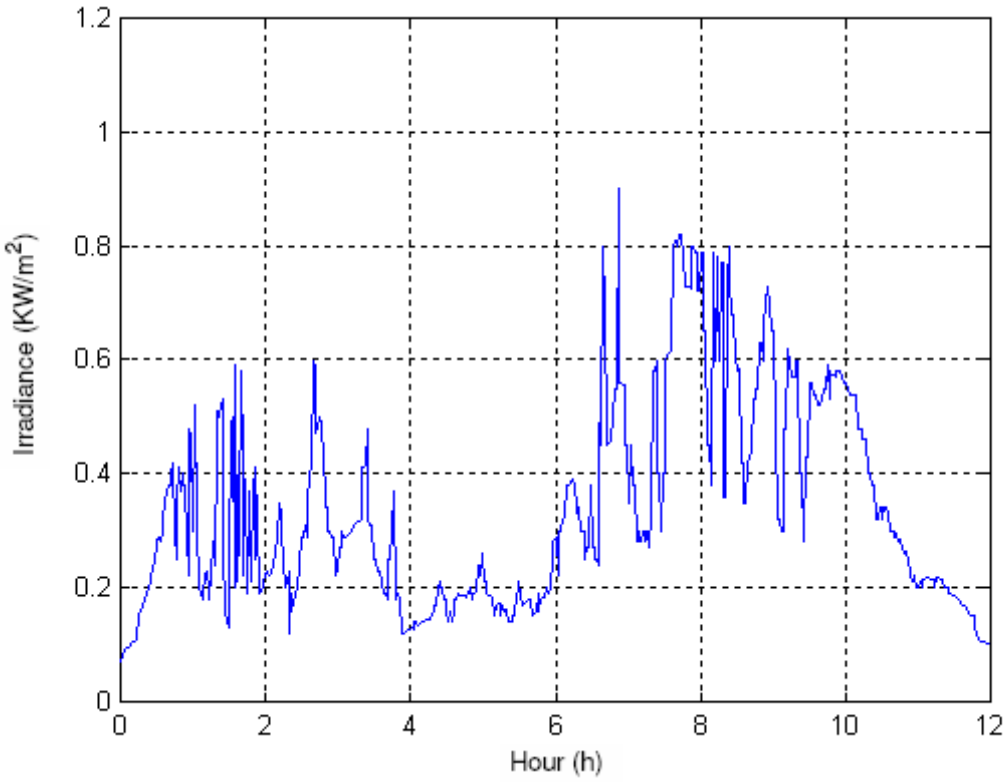

Figure 4-9: Irradiance data for a cloudy day in Barcelona, Spain.

Using the first set of data (sunny day measurements) in the simulation to compare between the Pert & Observ algorithm and the IncCond algorithm, knowing that the irradiance changes gradually (no influence of cloud), we notice that the two algorithms locate and maintain the PV operating point very close to the MPPs without considerable difference in their performance as shown in figure 4-10. However, the different performances of the algorithms are visible when the second set of data is used (cloudy day measurement where the irradiance changes rapidly), so the MPP tracking is supposed to be challenging. For both algorithms, the deviations of operating points from the MPPs are obvious when compared to the results of a sunny day.

The Incremental Conductance algorithm is supposed to overcome the disadvantages of the Pert & Observ algorithm under rapidly changing atmospheric conditions. The simulation result in figure 4-11 shows that the Pert & Observ algorithm has slightly larger deviations than the IncCond algorithm and it has some erratic behaviors (such as the large deviation pointed by the red arrow) which are also observable in the plot of the IncCond algorithm. To make better comparison between the two, total electric energy produced during a 12-hour period is calculated and tabulated in Table 4-1.

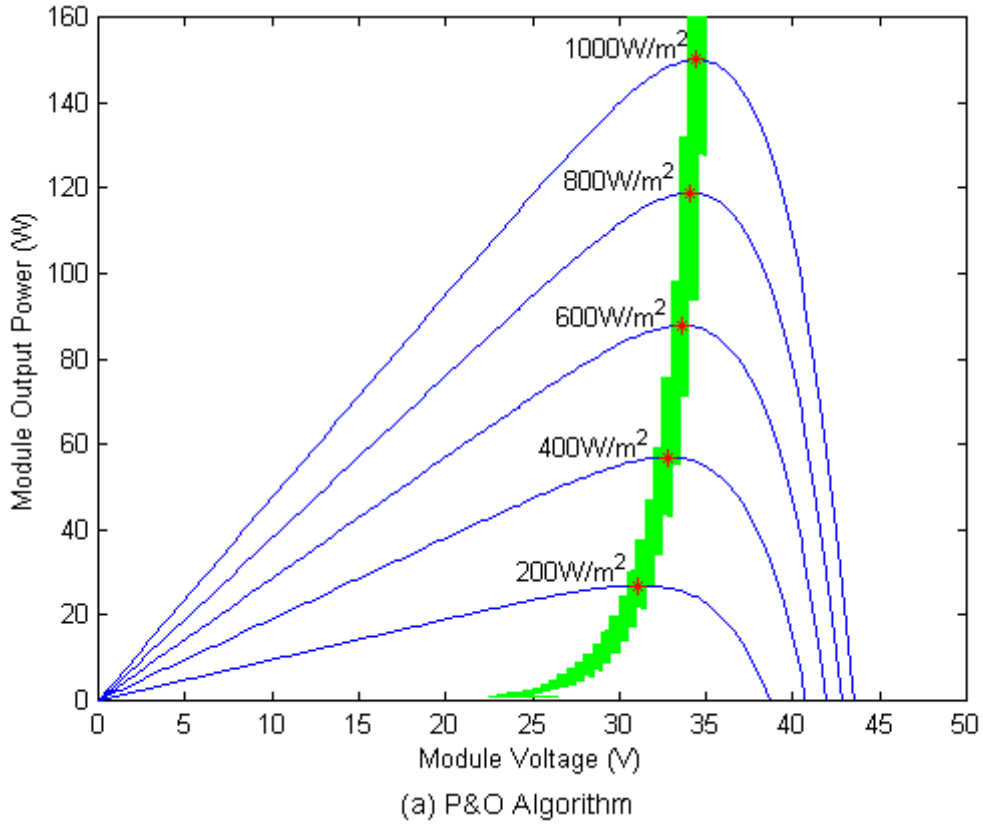

(a) P&O Algorithm

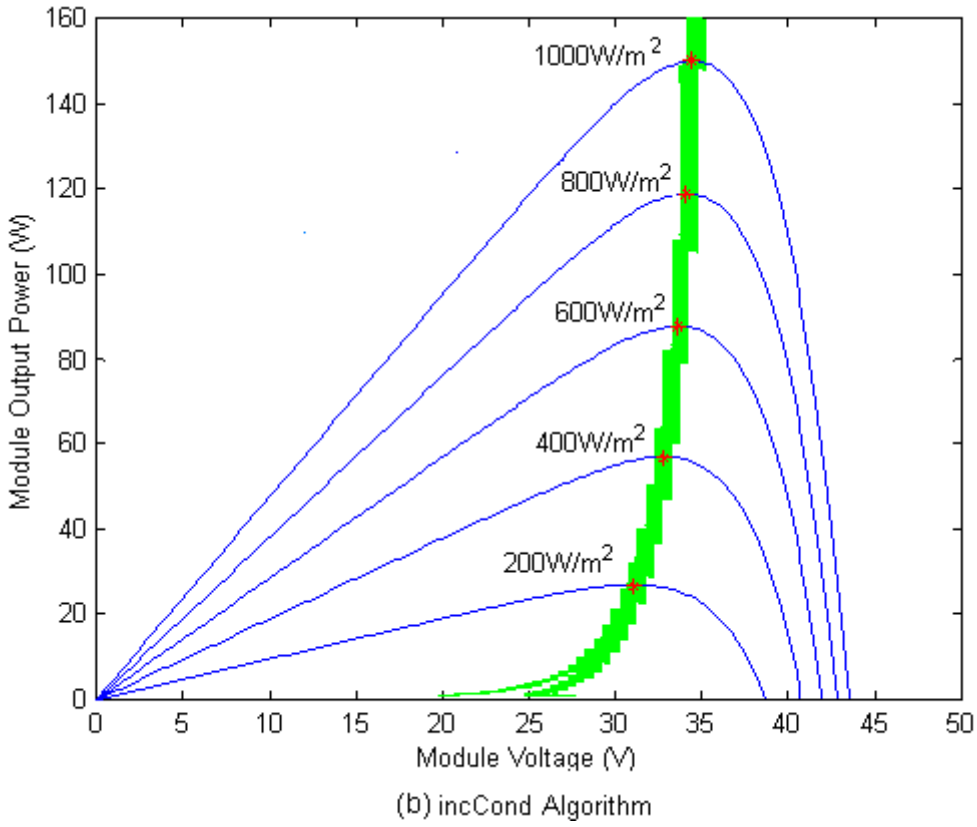

(b) incCond Algorithm

Figure 4-10: Traces of MPP tracking on a sunny day (25°c).

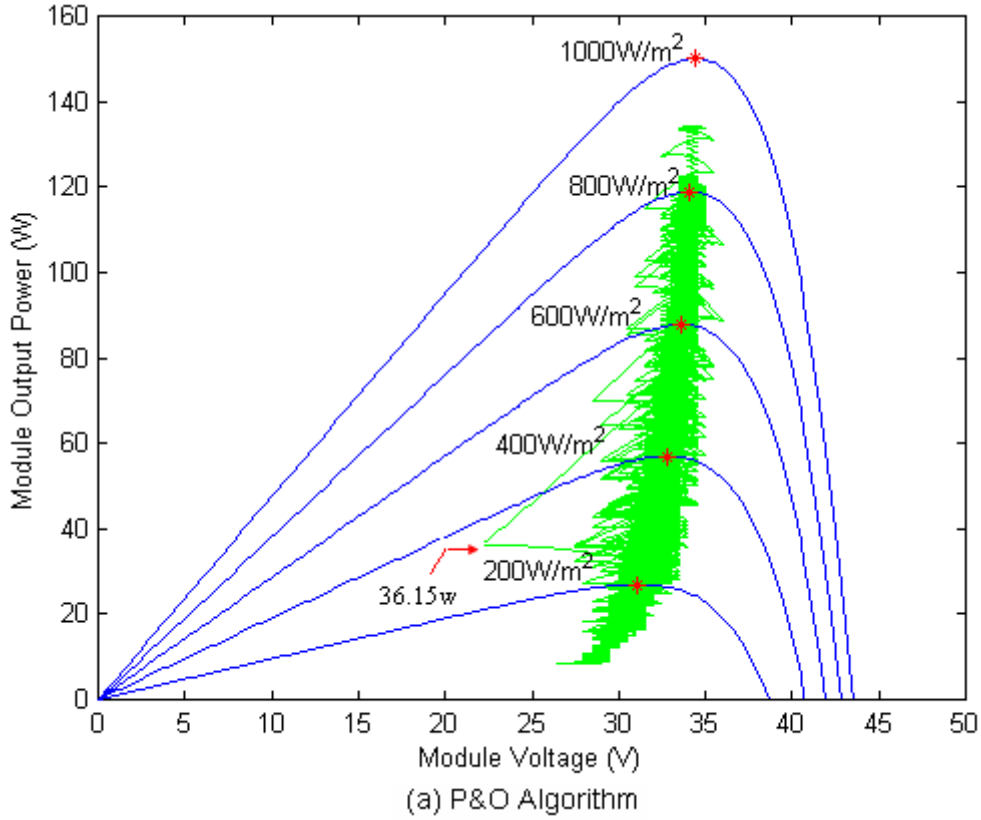

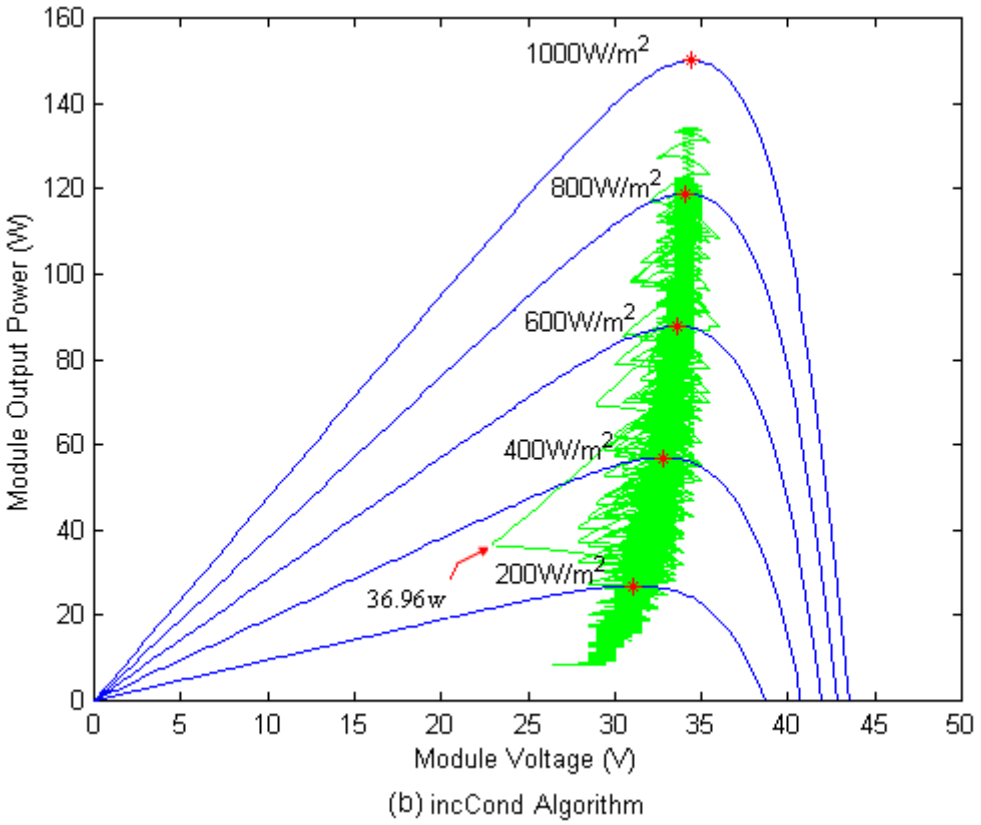

Figure 4-11: Traces of MPP tracking on a cloudy day (25°c).

	Pert & Observ algorithm	IncCond algorithm
Total Energy (simulation)	**576.4358 W/h**	**576.4967 W/h**
Total Energy (theoretical max)	**577.3323 W/h**	**577.3323 W/h**
Efficiency	**99.84%**	**99.85%**

Table 4-1: Comparison of the P&O and IncCond algorithms on a cloudy day.

As the table 4-1 shows, the total energy produced by the IncCond algorithm is closely larger than that of the P & O algorithm. The MPPT efficiency is measured by the following relation:

Efficiency = {Total Energy (simulation)} ÷ {Total Energy (theoretical max)} × 100%. (4.10)

The result shows that the efficiency is good for both algorithms even in cloudy conditions. However, the efficiency is slightly better with the IncCond algorithm. There are other studies show exactly the same results [3]; the simulation showed the efficiency of 99.85% for the P& O algorithm and 99.86% for the IncCond algorithm. The experimental results showed 96.5% and 97.0%, respectively, for a partly cloudy day [3].

4.9- SIMULATION AND PERFORMANCE OF MPPT WITH RESISTIVE LOAD:

The MPPT with a resistive load is implemented in MATLAB simulation and verified. The simulation results in Section 4.8 have shown that there is no great advantage in using the more complex IncCond algorithm, and the P&O algorithm provides satisfactory results even in the cloudy condition.

The selection of the P&O algorithm permits the use of the output sensing direct control method which eliminates the input voltage and current sensors. The MPPT design, therefore, chooses the P&O algorithm and the output sensing direct control method because of the advantage that allows of a simple and low cost system.

4.9.1- Output Sensing Direct Control:

The output sensing method measures the power change of PV at the output side of converter and uses the duty cycle as a control variable. This control method is simple and uses only one control loop, and it performs the adjustment of duty cycle within the MPP tracking algorithm. The way how to adjust the duty cycle is based on the theory of load matching explained in Section 3.4.

The following simulation illustrates the relationship between the output power of the converter and the switch duty cycle. In the simulation, a BP SX 150S PV module is coupled with the ideal boost converter with a resistive load (50Ω). The duty cycle is varied from 0 to 1 with 1% step, and the converter output power is plotted in Figure 4-12.

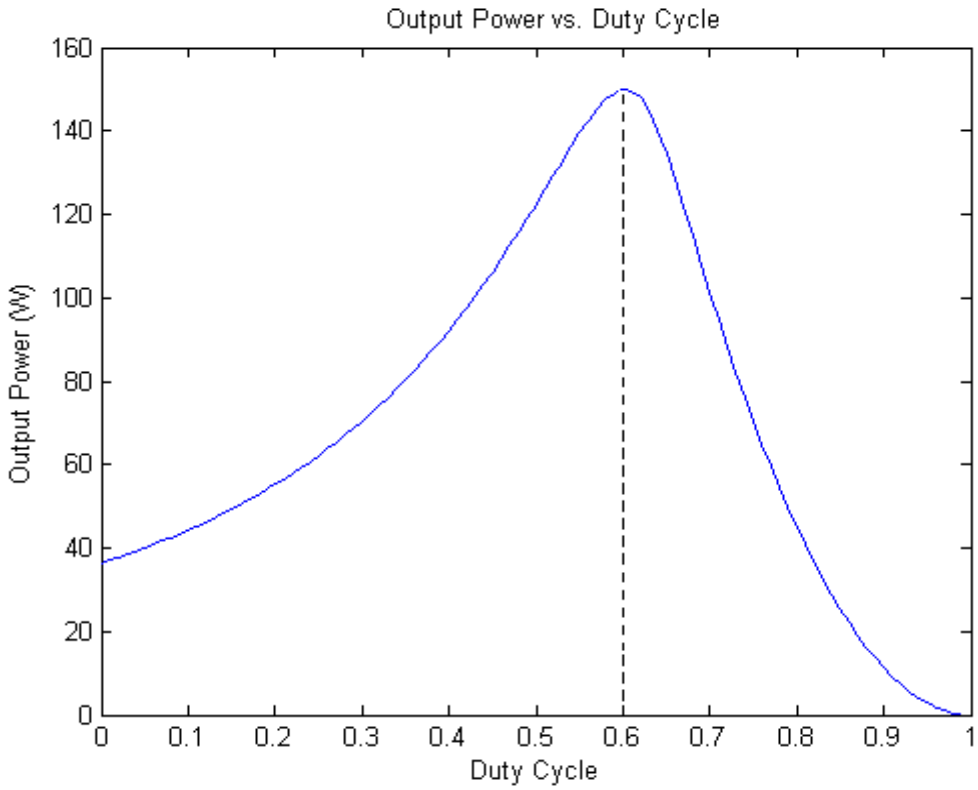

Figure 4-12: Output power of boost converter vs. its duty cycle (1KW/m^2, 25^{o}c).

As shown in the figure 4-12, the output power of the converter varied with the changes of the duty cycle and it reach the peak at the duty cycle of 0.6.

This control method employs the P&O algorithm to locate the MPP. Figure 4-13 shows the flowchart of algorithm [3]. In order to accommodate duty cycle as a control variable, the P&O algorithm used here is a slightly modified version from that previously introduced, but the

way how it works is exactly the same. The algorithm perturbs the duty cycle and measures the converter output power. If power increases, the duty cycle is further perturbed in the same direction; otherwise the direction will be reversed.

When the converter output power reaches the peak, the PV module or array is supposed to be operating at the Maximum Power Point.

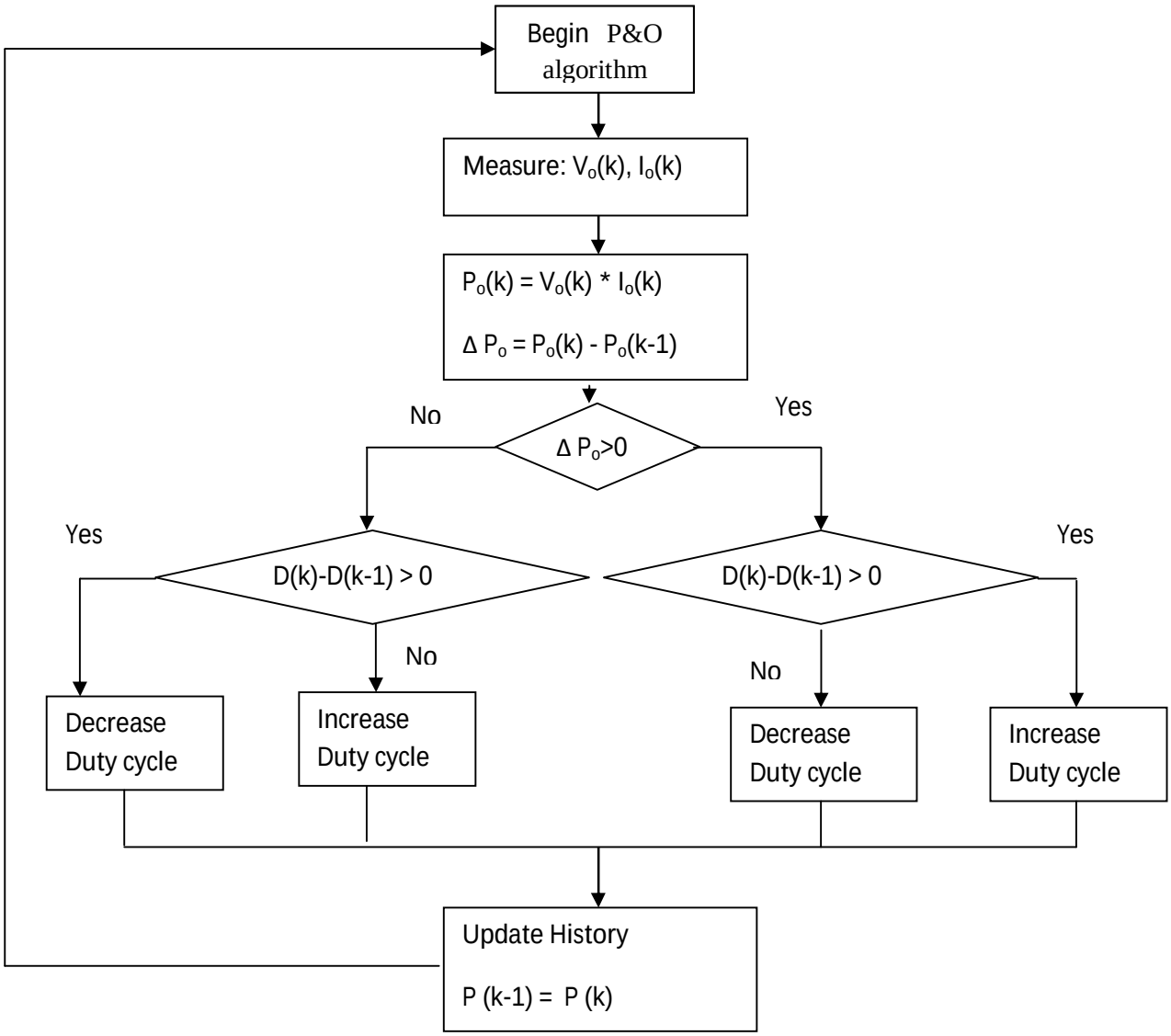

Figure 4-13: Flowchart of P&O algorithm for the output sensing direct control method.

As the flowchart explain, first the algorithm measure the converter output voltage and current, then the output power $P_o(k)$ and its variation (ΔP_o) is calculated at each step. If the variation in the output power is positive then the variation on the duty cycle kept on the same direction, otherwise the direction of the perturbation on the duty cycle will be reversed.

4.9.2- MPPT limitations:

The main drawback of MPPT is that there is no regulation on output while it is tracking a maximum power point. It cannot regulate both input and output at the same time.

The example of load matching in Section 3.4 is elaborated here to show how the output voltage and current will change with varying irradiation. The maximum power transfer occurs when the input impedance (resistance) of converter matches the optimal impedance (resistance) of the PV Generator, as stated in the equation below:

$$R_{in} = R_{opt} = \frac{V_{MPP}}{I_{MPP}} \qquad (4.11).$$

Equation (3.3) rewritten here for convenience:

$$R_{in} = \frac{V_s}{I_s} = (1-D)^2 \frac{V_o}{I_o} = (1-D)^2 R_{load} \qquad (4.12).$$

The equation (4.12) for the boost converter is solved for duty cycle (D):

$$D = 1 - \sqrt{\frac{R_{in}}{R_{load}}} \qquad (4.13).$$

The converter output voltage is given by:

$$V_o = \frac{1}{1-D} V_s \qquad (4.14).$$

the converter output current is given by:

$$I_o = (1-D) I_s \qquad (4.15).$$

The relation between R_{in} and R_{load} is:

$$R_{in} = (1-D)^2 R_{laod} \qquad (4.16)$$

The calculation results are tabulated in the tables below. PV module data are obtained from the MATLAB simulation model. Using the equations above, a set of data is collected for the resistive load of 50Ω and 60Ω at the constant module temperature of 25°c.

	PV Module			MPPT				
Irradiance	**V_{MPP}**	**I_{MPP}**	**P_{max}**	**R_{in}**	**D**	**V_o**	**I_o**	**R_{load}**
1000W/m²	**34.5V**	**4.35A**	**150.0W**	**7.92 Ohm**	**0.6020**	**86.6845V**	**1.7313A**	**50 Ohm**
800W/m²	**34.1V**	**3.48A**	**118.8W**	**9.80 Ohm**	**0.5573**	**77.0240V**	**1.5407A**	**50 Ohm**
600W/m²	**33.6V**	**2.61A**	**87.7W**	**12.9 Ohm**	**0.4921**	**66.1499V**	**1.3257A**	**50 Ohm**
400W/m²	**32.7V**	**1.73A**	**56.9W**	**18.8 Ohm**	**0.3868**	**53.3278V**	**1.0608A**	**50 Ohm**
200W/m²	**31.1V**	**0.87A**	**26.9W**	**35.9 Ohm**	**0.1527**	**36.7027V**	**0.7372A**	**50 Ohm**

Table 4.2: Load matching with the resistive load (50Ω) under varying irradiance.

	PV Module			MPPT				
Irradiance	**V_{MPP}**	**I_{MPP}**	**P_{max}**	**R_{in}**	**D**	**V_o**	**I_o**	**R_{load}**
1000W/m²	**34.5V**	**4.35A**	**150.0W**	**7.92 Ohm**	**0.6367**	**94.9581V**	**1.5804A**	**60 Ohm**
800W/m²	**34.1V**	**3.48A**	**118.8W**	**9.80 Ohm**	**0.5959**	**84.3756V**	**1.4064A**	**60 Ohm**
600W/m²	**33.6V**	**2.61A**	**87.7W**	**12.9 Ohm**	**0.5363**	**72.4636V**	**1.2102A**	**60 Ohm**
400W/m²	**32.7V**	**1.73A**	**56.9W**	**18.8 Ohm**	**0.4402**	**58.4177V**	**0.9684A**	**60 Ohm**
200W/m²	**31.1V**	**0.87A**	**26.9W**	**35.9 Ohm**	**0.2265**	**40.2058V**	**0.6730A**	**60 Ohm**

Table 4.3: Load matching with the resistive load (60Ω) under varying irradiance.

The results in tables 4.2 and 4.3 show that the output voltage and current V_o and I_o are varying and not regulated. If the application requires a constant voltage, batteries must be used to maintain the voltage constant.When the resistive load changes from 50Ω to 60Ω, the duty cycle of the converter changes even if the input is the same, which means that the design of the converter must satisfy the specifications of the source and the load at the same time. In other word, it is very important to select the appropriate size of the load, so that the capacity of PVG can be fully utilized.

4.9.3- Simulated System:

The simulated system consists of the BP SX 150S PV model, the ideal boost converter, the MPPT control, and the resistive load (50Ω).

The MATLAB function that models the PVG is the following:

$$I_a = bp\_sx150s(V_a, G, T) \tag{4.17}$$

The function, bp_sx150s, calculates the module current (I_a) for the given module voltage (V_a), irradiance (G in KW/m^2), and module temperature (T in ^{o}c).

The operating point of the PVG is determined by its relationship with the load resistance (R):

$$R = \frac{V_a}{I_a} \tag{4.18}$$

The irradiance (G) and the PVG temperature (T) for the function (4.17) are known variables, thus it is possible to say that (I_a) is a function of (V_a) thus: $I_a = f(V_a)$.

Substituting it into the equation (4.18) gives:

$$\begin{aligned} &R * I_a = V_a \\ &so \\ &V_a - R * I_a = 0 \end{aligned} \tag{4.19}$$

The final equation will be:

$$V_a - R * f(V_a) = 0 \tag{4.20}$$

Knowing the value of R enables to solve this equation for the operating voltage (V_a). MATLAB uses fzero function to do so. Putting (V_a) into the equation (4.17) gives the operating current (I_a).

The steady state analysis discussed in Section 3.5.1 provides sufficient modelling of the boost converter. The following equations describe the input/output relationship of voltage and current. The equations are given by:

$$V_o = \frac{1}{1-D} V_s \tag{4.21}$$

$$I_o = (1 - D)I_s \qquad (4.22).$$

Where: V_o is the boost converter output voltage.

I_o is the boost converter output current.

D is the boost converter duty cycle.

The flowchart explains the operation of the simulated system, is shown in figure 4-14 below:

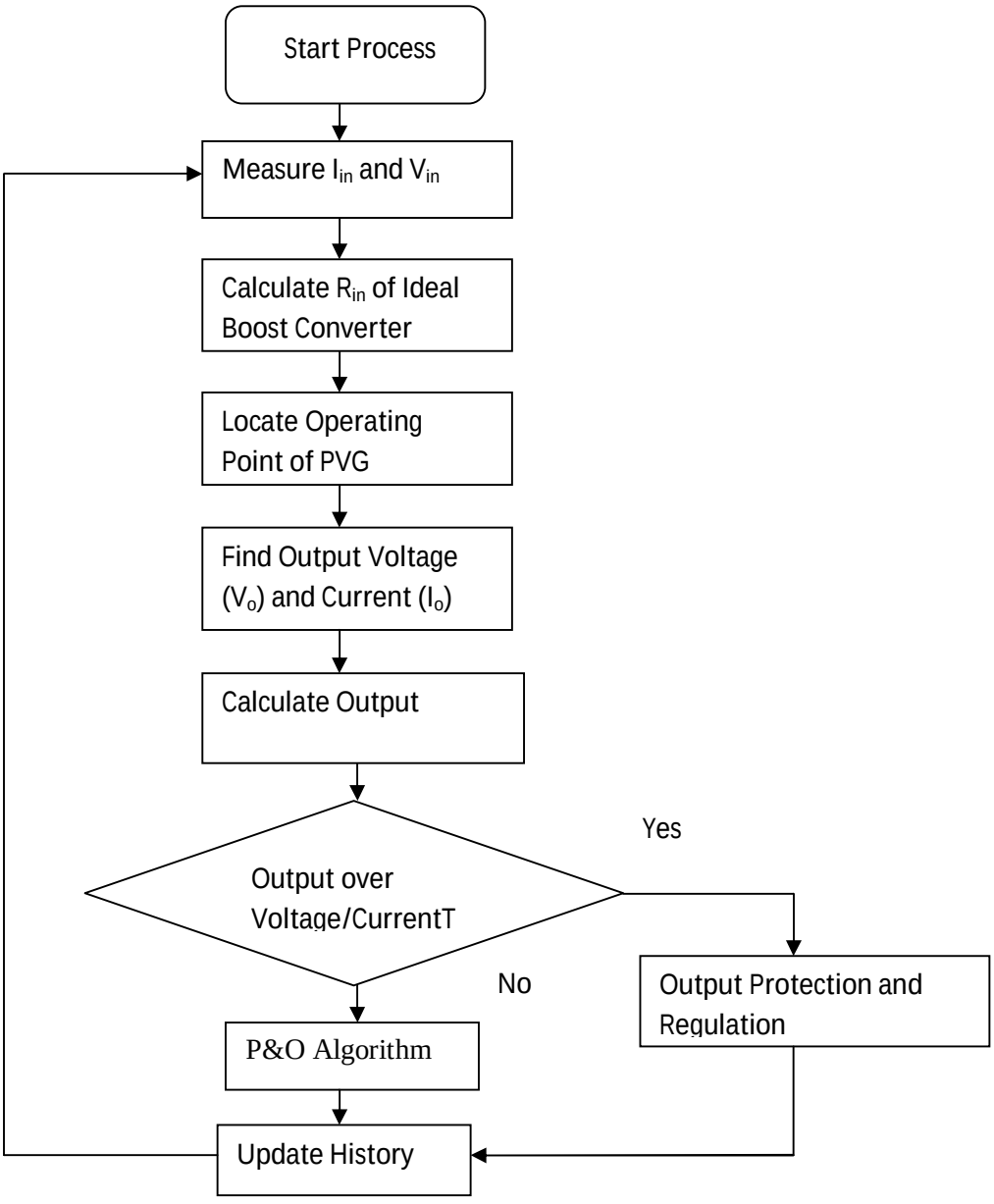

Figure 4-14: MPPT simulation flowchart for resistive load.

The control algorithm contains two loops, the main loop for MPPT and a second loop for output protection. During normal operation, the algorithm operates in MPPT mode. When the load cannot absorb all the power produced by the PVG, its voltage or/and current will exceed the allowable limits. To protect the load from failure, the control algorithm stops operating in MPPT mode and activate the output protection. Then, it regulates the output so that it does not exceed the safe limits. In the simulation, it sets when the output voltage goes beyond 86.7V or 1.75A for the output current for the resistive load R =50 Ω.

The simulation is performed under linearly increasing irradiance varying from 200w/m^2 to 1000W/m^2 with a moderate rate of 0.3W/m^2 per sample. Figure 4-15 (a) and (b) show that the locus of operating point is staying close to the MPPs.

Figure 4-15 (c) shows the relationship between the output power of converter and its duty cycle. Figure 4-15 (d) shows the current and voltage relationship of converter output. Since the load is resistive, the current and voltage increase linearly with the slope of $1/R_{load}$ on the I-V plane.

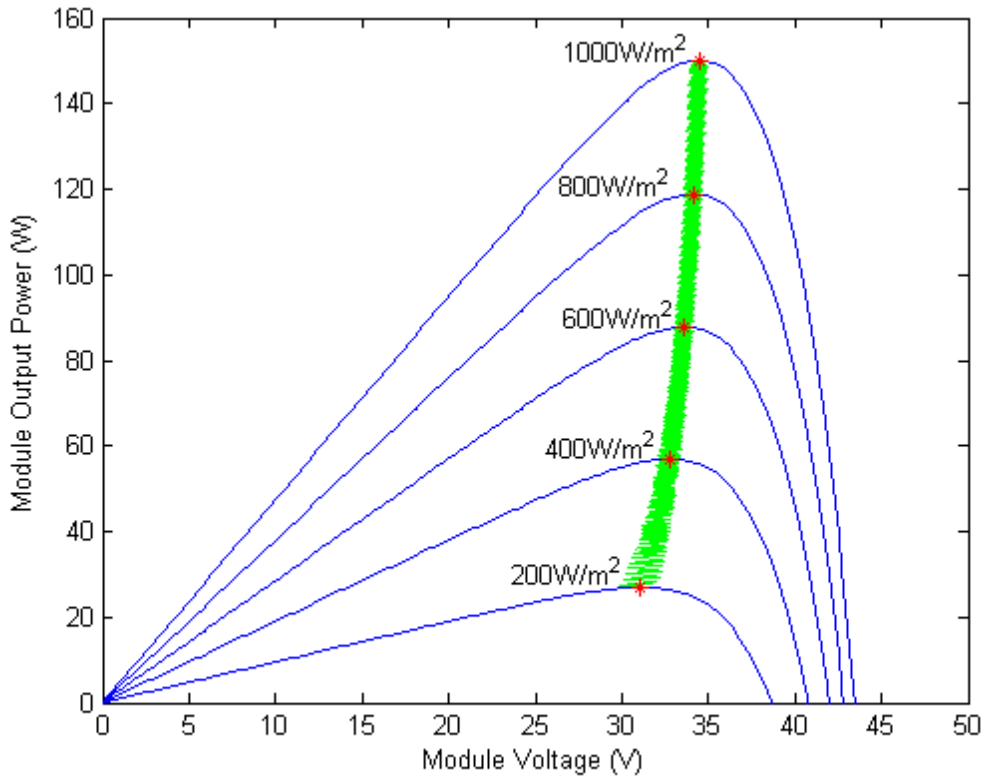

(a) PV Power vs. Voltage

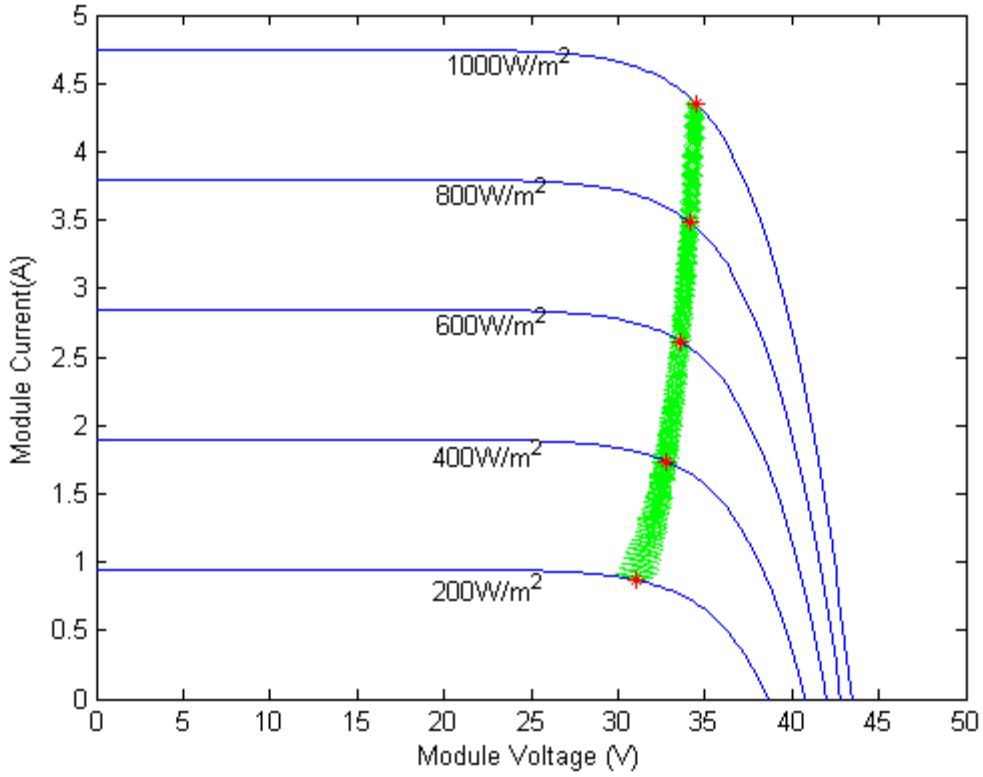

(b) PV Current vs. Voltage

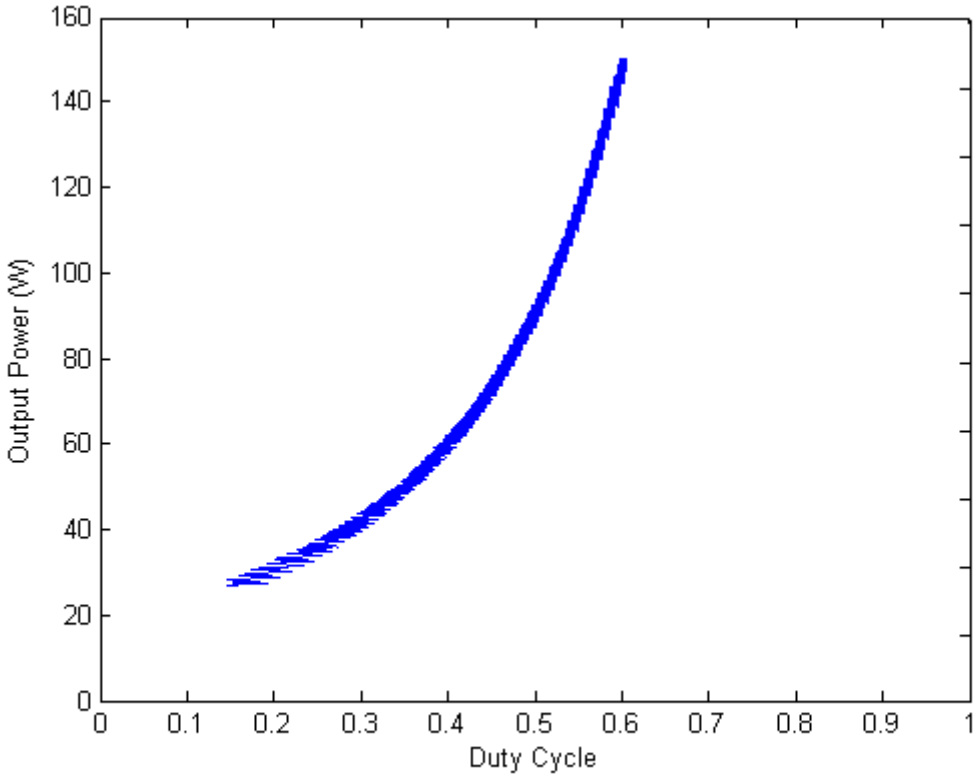

(c) Output Power vs. Duty Cycle

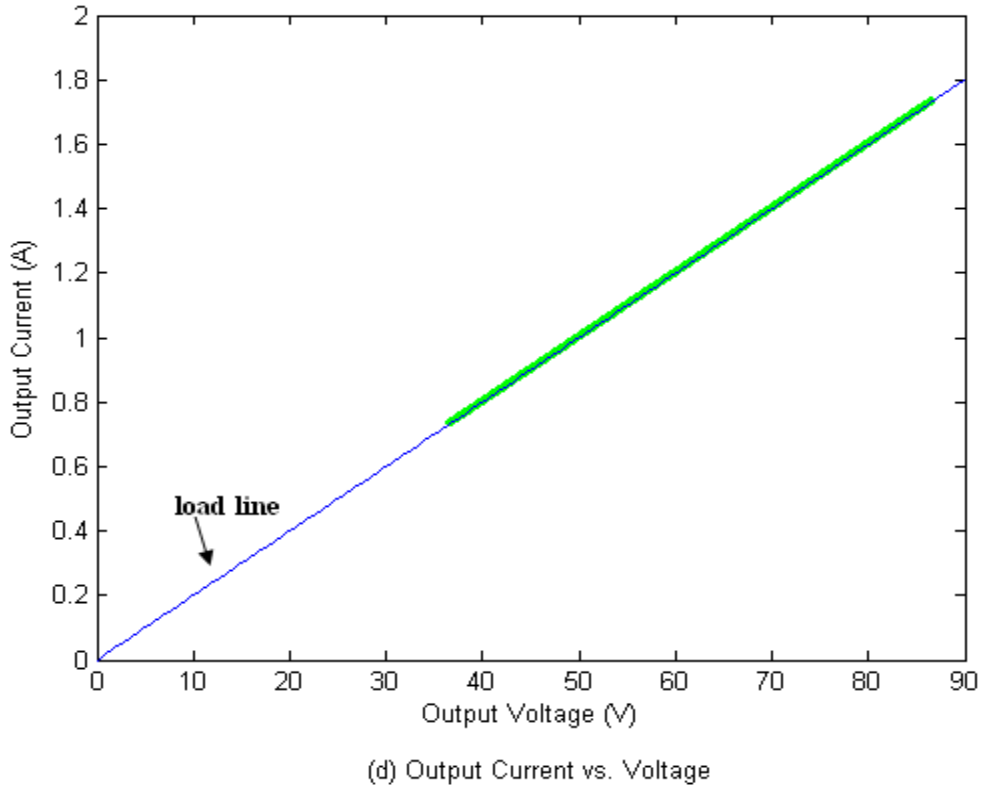

(d) Output Current vs. Voltage

Figure 4-15: MPPT simulations with the resistive load of 50Ω (200 to 1000W/m^2, 25°c).

4.9.4- System with MPPT vs. direct-coupled system:

To see the results of using MPPT in our system and how it increase the efficiency by extracting the maximum power from the PV module, a comparison is made between the system with MPPT and the direct coupled system. The irradiance data used here are the measurements of a sunny day in Bechar, Algeria. The total electric energy produced during a 12-hour period is calculated and tabulated in Table 4-4.

	With MPPT	**Without MPPT**
Total Energy (simulation)	**1.0607 kW**	**342.2825 W**
Total Energy (theoretical max)	**1.0831 kW**	**1.0831 kW**
Efficiency	**97.93 %**	**31.60 %**

Table 4-4: Energy production and efficiency of PV module with and without MPPT.

The results show that the PVG system without MPPT has poor efficiency (31.60 %) because of mismatching between the PV module and the resistive load.

On the other hand, it shows that the system with MPPT can utilize more than 97 % of PVG capacity.

If we change the value of the load to 60Ω, the limit of 86.7V will be exceeded during the increasing irradiance. The output protection maintains the voltage around 86.7V. Figure 4-16 (a) shows that the PVG is not operating at the MPP and sending the power less than the maximum after the irradiance reaches at a little over 800W/m^2, and as we said previously, this result indicates the importance of selecting an appropriate size of load, thus it can fully utilize the total capacity of PV module or array.

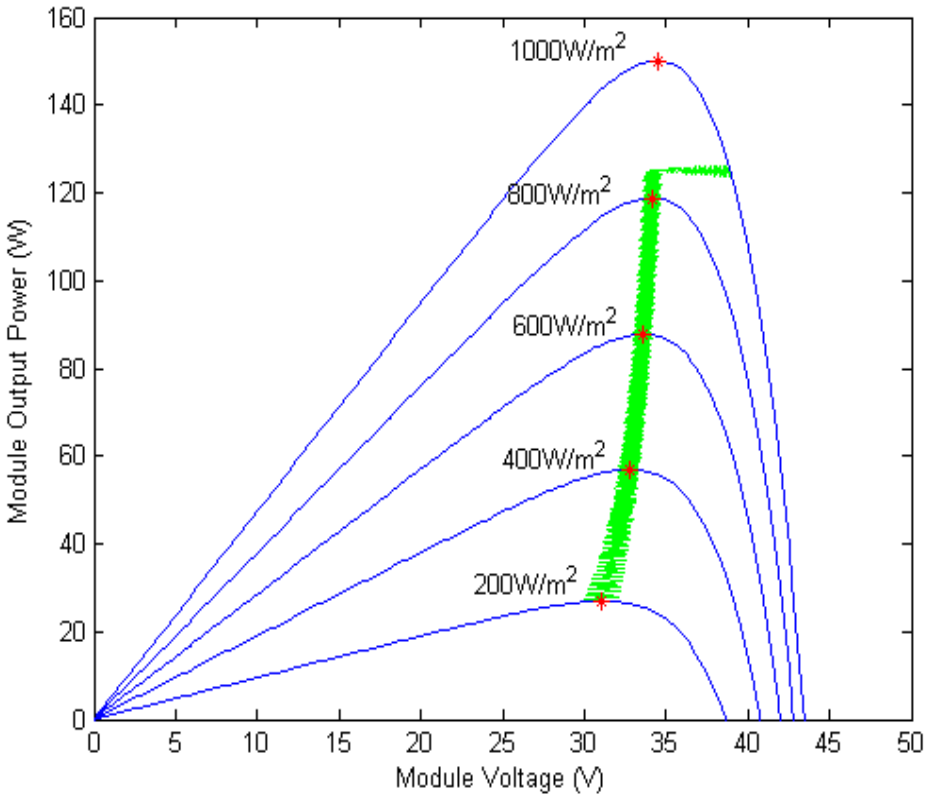

(a) PV Power vs. Voltage

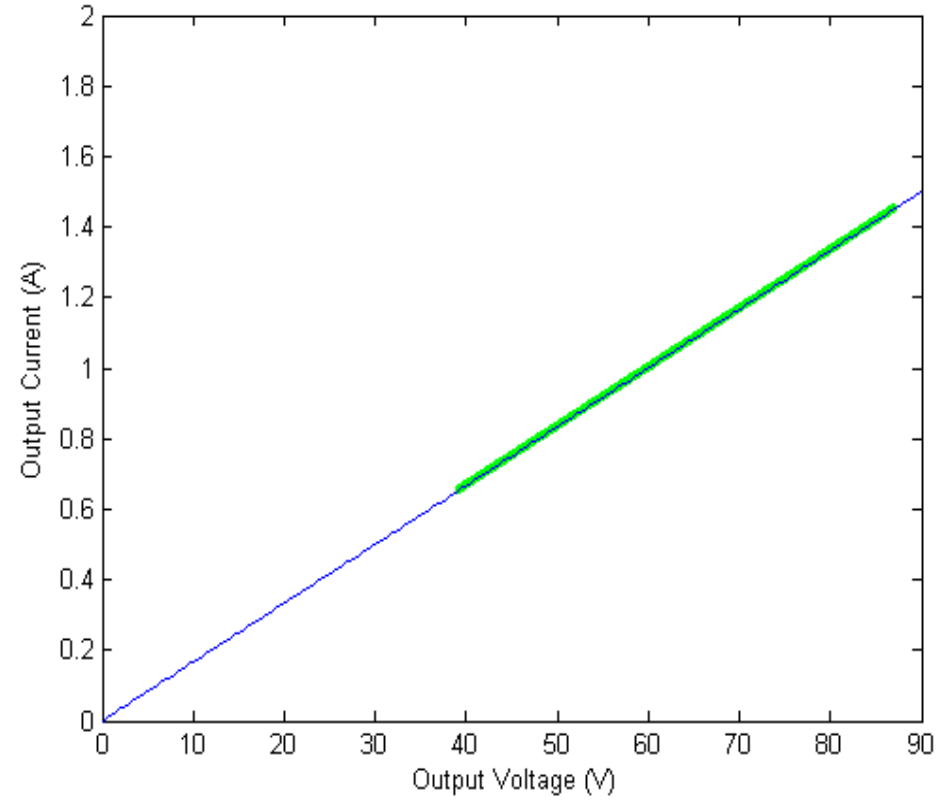

(b) Output Current vs. Voltage

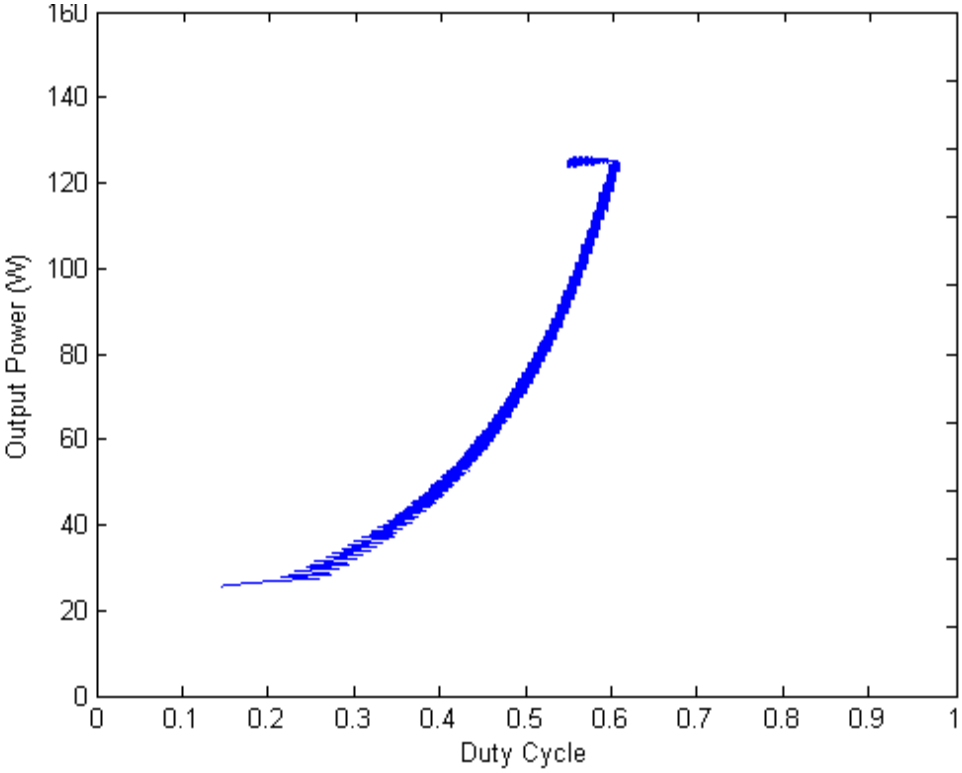

(c) Output Power vs. Duty Cycle

Figure 4-16: Output protection & regulation for 60Ω load.

4.10- CONCLUSION:

Comparative tests for the two MPPT algorithms, the perturbation and observation (P&O) algorithm and the incremental and conductance (IncCond) algorithm using actual irradiance data in the two different weather conditions have been undertaken. The IncCond algorithm shows slightly better performance in terms of efficiency compared to the P&O algorithm under cloudy weather conditions. Even a small improvement of efficiency could bring substantial savings if the system is large. However, it could be difficult to justify the use of IncCond algorithm for small low-cost systems as the cost and availability are the two major aspect of system design and the IncCond algorithm will require four sensors more than the P&O algorithm and also it need more control loops.

A comparative study of the PV system with resistive load with MPPT vs. direct-coupled system has been undertaken. The results show that the system with MPPT can utilize more than 97 % of PVG capacity. On the other hand the system without MPPT has poor efficiency (31.60 %).

.

Chapter 5: MPPT for water pumping system.

5.1- INTRODUCTION:

MPPT systems are used with non linear source for which a max power point exists for any given operation condition.

This is a case for PVG used to power a motor pumping system as described in the present chapter.

5.2- PHOTOVOLTAIC PUMPING SYSTEM:

Safe drinking water is an important need for the population around the word, in developing countries it is still a problem to bring water for all population. To overcome this problem many water pumping programs are made [2]. Photovoltaic power source is used for water pumping systems and it is the most promising area of PV applications.

PV pumping system is used to ensure water supply in remote areas because no electricity supply is available.

The use of water pumps fed by photovoltaic system has many advantages such as low maintenance, ease of installation and reliability. However, two main obstacles for using solar energy are exist, the high initial cost and the very low PV cell conversion efficiency [27].

Many studies have been done on ways of sizing, matching and adapting PV pumping systems. To optimize such installation, the choice of the drive system which suits the PV source, type of pumps to use and ways to control the whole system must be studied [28].

A typical PV pumping system consists of photovoltaic cell array, a power conditioner and the load. Also other accessories such as energy storage (batteries), water storage, cabling, transducers and protection are needed.

5.3- SYSTEM CONFIGURATIONS OF PV PUMPING SYSTEM:

Photovoltaic water pumping system has different system configurations:

- The first configuration is the directly coupled system, where a PV array is directly coupled to a DC motor and a pump. Such system is simple and reliable, but it does not operate continuously at its optimum point due to the continuous variation of solar radiation.

- The second configuration is PV pumping system with DC motor using maximum power point tracking (MPPT) to improve the efficiency of the system.

- The third configuration is PV pumping system with AC motor using maximum power point tracking (MPPT). However, in this case some extra conditioning circuit is needed.

5.4- POWER CONDITIONING STAGE:

The power conditioning stage mainly consist of a DC/DC converter which can be step down or step up or step down/step up converter.

If an AC motor is used for PV pumping system, an inverter must be included in order to perform the DC/AC conversion stage.

5.5- PHOTOVOLTAIC PUMPING SYSTEM USING A DC MOTOR:

Direct coupling of series, shunt, and separately excited DC motor PV pumping systems can be used. Separately exited and permanent magnet DC motors are more suitable for PV pumping systems. PM motors features high level dynamics, fast response, and high efficiency [4]-[28]-[31].

For better adaptation of the load to the source, MPPT technique is used to maximises the output power drawn from the PV generator and therefore improves the performance of the whole system as well.

5.5.1- I-V characteristic of DC motor:

The PM motors are well suited for PV pumping system; Figure 5-1 shows a simplified model of a PMDC motor. When the motor rotating generates a back emf, E is proportional to the angular speed (*w*) of the rotor. The DC voltage equation for the armature circuit is:

$$V = I * R_a + K * \omega \quad (5.1)$$

Where: R_a is the armature resistance.

The back emf is $E = K * \omega$ where: K is the constant, and ω is the angular speed of rotor in rad/sec.

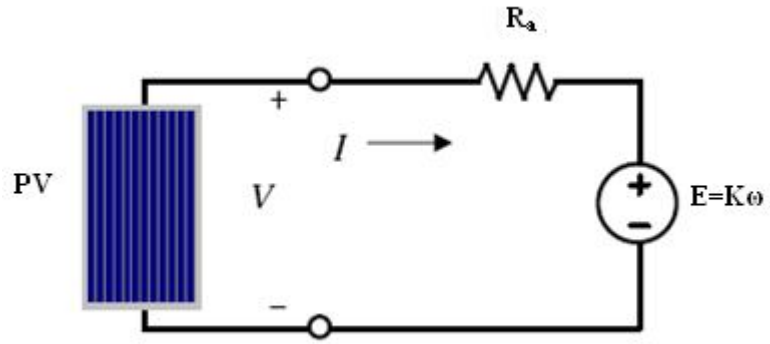

Figure 5-1: Electrical model of permanent magnet DC motor.

Figure 5-2 [4]-[32] shows a typical current-voltage relationship (I-V curve) of a DC motor. Applying the voltage to start the motor, the current rises rapidly with increasing voltage until the current is sufficient to create enough starting torque to overcome static friction and get motor rotating. At start-up (ω = 0), there is no effect of back emf, therefore the starting current builds up linearly with the slope of $1/R_a$ on the I-V plot as shown in Figure 5-2. Once it starts to run, the back emf takes effect and makes the current rate of rise slower with increasing voltage.

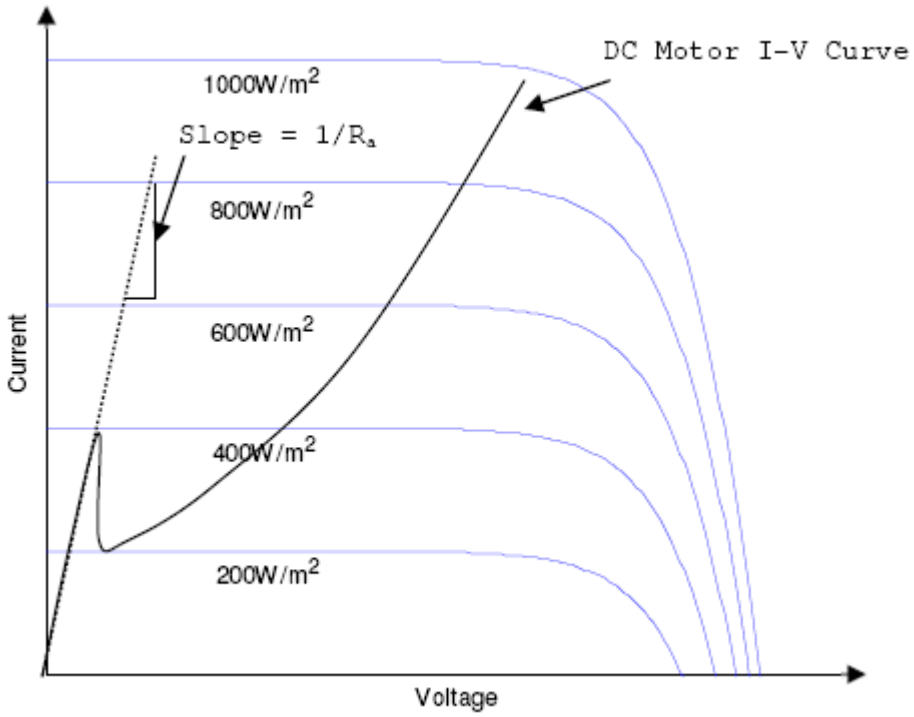

Figure 5-2: PV I-V curves with varying irradiance and a DC motor -pump I-V curve.

Under steady state operation point when we have a direct coupled PV pumping system with a DC motor, it is seen that the intersection between the I-V characteristics of the motor and the I-V characteristic of the PV generator is not at the optimum point as shown in figure 5-2. For this example, the water pumping system would not start operating until irradiance reaches at 400W/m^2. Once it starts to run, it requires as little as 200W/m^2 of irradiance to maintain the minimum operation. This means that the system cannot utilize a fair amount of morning insolation because there is insufficient starting torque. Also, when the motor is operated under the safe condition for a long time, it may result in shortening of the life of the motor due to input electrical energy converted to heat rather than to mechanical output.

For the PV source the power produced at the MPP is relatively low-current and high-voltage which is opposite of those required by the pump motor, so the MPPT is used to overcome this mismatching and obviously increase the efficiency by converting the power into high-current and low-voltage which satisfies the pump motor characteristics. The MPPT could start the pump motor at 50W/m^2 of irradiance.

5.5.2- Pump:

The pump converts input kinetic power into fluid output power. The output power is represented by the delivery of the pump in terms of flow-rate and head.

The most used pumps are [2]-[32]:

- Centrifugal pumps, which are more suitable for small to medium head, have their power output increased with speed accordingly.

- Positive displacement pumps, suitable for deep wells have a flow-rate which is normally independent of head. On the other hand, have a water output proportional to speed.

5.6- STEADY STATE PERFORMANCE OF PV PUMPING SYSTEM USING A DC MOTOR-PUMP:

The proposed system is very simple and consists of a single PV module, a maximum power point tracker (MPPT), and a DC water pump.

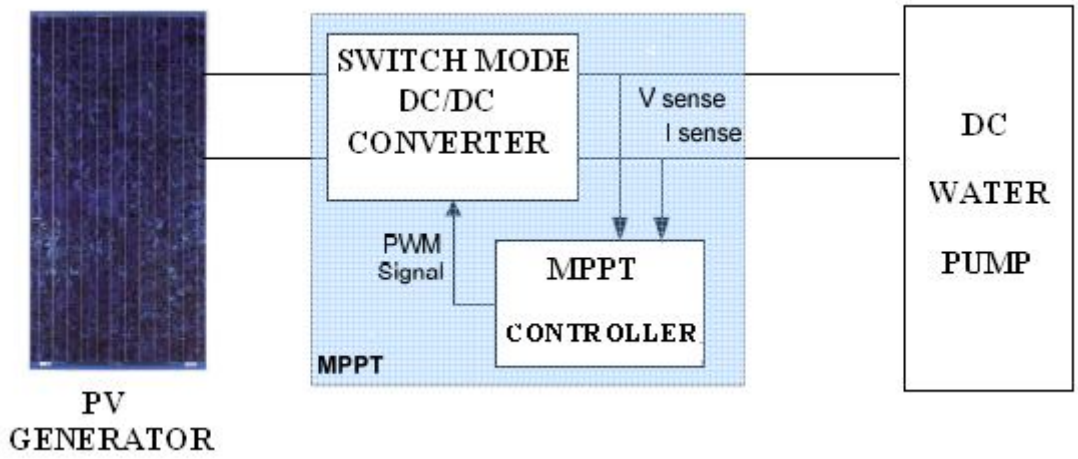

Figure 5-3: block diagram of the proposed PV water pumping system.

The DC water pump chosen here for its size and cost is the Kyocera SD 12-30 submersible solar pump. It is a diaphragm-type positive displacement pump equipped with a brushed permanent magnet DC motor and designed for use in standalone water delivery systems,

specifically for water delivery in remote locations. Flow rates up to 17.0L/min and heads up to 30.0m (100ft.) [33]. The typical daily output is between 2,700L and 5,000L. The rated maximum power consumption is 150W. It operates with a low voltage (12~30V DC), and its power requirement is as little as 35W.

The flow rate of water in positive displacement pumps is directly proportional to the speed of the pump motor, which is governed by the available driving voltage. They have constant load torque to the pump motors, and it is expressed by the total dynamic head in terms of its equivalent vertical column of water [33].

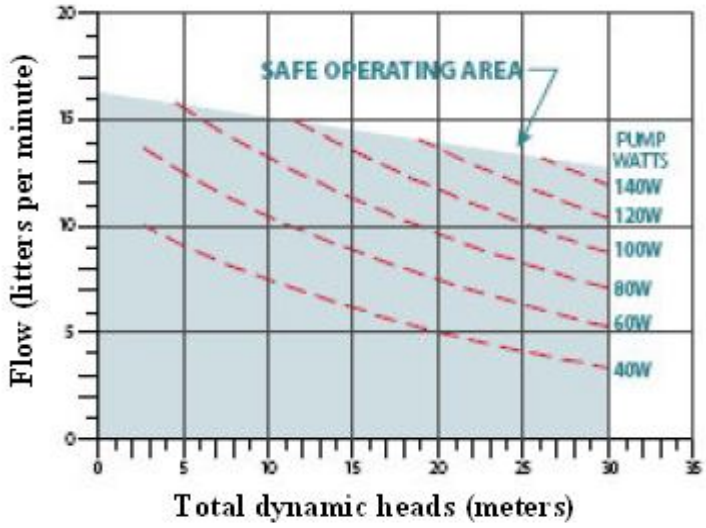

Figure 5-4: Kyocera SD 12-30 water pump performance chart [33].

To model the permanent magnet DC motor we apply a constant field. Since the water pump is a positive displacement type, the load torque is also constant. The value is selected to draw the maximum power of 150W at the maximum voltage of 30V. The parameters of DC machine, which correspond to the actual pump-motor are unknown, thus they are chosen by modification of the default values and estimation from other references.

The DC motor-pump load is represented by a variable resistance that changes with the variations of the voltage source as expressed by equation (5.2). Then, the change of load resistance (R_{load}) is observed, as shown in Figure 5-5. The plot data are transferred to MATLAB, and the cubic curve fitting tool in MATLAB provides the equation of the curve shown below:

$$R_{load} = 9.5 \times 10^{-5} \cdot V_o^3 - 8.7 \times 10^{-3} \cdot V_o^2 + 0.37 \cdot V_o + 0.2 \qquad (5.2)$$

Where: V_o is the output voltage of the converter. This equation characterizes the DC pump motor, and MATLAB uses it in the simulations.

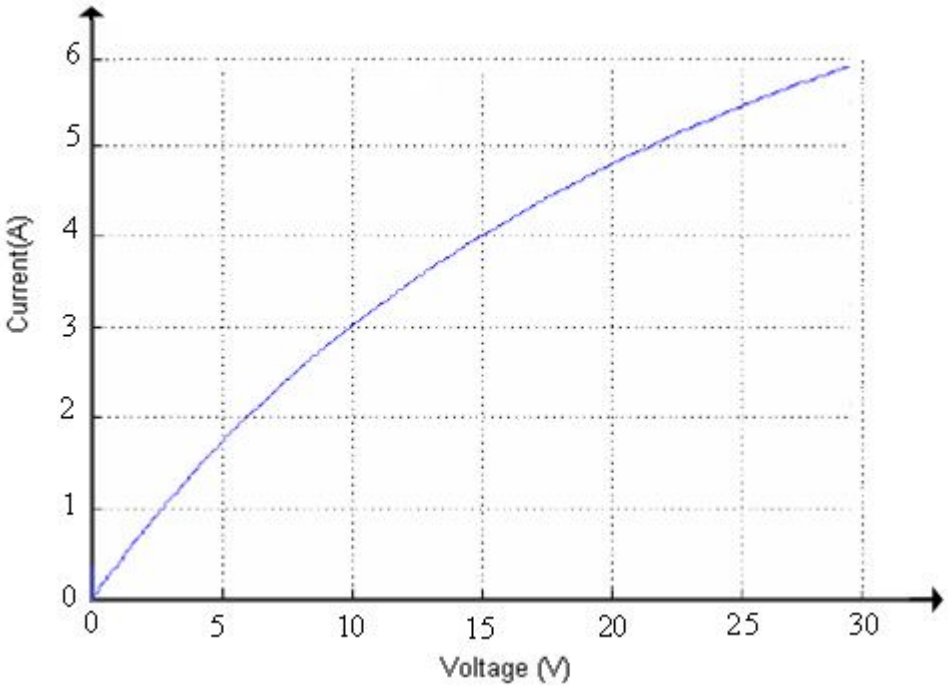

Figure 5-5: SIMULINK plot of $1/R_{load}$.

The simulation is carried out in a similar manner as that for the resistive load. The irradiance is increased linearly from 20w/m^2 to 1000w/m^2 with the same rate of 0.3w/m^2 per sample. However, instead of using a boost converter for the MPPT; a buck-boost converter is used for water pumping system.

For water pumping systems, the output voltage needs to be stepped down to provide a higher starting current for a pump motor. The buck converter is the simplest topology and easiest to understand and design, however it exhibits the most strict destructive failure mode of all configurations; the buck converter provide a high current for the output, when the RMS value of this current squared and multiplied by the equivalent series resistance (ESR) of the affected capacitor (the capacitor is the weakest part in the circuit), results in heating. Excessive heating can reduce component lifetime and even trigger a catastrophic failure [34].

Also the buck converter cannot operate at the MPP under all conditions. Thus, the additional boost capability can increase the overall efficiency.

Figure 5-6 (a) and (b) show that the locus of operating point staying close to the MPPs throughout the simulation. Figure 5-6 (c) shows the relationship between the output power of converter and its duty cycle. Figure 5-6 (d) shows the current and voltage relationship of converter output which is equal to the DC motor load.

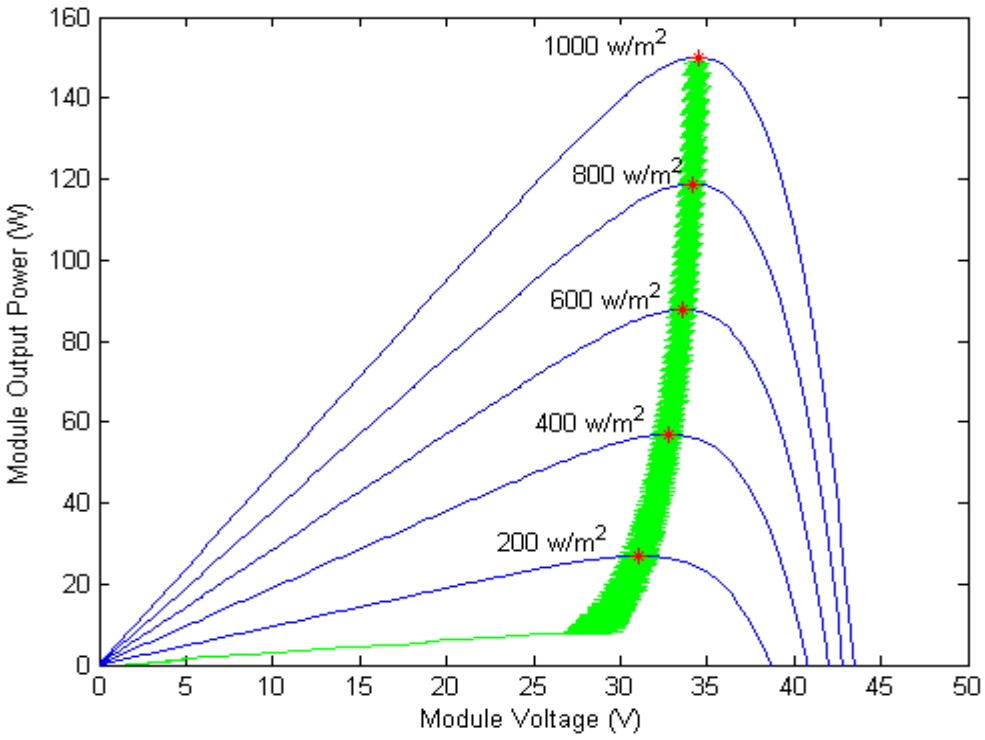

(a) PV Power vs. Voltage

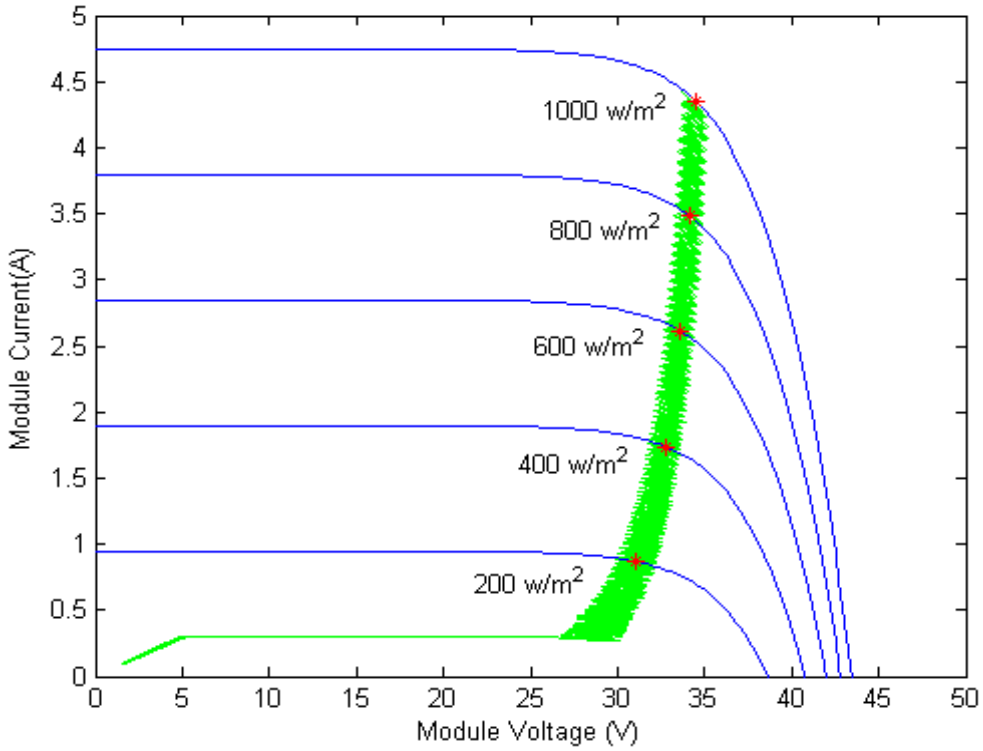

(b) PV Current vs. Voltage

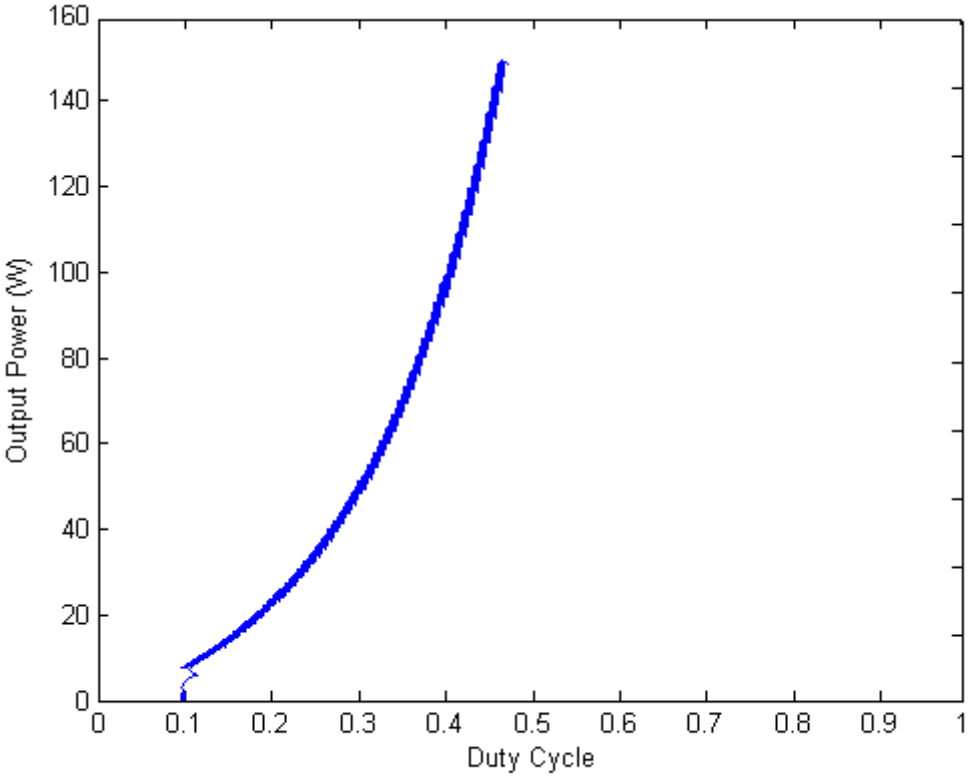

(c) Output Power vs. Duty Cycle

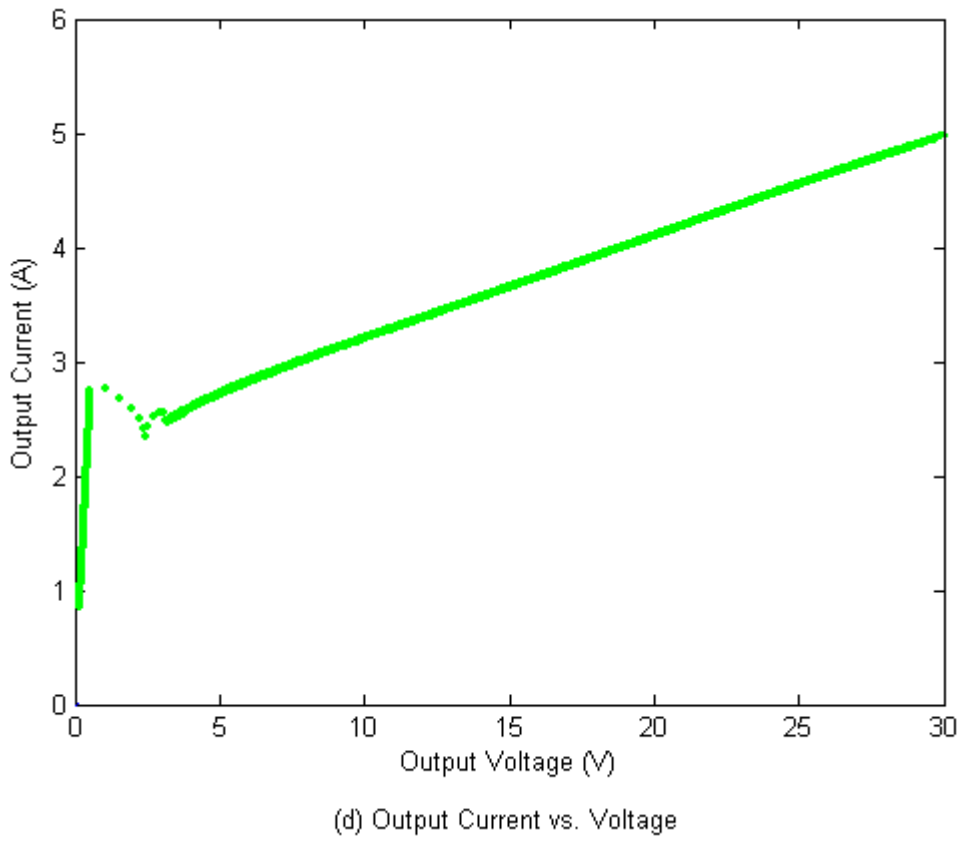

(d) Output Current vs. Voltage

Figure 5-6: MPPT simulations with the DC pump motor load (20 to 1000W/m^2, 25^oC).

Figure 5-6 (d) shows that the output current rises rapidly with increasing voltage until the current is sufficient to create enough torque to start the motor. Once it starts to run, the back emf takes effect and drops the current, therefore the current rises slowly with increasing voltage. It is observed that those characteristics are the same as the characteristics of the DC motor -pump I-V curve shown in figure 5-2; therefore it can be concluded that the simple MATLAB model of DC motor used here is valid.

It is said earlier that the buck-boost converter is more efficient then the buck converter for the pumping system due to the boost function, figure 5-7 show the simulation of the same system but with the buck converter. It is clearly seen that the buck converter cannot truck the MPP for all conditions.

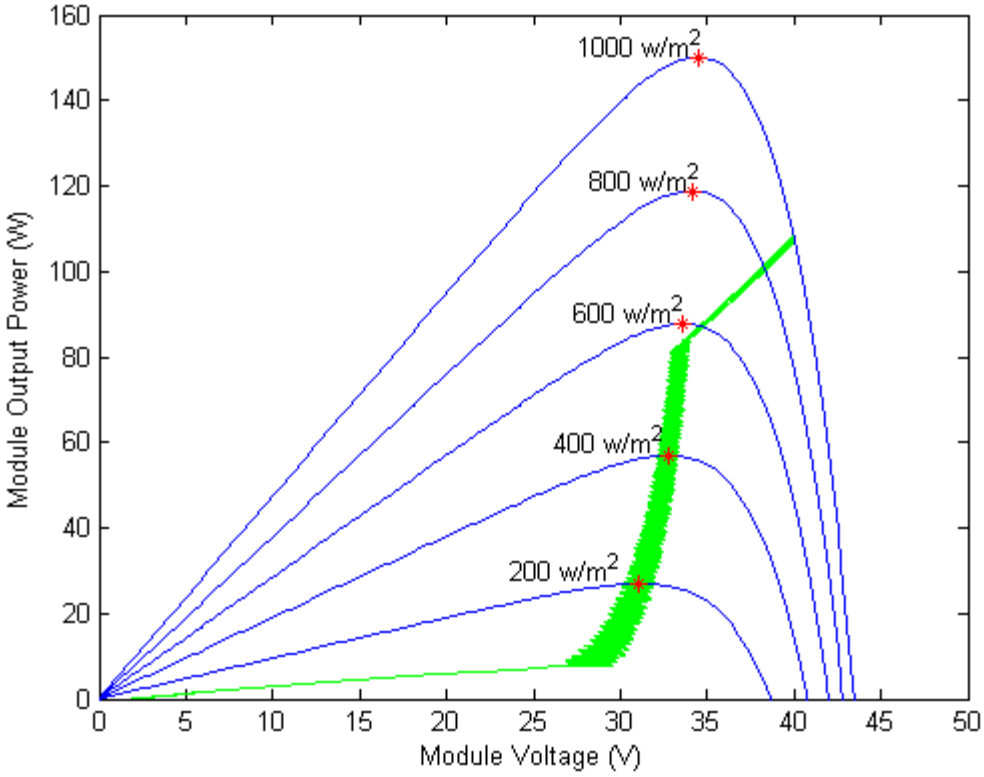

(a) PV Power vs. Voltage

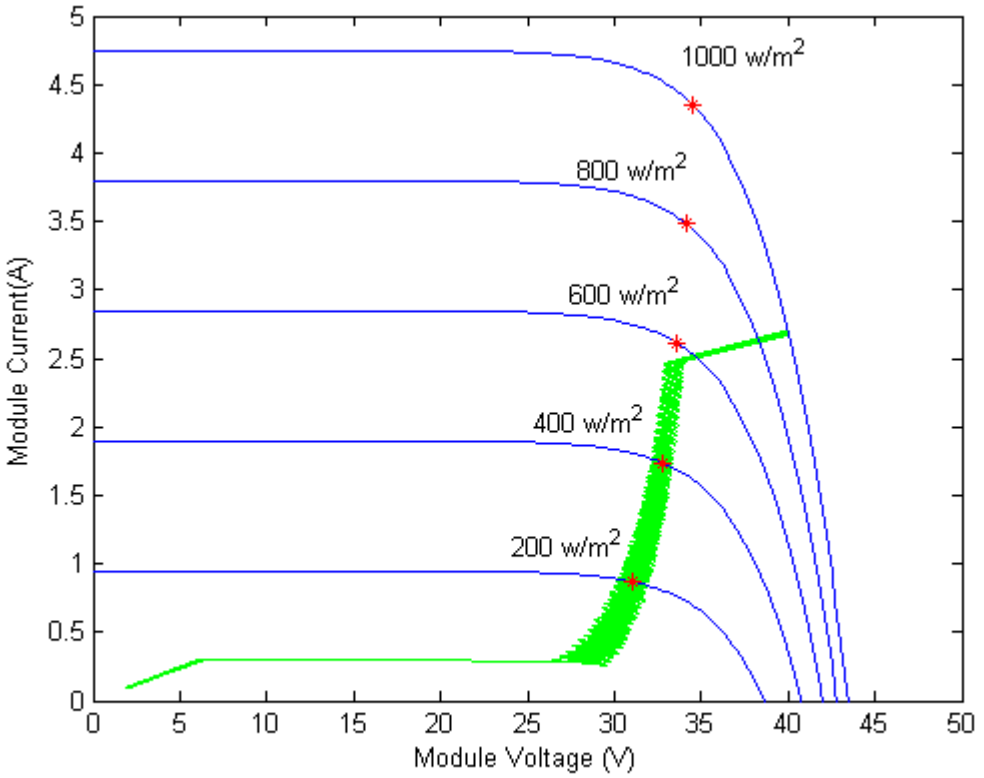

(b) PV Current vs. Voltage

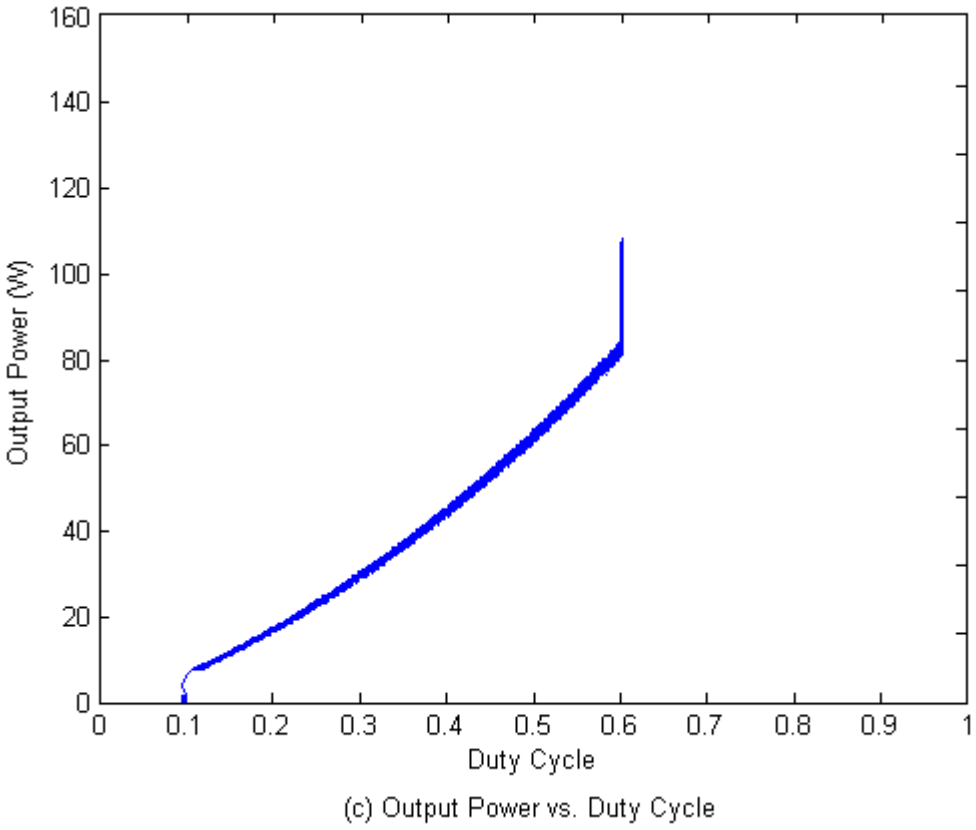

Figure 5-7: MPPT simulations with the DC pump motor load with a buck converter (20 to 1000W/m^2, 25^{o}C).

5.7- PUMPING SYSTEM WITH DC MOTOR USING MPPT vs. DIRECT-COUPLED SYSTEM:

The PV water pumping system with MPPT simulated in the previous section is compared with the direct-coupled PV water pumping system without MPPT. The irradiance data used here are the measurements of a sunny day in Bechar, Algeria; introduced in Section 4.8. The total electric energy produced during a 12-hour period is calculated and tabulated in Table 5-1.

	With MPPT	Without MPPT
Total Energy (simulation)	**1.0682 KW**	**0.6605 KW**
Total Energy (theoretical max)	**1.0831 KW**	**1.0831 KW**
Efficiency	**97.26 %**	**60.98 %**

Table 5-1: Energy production and efficiency of PV module with and without MPPT.

The results show that the PV water pumping system without MPPT has poor efficiency (60.98 %) because of mismatching between the PV module and the DC pump motor load.
On the other hand, it shows that the system with MPPT can utilize more than 97 % of PV capacity. Assuming a DC-DC converter has efficiency more than 90 %, the system can increase the overall efficiency by more than 25 % compared to the system without MPPT.

Another comparison of the two systems can be done in terms of flow rates and total volume of water pumped. As shown in Figure 5-5, the flow rate of Kyocera SD 12-30 water pump is proportional to the power delivered. When the total dynamic head is 30m, the flow rate per watt is approximately 86.7cm^3/W·min. The minimum power requirement of pump motor is 35W [33]; therefore as long as the output power is higher than 35W, it pumps water with the flow rate above. Using the same test condition, the flow rates of pump are obtained from the MATLAB simulations and shown in Figure 5-8.

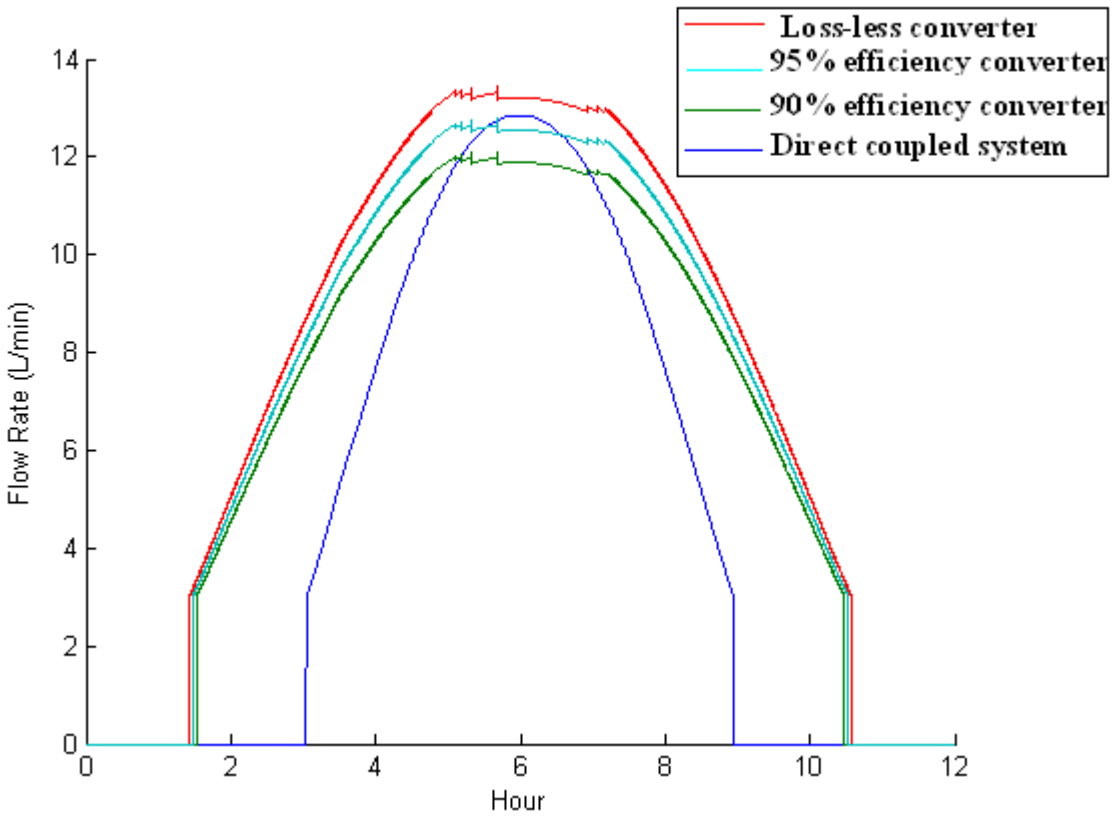

Figure 5-8: Flow rates of PV water pumps for a 12-hour period Simulated with the irradiance data of a sunny day (total dynamic head = 30m).

It is clearly seen that the performance of the pumping system is improved if the output power of the photovoltaic generator is optimal. As shown in figure 5-8, the direct-coupled PV water pumping system performance is lower compared to the system with MPPT even if the converter is 90 % or 95 % efficiency, for the first two hours the pump stays at rest while the same system with MPPT is already pumping water. Similarly, it goes idle nearly two hours earlier than the system with MPPT in the afternoon. The flow rate of water is also lower throughout the operating period.

Around the middle of the day, we observe that the direct-coupled system has a better performance than the system of the 90 % efficiency converter and approximately the same performance as the 95 % efficiency converter due to the high irradiance at this time.

The total volume of water pumped for the 12-hour period is also calculated for both systems. The results are tabulated below.

	With MPPT			Without MPPT
	Loss-les converter	**95 % Efficiency converter**	**90 % Efficiency converter**	
Total volume pumped for 12 hours (simulation).	**5.3746 m^3**	**5.0892 m^3**	**4. 8033 m^3**	**3.2708 m^3**

Table 5-2: Total volume of water pumped for 12 hours simulated with the irradiance data of a sunny day (total dynamic head = 30m).

The results show that MPPT offers significant performance improvement. It enables to pump up to 64 % more water than the system without MPPT. Even if the efficiency of converter is set to 90%, it can still pump 46 % more water than the system without MPPT. The results show also that 5 % improvement in the converter efficiency can increase the pumped water approximately by 286 L per day which is approximately 5 % of the volume of pumped water.

5.8- PHOTOVOLTAIC PUMPING SYSTEM USING INDUCTION MOTOR:

Water pumping system using induction motors can be very attractive; such a system is more reliable and requires much less maintenance as compared to DC driven system. The only disadvantage of the induction motor based PV pumping system is the increased cost of more complex control circuit.

The simplest and cheapest type of AC motor is the squirrel-cage induction motor. Its low cost and rugged construction make it the most commonly used motor for PV applications [37].

5.8.1- General Description:

Figure 5-9 shows the bloc diagram of photovoltaic pumping system with induction motor, the whole system is composed of a PV generator, a power dc–dc adapter, a natural

sinusoidal PWM voltage source inverter and a squirrel cage induction motor driving a centrifugal pump.

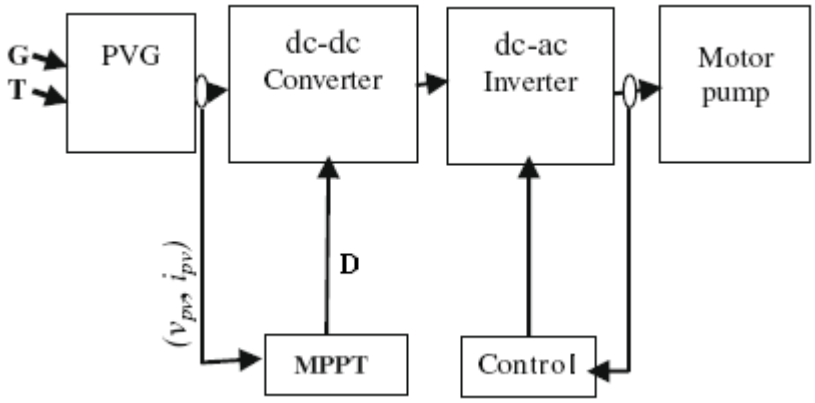

Figure 5-9: PV pumping scheme structure.

- **DC-DC Converter:**

The DC-DC converter is an impedance adapter; it is used to force the PV array to deliver the maximum power to the load.

- **The Inverter:**

The inverter is used to convert the dc voltage into three-phase ac voltage to supply the induction motor driving the pump. The output voltage of the inverter is sinusoidal with variable amplitude and frequency according to the solar radiation. The current is modulated sinusoidally to obtain a high efficiency.

- **Induction Motor:**

AC motors are generally used for medium- to high-power demand applications. Induction motors with squirrel-cage rotors are available in either single phase or three phases. An induction motor operates at nearly constant speed. However, the speed of an induction motor can be varied with electronic converters (inverters). Using inverters to control induction motor speeds is highly efficient over wide speed and load ranges [2].

- **Pump:**

The pump represents the mechanical load of the induction motor and its size determins the power ratings of the other system components, including the necessary PV peak power [38].

Submersible centrifugal pumps are best for high flow rates (25–100 l/min) and medium heads (10–30 meters). They are used for PV pumping system with induction motor [37].

The flow head characteristic of a centrifugal pump can be given by the following expression [37]:

$$H = a_1\omega^2 + a_2\omega Q + a_3 Q^2 \quad (5.3)$$

Where a_1, a_2 and a_3 are geometric parameters characterizing the pump.

Q: Flow rate of the pump (m^3/h).

H: Total height (m).

ω: The motor speed.

5.8.2- Control Techniques:

Recent research has focused on achieving the most energy efficient control algorithms for AC machine-pump loads in which MPPT tracking and maximum motor and pump efficiency are the system performance targets [29].

Alike DC motors, the induction motor characteristics severely affected by the non linear characteristic of the PV source. So two optimisation techniques are used [29]:

- The PV generator maximum power is tracked.
- The induction motor is controlled to achieve maximum efficiency.

➢ MPPT:

We can use the MPPT on an induction motor-PV pumping system in different stages, In the DC-DC converter or in the inverter [27]-[36].

When the inverter with MPPT is used (without a DC-DC converter stage), the available PV power is utilized more efficiently. In this case, the inverter acts as both a variable-frequency source to control the output of the PVG and the water pump [2]-[29]-[39].

➢ PWM Controller:

To optimize the PV pumping system, the induction motor has to be controlled to achieve maximum efficiency. Two control techniques are used: the scalar control and the vector control.

Different studies show that the “V/f” law is sufficient to control pumping systems, especially as this type of applications does not require high dynamic performance [40].

The conventional V/f control operation of the system will have to be modulated according to the climatic conditions in order to ensure a maximal PV pumping operation during the day.

5.9- STEADY STATE PERFORMANCE OF A PV PUMPING SYSTEM USING AN INDUCTION MOTOR:

The simulated system consists of the 42 BP solar polycrystalline panel (AEG PC4050), the ideal boost converter, the MPPT control, an inverter and the induction motor-pump load.

5.9.1- PV Generator:

The PV generator consists of 42 modules arranged in three parallel strings with fourteen in each and connected to the dc–dc converter. The maximum power delivered by this PV generator is 2.1 KW. For several climatic conditions (irradiance and ambient temperature), an example of simulated I–V characteristic for the 2100 W photovoltaic plant are given by figure 5-10:

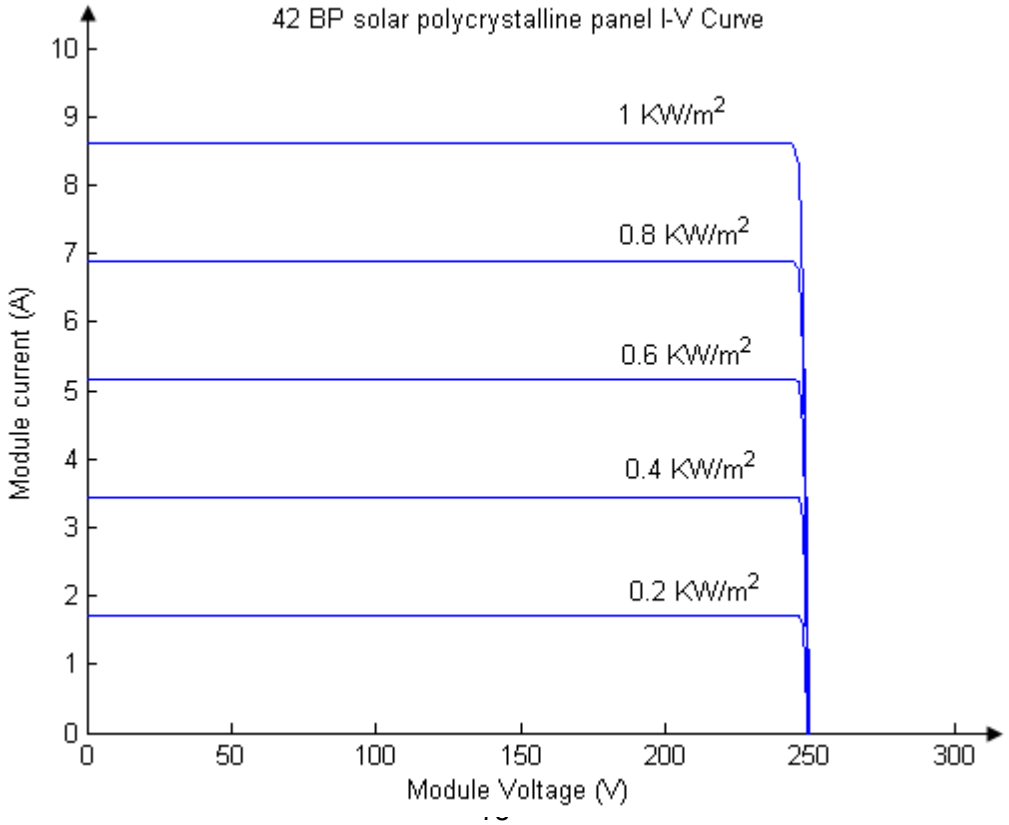

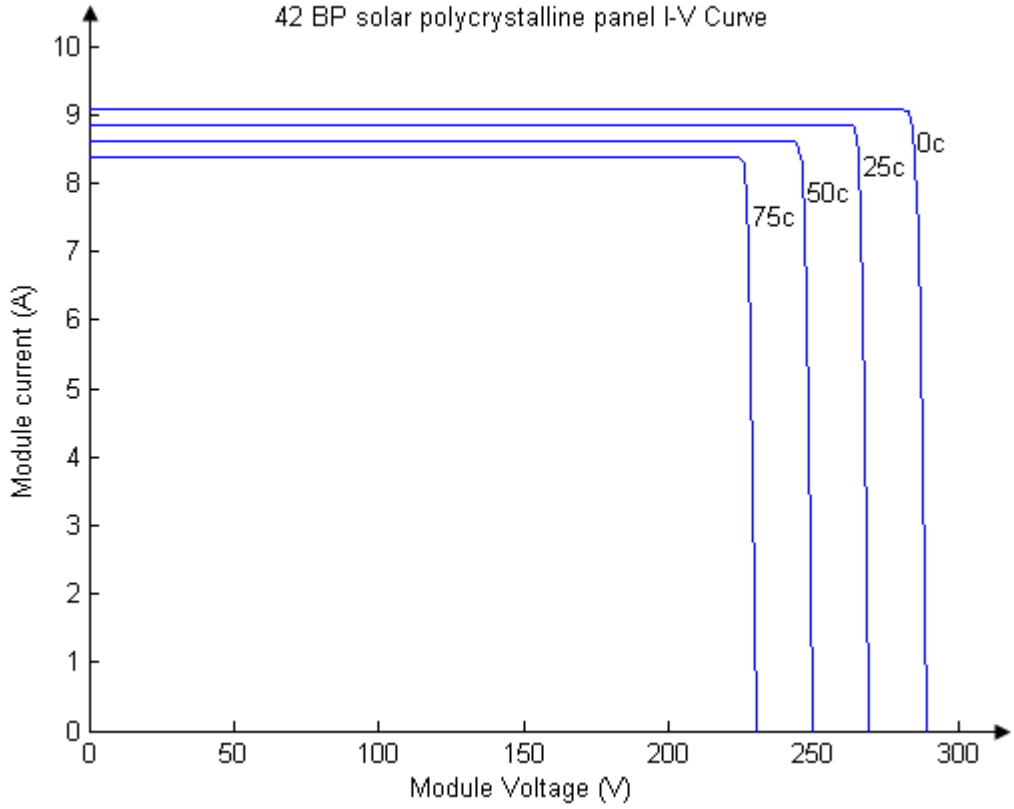

Figure 5-10: I-V curves of 42 BP solar polycrystalline panel at various climatic conditions Simulated with the MATLAB model.

5.9.2- The Induction Motor:

In the simulated PV pumping system, A Squirrel-cage induction motor of 1.5 kW, 220 / 380V, 4 poles, 1420 tr/min, 50 Hz. Rs = 4.85 Ω; Rr = 3.805 Ω; Xs = 2.513 Ω; Xr = 2.513 Ω; Xm = 81.05 Ω ; Rm = 500 Ω is used.

A per phase equivalent circuit model is used for modeling of the induction motor. As shown in figure 5-11, R_s and X_s are the per phase resistance and leakage reactance of the stator winding, R'_r and X'_r are the rotor resistance and reactance referred to the stator. R_m represents the resistance for excitation (or core) loss and X_m is the magnetizing reactance.

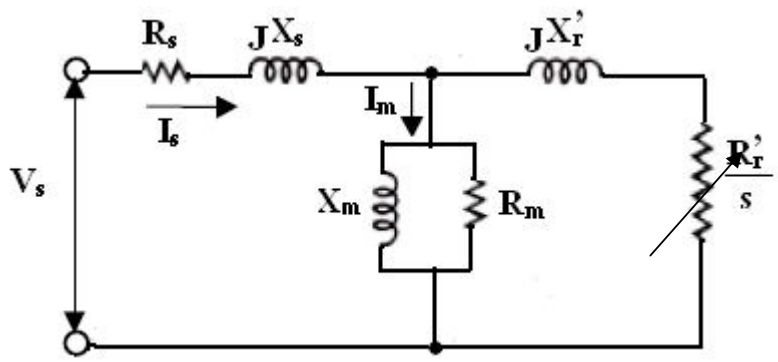

Figure 5-11: circuit model of the induction motor [14].

The equivalent impedance of the induction motor is:

$$Z = Z_s + Z_{RF} \tag{5.4}$$

Z_s: is the Stator impedance (R_s+jX_s).

Z_{RF}: is the equivalent per phase impedance seen by the stator across the motor gap ($Z_r \| Z_m$).

$$Z = Z_s + Z_r \| Z_m \tag{5.5}$$

The Gap power (power passing from the stator to the rotor through the air gap) is:

$$P_g = 3(I_s)^2 R_r / s \tag{5.6}$$

The developed power is:

$$P_d = P_g(1 - s) \tag{5.7}$$

5.9.3- The Inverter:

The dc–ac inverter provides three-phase system of voltages which is variable in amplitude and frequency according to the solar radiation. They vary from 0.1 up to 1 time the rated voltage and frequency. It depends of the loads and climatic conditions [27].

The switching frequency is equal to 2 kHz. The phase voltage is given by the following expression:

$$\begin{bmatrix} v_{as} \\ v_{bs} \\ v_{cs} \end{bmatrix} = \frac{V_{PV}}{3} \begin{bmatrix} 2 & -1 & -1 \\ -1 & 2 & -1 \\ -1 & -1 & 2 \end{bmatrix} \begin{bmatrix} f_{ca} \\ f_{cb} \\ f_{cc} \end{bmatrix} \quad (5.8)$$

With V_{pv} is the input voltage. f_{ca}, f_{cb} and f_{cc} are the PWM control signals.

The V/f ratio can be regulated in a constant or variable way, according to requirements of drive. It varies with the climatic conditions. For example, for lower irradiances, before 09 h: 00 or after 17 h: 00, the inverter frequency is lower than 10 Hz. In order to start or to maintain the functioning of the system the V/f ratio changes instantaneously [29]. The V/f law is defined as [27]:

$$\frac{V}{f} = 1.10^{-11}G^4 - 3.10^{-8}G^3 + 3.10^{-5}G^2 - 1.17.10^{-2}G + 3.92 \quad (5.9)$$

Supposing that the inverter is ideal and the system is balanced and the operation is at steady state, the RMS values of currents and voltages are used in simulations.

5.9.4- Simulation and results:

The simulation is carried out in a similar manner as previously; the perturbation and observation algorithm is used to take out the maximum power from the source (MPPT) by adjusting the duty cycle of the boost converter (to have impedance matching). The irradiance data used here are the measurements of a sunny day in Bechar, Algeria; introduced in Section 4.8. Figure 5-12 (a) and (b) show that the locus of operating point staying close to the MPPs throughout the simulation. Figure 5-12 (c) shows the relationship between the output power of converter and its duty cycle. Figure 5-12(d) shows the current and voltage relationship of converter output.

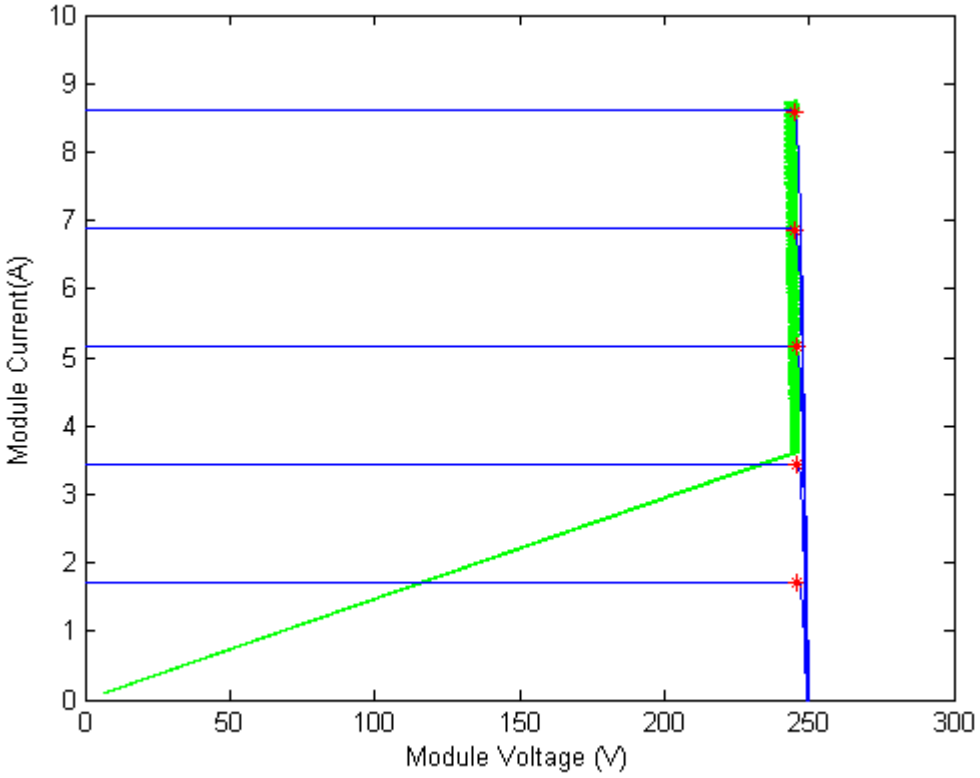

(b) PV Current vs. Voltage

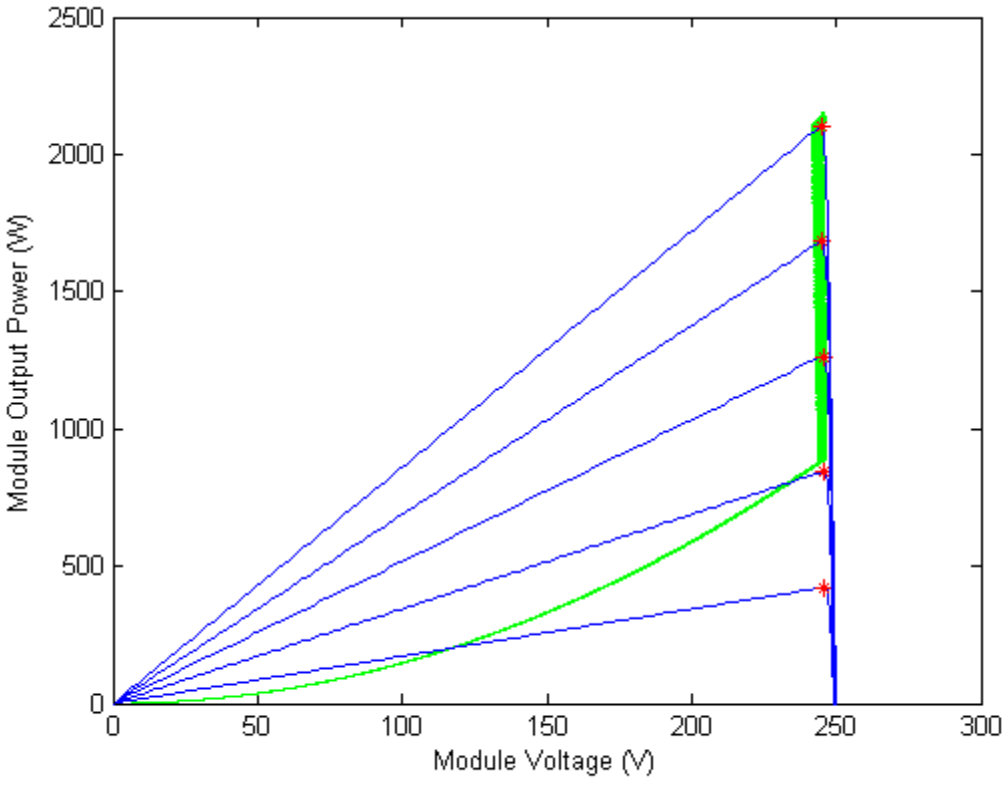

(a) PV Power vs. Voltage

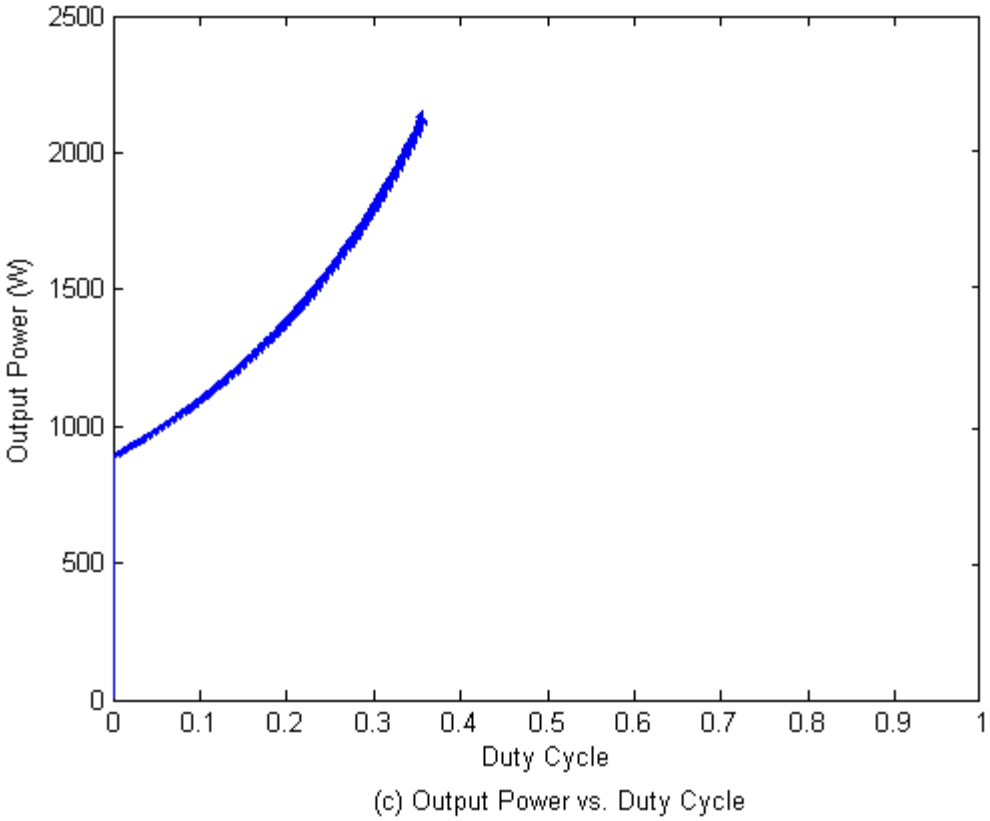

(c) Output Power vs. Duty Cycle

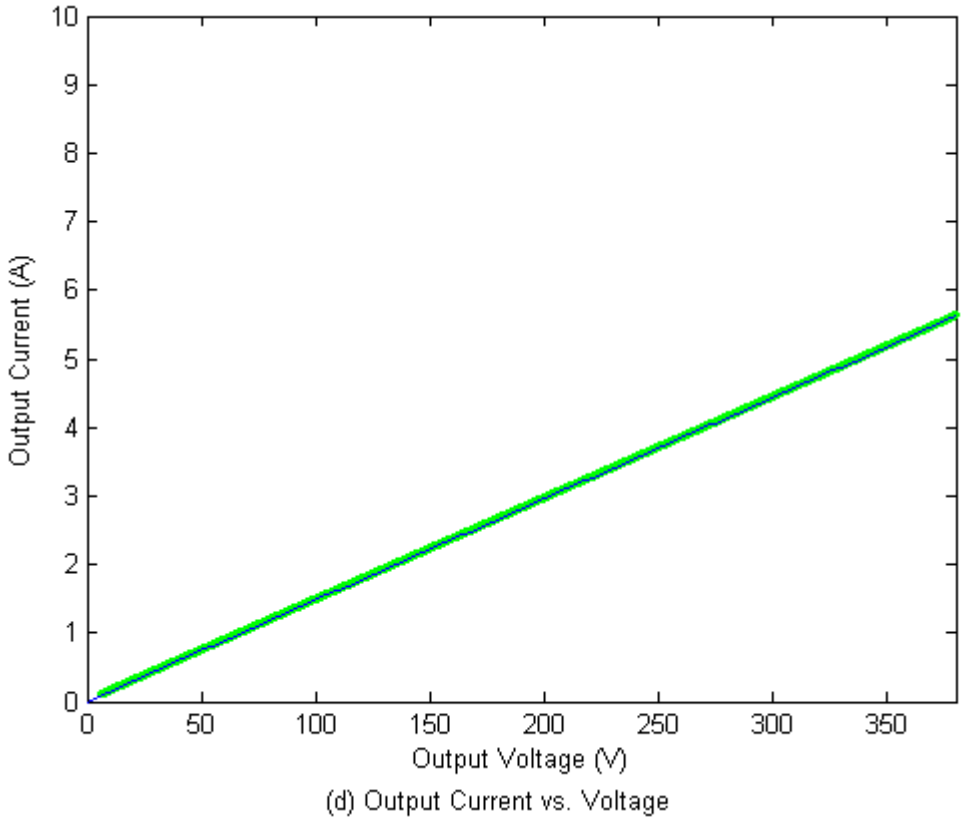

(d) Output Current vs. Voltage

Figure 5-12: MPPT simulations with the induction motor-pump load (20 to 1000W/m^2, 25^{o}C).

Figure 5-13 shows the developed power of the induction motor, the maximum power produced is about 1500W.

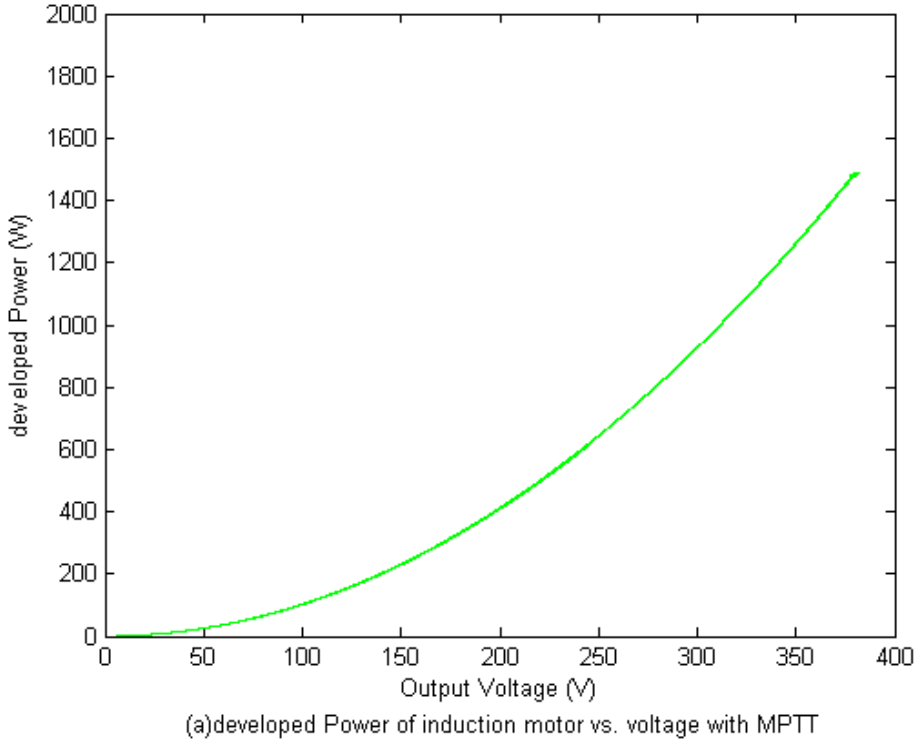

Figure 5-13: the developed power of the induction motor.

The total electric energy produced by the PV panel during a 12-hour period is calculated; also the developed power produced by the induction motor is calculated.

Total Energy (theoretical max)	**15.43 KW**
Total Energy (simulation)	**14.718 KW**
Developed Energy of the induction motor	**10.243 KW**
Efficiency η_1	**95.38 %**
Efficiency η_2	**69.6%**
Efficiency η	**66.38 %**

Table 5-3: Energy production and efficiency of PV pumping system with MPPT.

As we see in table 5-3, η_1 which is the efficiency of the MPPT is very high, about 95.38% and η_2 which is the efficiency of the induction motor is 69.6 % so as a result the total efficiency of the system is 66.38 %.

To see the impact of the MPPT in the efficiency of the system, we do a comparison between the previous system and the same system without MPPT. The results are tabulated in table 5-4:

Total Energy (theoretical max)	**15.43 KW**
Total Energy (simulation)	**8.1522 KW**
Developed Energy of the induction motor	**5.1146 KW**
Efficiency η_1	**55.23 %**
Efficiency η_2	**62.72 %**
Efficiency η	**34.64 %**

Table 5-4: Energy production and efficiency of PV pumping system without MPPT.

The results show that the PV water pumping system without MPPT has poor efficiency (34.64%) because of mismatching between the PV module and the induction motor pump load, the PV module produce only 55.23 % of its capacity. On the other hand, the previous results show that the system with MPPT can utilize more than 95 % of PV capacity.

In reality the electronic circuits like DC-DC converters and DC-AC inverters are not 100 % efficient, diode loss, switching loss in a Power-MOSFET, resistive losses in inductors and capacitors and harmonics degrade the performance of the system.

In practice, the efficiency of DC-DC converter is between 90 to 95 % and the efficiency of the inverter is about 95 %. We can have more realistic results by taking in consideration the system losses.

Figure 5-14 shows a comparison of the developed power of the induction motor for a loss-less converters, a 90 % efficiency converter, and a 95 % efficiency converters and a direct coupled system. From those plots it can be said that the PV pumping system with MPPT gives better performance than the system without MPPT even if the electronic converters are not 100 % efficient. Table 5-5 gives the developed power in 12 hours of each system.

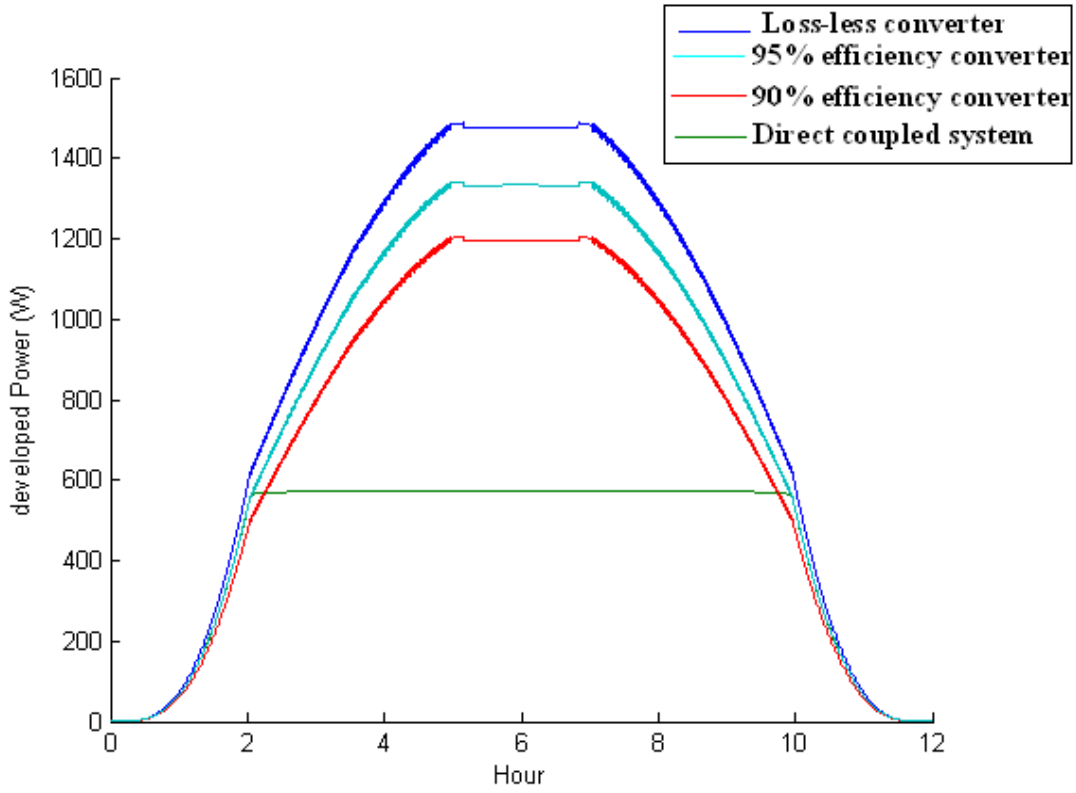

Figure 5-14: the developed power of the induction motor for different converters efficiencies.

	With MPPT			Without MPPT
	Loss-les converter	**95 % Efficiency converter**	**90 % Efficiency converter**	
The developed power for 12 hours.	**10.243 KW**	**9.245 KW**	**8.297 KW**	**5.115 KW**

Table 5-5: Energy production of PV pumping system for different converters efficiencies and direct coupled system.

A further comparison can be made in terms of flow rates and total volume of water pumped per day. As shown in Figure 5-15, the maximum flow rate of the pumped water for loss-less converter is about 42 l/min, for the 95 % efficiency converter is about 37 l/min, for the 90 % efficiency converter about 33 l/min and for direct coupled system the flow rate is approximately 16 l/min. Those results indicate the large difference in performance between the system with MPPT and the system without MPPT.

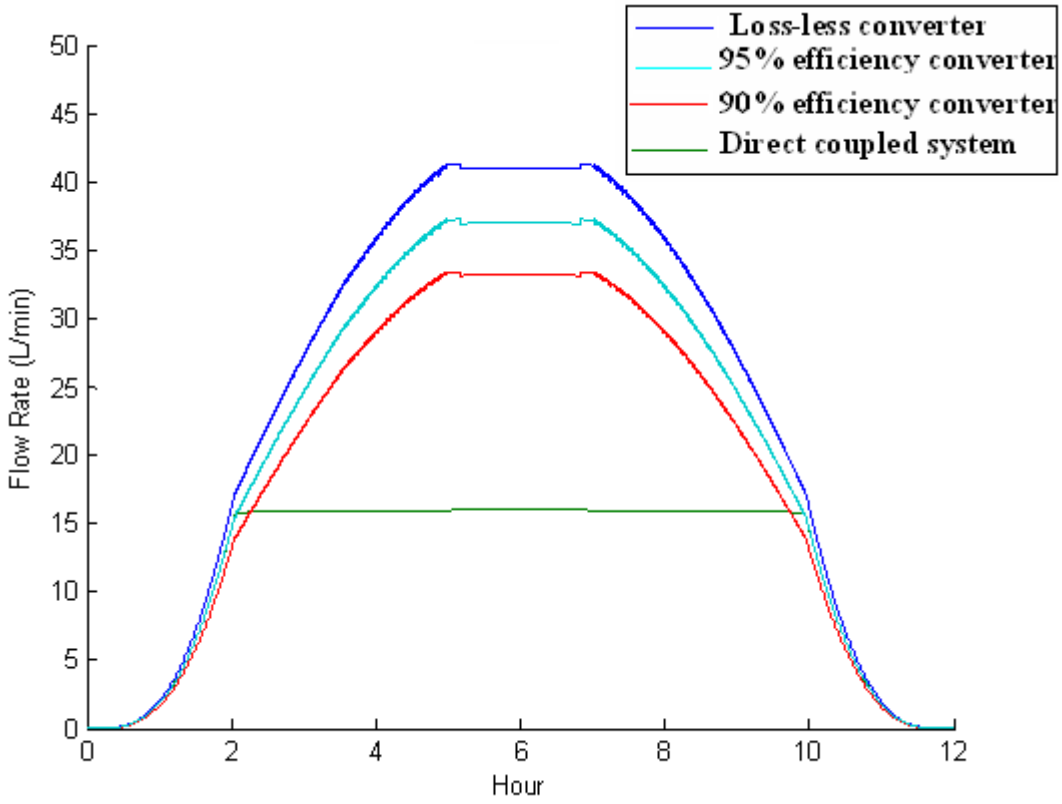

Figure 5-15: Flow rates of PV water pumps for a 12-hour period Simulated with the irradiance data of a sunny day (total dynamic head about 50m).

The total volume of water pumped for the 12-hour period is also calculated for both systems. The results are tabulated below. The results show that the system with MPPT can pump up to 50 % more water than the system without MPPT. Also the plots show that a 5 % improvement in the converter efficiency can increase the pumped water in a day by 10.25 %.

	With MPPT			Without MPPT
	Loss-les converter	**95 % Efficiency converter**	**90 % Efficiency converter**	
Total volume pumped for 12 hours of a day light	**17.07m^3**	**15.41m^3**	**13.83m^3**	**8.52m^3**

Table 5-6: Total volume of water pumped for 12 hours simulated with the irradiance data of a sunny day (total dynamic head about 50m).

5.10- CONCLUSION:

From the computed result, the MPPT process applied to a PV pumping system can achieve higher efficiency.

For the pumping system with DC motor-pump load, the MATLAB simulation verifies functionality and benefits of MPPT. Comparisons between the system with MPPT and the system without MPPT in terms of total energy produced and total volume of water pumped a day has been undertaken. The results validate that MPPT can significantly increase the efficiency (97 %) of energy production from PV generator and the performance of the PV water pumping system compared to the system without MPPT (60 %) even if the converter is not 100 % efficient.

The pumping system with an induction motor pump load composed of a PV panel, a DC-DC converter for MPPT, DC-AC inverter for power conversion and the induction motor-pump load. As the pumping system with a DC motor, the performance of the pumping system with an induction motor verifies the functionality and benefits of MPPT. We can conclude that the system with MPPT has better performance than the system without MPPT (the efficiency is about 66% for the system with MPPT and 33 % for the system without MPPT). Because of the robust, maintenance free and low cost characteristics of 3-phase induction motors; it is evident that induction motor based PV water pumping systems will become very popular in the near future.

6.1- GENERAL CONCLUSION:

This thesis presents a study of maximum power point tracking (MPPT) for photovoltaic (PV) systems and its different applications for different loads. The modeling of the PV module based on a simplified version of the two diode model achieves good matching with data sheet information.

The MPPT ensure impedance matching between the PV generator and the load for maximum power transfer by controlling the duty cycle of the DC-DC converter.

Two MPPT algorithms are simulated to achieve maximum power transfer; the Perturbation and Observation (P&O) algorithm and the Incremental and Conductance (IncCond) algorithm. The IncCond algorithm shows slightly but better performance in terms of efficiency compared to the P&O algorithm under cloudy weather condition. A small improvement of efficiency could bring substantial savings if the system is large. However, it could be difficult to justify the use of IncCond algorithm for small low-cost systems as the cost and availability are the two major aspect of system design and the IncCond algorithm will require four sensors more than the P&O algorithm and also it need more control loops. For this reasons, the (P&O) algorithm is chosen.

The comparative study of the PV system with resistive load with MPPT vs. direct-coupled system shows that the PV system without MPPT has poor efficiency (as defined in the text) because of mismatching between the PV module and the load. On the other hand, it shows that the system with MPPT can utilize more than 97 % of PV theoretical capacity. However, MPPT has some limitations; one of its main drawbacks is that there is no regulation on the output while it is tracking a maximum power point. It cannot regulate both input and output at the same time. If the application requires a constant voltage, it must employ batteries to maintain the voltage constant. In addition to that, if the value of the load resistance changes the duty cycle of the converter changes even if the input is the same; this means that the design of the converter must satisfy the specifications of the source and the load at the same

time. Thus, it is very important to select the appropriate size of the load, so that the full capacity of the PV module and array is utilized.

The PV pumping system with DC motor-pump has been studied and simulations carried out using SimPowerSystems in SIMULINK. The model is then transferred into MATLAB. Simulation of the whole system is performed and the functionality and benefits of MPPT verified. Comparison of the system performance with and without MPPT in terms of total energy produced and total volume of water pumped a day is under taken. The Results show that the system with MPPT can utilize more than 97 % of PV capacity and it is able to pump up to 64 % more water than the system without MPPT. Even if the efficiency of converter is set to 90%, it can still pump 46 % more water than the system without MPPT. The results show also that 5 % improvement in the converter efficiency can increase the pumped water approximately by 286 l per day which is approximately 5 % of the volume of pumped water.

Study of a PV pumping system with an inverter fed induction motor driving a pump is then carried out. The induction motor is modeled using the per-phase equivalent circuit. A comparison between the system with MPPT and the system without MPPT is undertaken.
We can conclude that the system with MPPT has much better performance than the system without MPPT; the efficiency is about 66% for the system with MPPT and 33 % for the system without MPPT.
A further comparison has been made in terms of flow rates and total volume of water pumped per day. The results show that the system with MPPT can pump up to 50 % more water than the system without MPPT. Also the plots indicate that a 5 % improvement in the converter efficiency can increase the pumped water in a day by 10.25 %.

SUGGESTION FOR FURTHER WORK:

Correct modeling of the DC-DC converter and DC water pump is an important area of study. A more realistic model of the DC-DC converter would involve diode losses, switching losses in a Power switch, and resistive losses in inductors and capacitors.

The model used for simulations of DC water pump gives results within a reasonable range. The model accuracy is, however, uncertain because the parameters are only estimates. If tests could be run on the real water pump motor or an equivalent sized motor to determine reasonable entries to SIMULINK block parameters, this could lead to more accurate simulation runs. Also, simply increasing the size of system and using a larger motor (5hp or above) could allow for better results in SUMILINK, though many PV water pumps rarely use such large motors.

Also a more accurate modeling of the induction motor together with the inverter is in order.

Special attention will be devoted to minimizing losses in all system parts, through the use of different converter topologies.

Practical implementation of the system is considered as the next step. It may involve implementation of: a DSP or a microcontroller, a method of supplying power to the controller, signal conditioning circuits for A/D converters, a driving circuit for Power- MOSFET, DC-DC converters, and a water level sensor that detects when the water reservoir reaches full.
It will involve performance analysis on the actual system and comparisons with simulations.

REFERENCES :

[1]: Minwon Parks and In-Keun Yu: "A Novel Real-Time Simulation Technique of Photovoltaic Generation Systems Using RTDS" IEEE TRANSACTIONS ON ENERGY CONVERSION, VOL. 19, NO. 1, MARCH 2004.

[2]: Achour Betka: "Perspectives for the Sake of Photovoltaic Pumping Development in the South" thesis submitted for the award of the degree of PHD University of Batna.

[3]: Akihiro Oi "Design and Simulation of Photovoltaic Water Pumping" thesis for the degree of Master of Science in Electrical Engineering, California Polytechnic State University, 2005.

[4]: Mirjana Milosevic: "On the Control of Distributed Generation in Power System" thesis for the degree of Doctor of Technical Sciences, Swiss Federal Institute of Technology Zurich, 2007.

[5]: Chihchiang Hua, *Member, IEEE,* Jongrong Lin, and Chihming Shen: "Implementation of a DSP-Controlled Photovoltaic System with Peak Power Tracking" IEEE TRANSACTIONS ON INDUSTRIAL ELECTRONICS, VOL. 45, NO. 1, FEBRUARY 1998.

[6]: Geoff Walker: "Evaluating MPPT Converter Topologies Using MATLAB PV Model" University of Queensland, Australia.

[7]: Adedamola Omale: "Analysis, Modelling and Simulation of Optimal Power Tracking of Multiple-Modules of Paralleled Solar Cell Systems" the Florida State University, 2006.

[8]: Daniel F.Butay, Michael T.Miller: “Maximum Peak Power Tracker: A Solar Application” Worcester Polytechnic Institute, 2008.

[9]: BP SX 150 DATA SHEET.

[10]: Mohammad A. S. Masoum, Hooman Dehbonei, and Ewald F. Fuchs, Fellow: “Theoretical and Experimental Analyses of Photovoltaic Systems with Voltage- and Current-Based Maximum Power-Point Tracking” IEEE TRANSACTIONS ON ENERGY CONVERSION, VOL. 17, NO. 4, DECEMBER 2002.

[11]: D. Shmilovitz: “On the Control of Photovoltaic Maximum Power Point Tracker Via Output Parameters” IEE Proc.-Electr. Power Appl., Vol. 152, No. 2, March 2005.

[12]: Vikrant.A.Chaudhari: “Automatic Peak Power Tracker for Solar PV Modules Using DSPACER Software” Thesis for the award of the Degree of Master of Technology in Energy, July 2005.

[13]: DC-DC Converter: Copyright © G.Ledwich 1998.

[14]: Muhammad H.Rashid: “Power Electronics. Circuits; Devices, and Applications” third Edition 2004.

[15]: Jacar Electronics Reference Data Sheet: DC-DC Convrter.PDF (Copyright © Jacar Electronics, 2001).

[16]: Mohamad A. S. Masoum, Seyed Mahdi Mousavi Badejani, and Ewald F. Fuchs, Fellow, IEEE:” Microprocessor-Controlled New Class of Optimal Battery Chargers for Photovoltaic

Applications" IEEE TRANSACTIONS ON ENERGY CONVERSION, VOL. 19, NO. 3, SEPTEMBER 2004.

[17]: Toshihiko Noguchi, Member, IEEE, Shigenori Togashi, and Ryo Nakamoto: "Short Current Pulse-Based Maximum-Power-Point Tracking Method for Multiple Photovoltaic-and-Converter Module System" IEEE TRANSACTIONS ON INDUSTRIAL ELECTRONICS, VOL. 49, NO. 1, FEBRUARY 2002.

[18]: http://re.jrc,ec.europa.eu/pvgis/apps/radmonth,php?en=&europe= , this sit was perpetrated by Thomas Huld and Marcel Suri, PVGIS © European Communities,2001-2007.

[19]: Wu Libo, Zhao Zhengming, Senior Member, IEEE, and Liu Jianzheng: "A Single-Stage Three-Phase Grid-Connected Photovoltaic System With Modified MPPT Method and Reactive Power Compensation" IEEE TRANSACTIONS ON ENERGY CONVERSION, VOL 22, NO.4, DESEMBER 2007.

[20]: Frede Blaabjerg, Remmus Teadorescu, Zhe Chen: "Power Converter and Control of Renewable Energy Systems" Aalborg University, Institute of Energy Technology Denmark.

[21]: S. Yuvarajan, Dachuan Yu, Shanguang Xu: "A novel power converter for photovoltaic applications" Electrical and Computer Engineering Department, North Dakota State University, published in Journal of Power Sources 135 (2004) 327–331, (SCIENCE DIRECT).

[22]: Miguel Angel Rodríguez Otero: "Power Quality Issues and Feasibility Study in a DC Residential Renewable Energy System" A thesis submitted in partial fulfillment of the

requirements for the degree of Master of Science in Electrical Engineering University of Puerto Rico, 2008.

[23]: W. Kramer, S. Chakraborty, B. Kroposki, and H. Thomas: “Advanced Power Electronic Interfaces for Distributed Energy Systems, Part 1: Systems and Topologies” A National Laboratory of the U.S. Department of energy Office of Energy Efficiency and Renewable Energy. Technical Report NREL/TP-581-42672. March 2008.

[24]: "http://en.wikipedia.org/wiki/Maximum_power_point_tracker". This page was last modified on 30 October 2009 at 22:33.

[25]: Richard A. Cullen President Blue Sky Energy, Inc: “What is Maximum Power Point Tracking (MPPT) and How Does it Work?” http://www.blueskyenergyinc.com.

[26]: Northern Arizona Wind & Sun: “All About MPPT Solar Charge Controllers, Theory, operation, and use of MPPT charge controllers for solar electric systems”.

[27]: Nejib Hamrouni *, Moncef Jraidi, Adne`ne Che´rif : “Theoretical and Experimental Analysis of the Behavior of a Photovoltaic Pumping System” High Engineering Faculty of Tunis PB 37, Belvedere, Tunis, Tunisia Received 29 November 2007; received in revised form 16 October 2008; accepted 2 March 2009 ; (SCIENCE DIRECT).

[28]: A. Moussi, A. Torki: “An Improved Efficiency Permanent Magnet Brushless DC Motor PV Pumping System”, LARHYSS Journal, N°.01, Mai 2002.

[29]: Dr. A. Moussi, A. Saadi, A. Betka, G.M. Asher: “Photovoltaic Pumping Systems

Technologies Trends” LARHYSS Journal, ISSN 1112-3680, n° 02, Juin 2003, pp. 127-150.

[30]: A. Saadi, A. Moussi:"Optimisation of Back-Boost Converter by MPPT Technique With Variable Reference Voltage Applied for Photovoltaic Water Pumping System Under Variable Weather Conditions" Asian Journal of Information Technology 6(2):222-229, 2007.

[31]: S. Singer, I. Appelbaum: "Starting Characteristics of Direct Current Motors Powered by Solar Cells" IEEE TRANSACTIONS ON ENERGY CONVERSION, Vol. 8, No. 1, March 1993.

[32]: Abdulrahman Mohammed AL-Ibrahim: "Optimum Selection of Direct-Coupled Photovoltaic Pumping System in Solar Domestic Hot Water Systems" thesis submitted for the award of the degree of doctor of philosophy (Mechanical Engineering) at the University of Wisconsin-Madison 1997.

[33]: Kyocera Solar Inc. SD Series Pumps (downloaded from www.kyocerasolar.com).

[34]: Josh Mandelcorn: "Capacitor choice is key in buck converter design" Group Technical Staff, Texas Instruments. eetindia.com.

[35]: M. Arrouf*, N. Bouguechal: "Vector control of an induction motor fed by a photovoltaic generator" Department of Electrical Engineering, Faculty of Engineering Sciences, University of Batna, Algeria. (SCIENCE DIRECT).

[36]: Mehmet Akbaba : "Matching induction motors to PVG for maximum power transfer" Department of Electrical and Electronics Engineering, University of Bahrain, (SCIENCE DIRECT).

[37]: N. Argaw, R. Foster and A. Ellis: "Renewable Energy for Water Pumping Applications in Rural Villages" New Mexico State University Las Cruces, New Mexico, July 2003.

[38]: Abdel-Karim Daud[a,*], Marwan M. Mahmoud[b]: “Solar powered induction motor-driven water pump operating on a desert well, simulation and field tests” [a] Palestine Polytechnic University, [b] An Najah, National University. 23 November 2004 (SCIENCE DIRECT).

[39]: Thierry Martire´ [a,b] , Christian Glaize [a,*], Charles Joubert [a], Benoıˆt Rouvie`re [b]: “A simplified but accurate prevision method for along the sun PV pumping systems” [a] Laboratoire d’E´ lectrotechnique de Montpellier (LEM), Universite´ de Montpellier II, CC079, Place Euge`ne Bataillon, F 34095Montpellier Cedex 5, France

[b] Apex BP-SOLAR – 1, Rue du Grand Cheˆne, F 34270 Saint Mathieu de Tre´ viers, France. June 2008 (SCIENCE DIRECT).

[40]: A. Ben Rhouma, J. Belhadj, X. Roboam: “Control and energy management of a pumping system fed by hybrid photovoltaic-wind sources with hydraulic storage: -static and dynamic analysis. –“U/f’’ and “F.O.C” controls methods comparison.” LSE-ENIT B.P 37 le Belvédère 1002 Tunis ESSTT, BP 56 Monfleury 1008 Jamel.Belhadj@esstt.rnu.tn

APPENDIX A : MATLAB functions and programs.

A.1 MATLAB Functions and Programs:

A.1.1 MATLAB Function for Modelling BP SX 150S PV Generator:

This MATLAB function (bp_sx150s1.m) is to simulate the current-voltage and the power-voltage relationships of BP SX 150S PV module and used in simulations throughout of this thesis.

```
function Ia = bp_sx150s1(Va,G,TaC)
k = 1.381e-23;
q = 1.602e-19;
n = 1.62;
Eg = 1.12;
TaK = 273 + TaC;
Ns = 72;
TrK = 298;
Voc_TrK = 43.5 /Ns;
Isc_TrK = 4.75;
a = 0.65e-3;
Vc = Va / Ns;
Isc = Isc_TrK * (1 + (a * (TaK - TrK)));
Iph = G * Isc;
Vt_TrK = n * k * TrK / q;
b = Eg * q /(n * k);
Ir_TrK = Isc_TrK / (exp(Voc_TrK / Vt_TrK) -1);
Ir = Ir_TrK * (TaK / TrK)^(3/n) * exp(-b * (1 / TaK -1 / TrK));
dVdI_Voc = -1.0/Ns;
```

```
Xv = Ir_TrK / Vt_TrK * exp(Voc_TrK / Vt_TrK);
Rs = - dVdI_Voc - 1/Xv;
Vt_Ta = n * k * TaK / q;
Ia=zeros(size(Vc));
for j=1:5;
Ia = Ia - (Iph - Ia - Ir .* ( exp((Vc + Ia .* Rs) ./ Vt_Ta) -1))...
./ (-1 - Ir * (Rs ./ Vt_Ta) .* exp((Vc + Ia .* Rs) ./ Vt_Ta));
End
```

A.1.2 MATLAB Script to Draw PV I-V Curves:

The following simple MATLAB script is used for Figure 2-10 to draw the I-V characteristics of various module temperatures. Other plots showing PV characteristics are done in similar ways using MATLAB.

```
clear;
G=1;
figure
hold on
for TaC =0:25:75
Va = linspace (0,48-TaC/8, 200);
Ia = bp_sx150s1(Va, G, TaC);
plot(Va,Ia)
%p=Va.*Ia;
%plot(Va,p)
end
title('BP SX 150S Photovoltaic Module I-V Curve')
xlabel('Module Voltage (V)')
ylabel('Module Current (A)')
```

```
axis([0 50 0 5])
gtext('0^oc')
gtext('25^oc')
gtext('50^oc')
gtext('75^oc')
hold off
```

A.1.3 MATLAB Function to Find the MPP:

This simple MATLAB function is to find the power, voltage, and current at the MPP of BP SX 150S PV module under the given irradiance and module temperature.

```
function [Pa_max, Imp, Vmp] = find_mpp(G, TaC)
Va = 12;
Pa_max = 0;
% Start process
while Va < 48-TaC/8
Ia = bp_sx150s1(Va,G,TaC);
Pa_new = Ia * Va;
if Pa_new > Pa_max
Pa_max = Pa_new;
Imp = Ia;
Vmp = Va;
end
Va = Va + .005;
end
```

A.1.4 MATLAB Script: P&O Algorithm:

This MATLAB script is to test the P&O algorithm under the sunny weather condition. Other testing is done in a similar way.

```
clear;
TaC = 25;
C = 0.5;
power=0;
G = 0.011;
Va = 26.0;
Ia = bp_sx150s1(Va,G,TaC);
Pa = Va * Ia;
Vref_new = Va + C;
Va_array = [];
Pa_array = [];
x=5.63:0.25:18.38;
y=[0.011 0.024 0.039 0.08 0.130 0.187 0.249 0.312 0.377 0.442 0.506 0.569 0.629 0.687
0.742 0.797 0.841 0.884 0.923 0.958 0.988 1.013 1.034 1.049 1.059 1.064 1.064 1.059 1.049
1.034 1.013 0.988 0.958 0.923 0.884 0.841 0.793 0.742 0.687 0.629 0.569 0.506 0.442 0.377
0.312 0.249 0.187 0.130 0.08 0.039 0.024 0.011];
xi=0:24/40000:24;
yi=interp1(x,y,xi,'cubic');
for Sample =1:40001
G = yi(Sample);
Va_new = Vref_new;
Ia_new = bp_sx150s1(Vref_new,G,TaC);
Pa_new = Va_new * Ia_new;
deltaPa = Pa_new - Pa;
power=power+Pa_new
% P&O Algorithm starts here
if deltaPa > 0
```

```
if Va_new > Va
Vref_new = Va_new + C; % Increase Vref
else
Vref_new = Va_new - C; % Decrease Vref
end
elseif deltaPa < 0
if Va_new > Va
Vref_new = Va_new - C; % Decrease Vref
else
Vref_new = Va_new + C; %Increase Vref
end
else
Vref_new = Va_new; % No change
end
Va = Va_new;
Pa = Pa_new;
Va_array = [Va_array Va];
Pa_array = [Pa_array Pa];
end
% Plot result
figure
plot (Va_array, Pa_array, 'g')
Va = linspace (0, 45, 200);
hold on
for G=.2:.2:1
Ia = bp_sx150s1(Va, G, TaC);
Pa = Ia.*Va;
plot(Va, Pa)
[Pa_max, Imp, Vmp] = find_mpp(G, TaC);
```

```
plot(Vmp, Pa_max, 'r*')
end
title('P&O Algorithm')
xlabel('Module Voltage (V)')
ylabel('Module Output Power (W)')
axis([0 50 0 160])
gtext('1000W/m^2')
gtext('800W/m^2')
gtext('600W/m^2')
gtext('400W/m^2')
gtext('200W/m^2')
hold off
```

A.1.5 MATLAB Script: incCond Algorithm:

This MATLAB script is to test the incCond algorithm under the cloudy weather condition. Other tests are done in a similar way.

```
clear;
TaC = 25;
C = 0.5;
E = 0.002;
G = 0.07;
Va = 27.2;
Ia = bp_sx150s1(Va,G,TaC);
Pa = Va * Ia;
Vref_new = Va + C;
Va_array = [];
Pa_array = [];
Pmax_array =[];
```

```
x=0:12/565:12;

y=[0.07 0.08 0.09 0.092 0.094 0.095 0.097 0.1 0.105 0.107 0.109 0.11 0.15 0.16 0.165 0.17
0.18 0.19 0.2 0.21 0.22 0.23 0.25 0.27 0.28 0.29 0.28 0.3 0.32 0.35 0.37 0.38 0.38 0.4 0.42 0.3
0.25 0.35 0.41 0.37 0.4 0.38 0.38 0.29 0.22 0.48 0.47 0.3 0.52 0.32 0.31 0.2 0.19 0.18 0.19
0.22 0.23 0.2 0.18 0.22 0.28 0.24 0.45 0.51 0.5 0.52 0.53 0.27 0.16 0.14 0.13 0.22 0.49 0.5 0.2
0.59 0.21 0.3 0.58 0.43 0.22 0.39 0.19 0.37 0.3 0.21 0.39 0.25 0.41 0.32 0.19  0.195 0.2 0.21
0.22 0.23 0.22 0.223 0.225 0.24 0.26 0.26 0.29 0.35 0.33 0.3 0.25 0.2 0.21 0.23 0.121 0.19
0.17 0.19 0.19 0.2 0.24 0.29 0.29 0.29 0.31 0.29 0.35 0.4  0.41 0.6 0.59 0.47 0.48 0.5 0.49
0.46 0.45 0.34 0.34 0.3 0.3 0.29 0.29 0.22 0.23 0.23 0.27 0.27 0.3 0.29 0.29 0.291 0.293 0.295
0.3 0.31 0.312 0.314 0.316 0.318 0.32 0.41 0.41 0.415 0.48 0.32 0.31 0.31 0.25 0.25 0.25 0.23
0.23 0.21 0.21 0.19 0.19 0.18 0.25 0.25 0.3 0.37 0.37 0.18 0.19 0.178 0.178 0.12 0.12 0.123
0.124 0.125 0.126 0.13 0.126 0.14 0.14 0.135 0.135 0.136 0.14 0.14 0.145 0.146 0.146 0.146
0.15 0.16 0.17 0.17 0.2 0.21 0.2 0.2 0.18 0.18 0.16 0.14 0.16 0.14 0.16 0.18 0.18 0.19 0.19
0.187 0.186 0.185 0.184 0.183 0.19 0.2 0.18 0.19 0.19 0.195 0.24 0.24 0.22 0.26 0.21 0.21
0.19 0.186 0.185 0.184 0.183 0.15 0.17 0.172 0.174 0.15 0.17 0.16 0.16 0.162 0.14 0.14 0.14
0.15 0.15 0.19 0.195 0.21 0.19 0.17 0.172 0.174 0.175 0.178 0.18 0.15 0.15 0.155 0.16 0.19
0.16 0.18 0.183 0.184 0.2 0.2 0.19 0.2 0.25 0.28 0.285 0.29 0.22 0.3 0.3 0.32 0.32 0.325 0.38
0.38 0.385 0.39 0.39 0.38 0.34 0.32 0.34 0.3 0.3 0.3 0.25 0.27 0.27 0.38 0.27 0.3 0.25 0.25
0.24 0.49 0.45 0.8 0.7 0.7 0.45 0.455 0.457 0.459 0.5 0.55 0.55 0.9 0.56 0.558 0.556 0.557
0.45 0.45 0.35 0.44 0.45 0.38 0.38 0.28 0.28 0.3 0.28 0.3 0.28 0.3 0.3 0.27 0.33 0.33 0.58 0.58
0.6 0.4 0.4 0.3 0.4 0.4 0.6 0.61 0.613 0.615 0.616 0.8 0.81 0.8 0.8 0.82 0.82 0.78  0.78 0.73
0.73 0.727 0.726 0.8 0.8 0.79 0.79 0.72 0.72 0.79 0.79 0.65 0.65 0.45 0.45 0.39 0.38 0.79 0.6
0.78 0.7 0.6 0.77 0.77 0.36 0.36 0.74 0.8 0.74 0.68 0.68 0.6 0.59 0.58 0.585 0.42 0.42 0.35
0.35 0.42 0.43 0.43 0.44 0.53 0.53 0.57 0.55 0.63 0.63 0.6 0.66 0.7 0.73 0.7 0.7 0.65 0.65 0.48
0.48 0.32 0.32 0.3 0.3 0.48 0.48 0.62 0.6 0.6 0.57 0.57 0.57 0.6 0.6 0.4 0.4 0.28 0.28 0.43 0.43
0.56 0.56 0.56 0.54 0.54 0.54 0.52 0.52 0.53 0.53 0.55 0.55 0.59 0.53 0.58 0.575 0.572 0.57
0.58 0.58 0.58 0.57 0.57 0.56 0.56 0.55 0.55 0.54 0.54 0.539 0.538 0.537 0.48 0.48 0.48 0.46
0.46 0.46 0.4 0.4 0.4 0.38 0.38 0.32 0.32 0.32 0.34 0.34 0.32 0.34 0.34 0.33 0.33 0.3 0.3 0.3
0.29 0.295 0.28 0.285 0.27 0.275 0.26 0.265 0.25 0.255 0.22 0.21 0.21 0.22 0.2 0.2 0.21 0.2
0.215 0.216 0.217 0.218 0.217 0.216 0.215 0.214 0.2 0.219 0.218 0.217 0.216 0.215 0.2 0.2
0.2 0.19 0.189 0.187 0.186 0.185 0.182 0.18 0.178 0.175 0.17 0.17 0.165 0.16 0.155 0.152
0.15 0.15 0.13 0.12 0.109 0.107 0.106 0.105 0.104 0.103 0.102 0.101 0.1];

xi=0:12/40000:12;

yi=interp1(x,y,xi,'cubic');

for Sample = 1:40001

G = yi(Sample);

Va_new = Vref_new;

Ia_new = bp_sx150s1(Vref_new,G,TaC);

deltaVa = Va_new - Va;

deltaIa = Ia_new - Ia;

% incCond Algorithm starts here
```

```
if deltaVa == 0
if deltaIa == 0
  Vref_new = Va_new;
elseif deltaIa > 0
  Vref_new = Va_new + C;
else
  Vref_new = Va_new - C;
end
else
if abs(deltaIa/deltaVa + Ia_new/Va_new) <= E
  Vref_new = Va_new;
else
if deltaIa/deltaVa > -Ia_new/Va_new + E
  Vref_new = Va_new + C;
else
  Vref_new = Va_new - C;
end
end
end
[Pa_max, Imp, Vmp] = find_mpp(G, TaC);
Va = Va_new;
Ia = Ia_new;
Pa = Va_new * Ia_new;
Va_array = [Va_array Va];
Pa_array = [Pa_array Pa];
Pmax_array = [Pmax_array Pa_max];
end
Pth = sum(Pmax_array)/3600;
Pact = sum(Pa_array)/3600;
```

```
figure
plot (Va_array, Pa_array, 'g')
Va = linspace (0, 45, 200);
hold on
for G=.2:.2:1
Ia = bp_sx150s1(Va, G, TaC);
Pa = Ia.*Va;
plot(Va, Pa)
[Pa_max, Imp, Vmp] = find_mpp(G, TaC);
plot(Vmp, Pa_max, 'r*')
end
title('incCond Method')
xlabel('Module Voltage (V)')
ylabel('Module Output Power (W)')
axis([0 50 0 160])
gtext('1000W/m^2')
gtext('800W/m^2')
gtext('600W/m^2')
gtext('400W/m^2')
gtext('200W/m^2')
hold off
```

A.1.6 MATLAB Script for MPPT with Output Sensing Direct Control Method:

This MATLAB script is to test the output sensing direct control method with the P&O algorithm. The load is a resistive load (50Ω).

```
clear;
% Define constants
TaC = 25;
```

```
Rload =50;
deltaD = .0035;
G = .2;
D = 0.15;
D_k_1 = 0.15;
Va_k_1 = 0;
Pa_k_1 = 0;
Vo_k_1 = 0;
Io_k_1 = 0;
Po_k_1 = 0;
% Set up arrays storing data for plots
Va_array = [];
Ia_array = [];
Pa_array = [];
Vo_array = [];
Io_array = [];
Po_array = [];
D_array = [];
% Take 3600 samples
for Sample = 1:3600
D_k = D;
% Calculate input impedance of ideal boost converter (Rin)
Rin = (1-D_k)^2 * Rload;
% Locate the operating point of PV module and
% calculate its voltage, current, and power
f = @(x) x - Rin*bp_sx150s1(x,G,TaC);
Va_k = fzero (f, [0, 45]);
Ia_k = bp_sx150s1(Va_k,G,TaC);
Pa_k = Va_k * Ia_k;
```

```
% Measure the outputs for ideal boost converter
Vo_k = 1/(1-D_k) * Va_k;
Io_k = (1-D_k) * Ia_k;
% Calculate new Po and deltaPo
Po_k = Vo_k * Io_k;
deltaPo = Po_k - Po_k_1;
% Output voltage and current protection (86V/1.5A Max)
if (Vo_k > 86.6) | (Io_k > 1.75) % '2%' margin added
if deltaPo >= 0
if D_k > D_k_1
D = D_k - deltaD; % Decrease duty cycle
else
D = D_k + deltaD; % Increase duty cycle
end
else
if D_k > D_k_1
D = D_k + deltaD; % Increase duty cycle
else
D_k = D_k - deltaD; % Decrease duty cycle
end
end
elseif (Vo_k > 86.6) | (Io_k > 1.75)
D = D_k; % No change
elseif D_k < 0.15
D = 0.15; % Set minimum duty cycle
elseif D_k > 0.65
D = 0.65; % Set maximum duty cycle
else
% P&O Algorithm starts here
```

```
if deltaPo > 0
if D_k > D_k_1
  D = D_k + deltaD; % Increase duty cycle
  else
D = D_k - deltaD; % Decrease duty cycle
end
elseif deltaPo < 0
if D_k > D_k_1
D = D_k - deltaD; % Decrease duty cycle
else
D = D_k + deltaD; % Increase duty cycle
end
else
D = D_k; % No change
end
end
% Update history
Va_k_1 = Va_k;
Ia_k_1 = Ia_k;
Pa_k_1 = Pa_k;
Vo_k_1 = Vo_k;
Io_k_1 = Io_k;
Po_k_1 = Po_k;
D_k_1 = D_k;
% Store data in arrays for plots
Va_array = [Va_array Va_k];
Ia_array = [Ia_array Ia_k];
Pa_array = [Pa_array Pa_k];
Vo_array = [Vo_array Vo_k];
```

```
Io_array = [Io_array Io_k];
Po_array = [Po_array Po_k];
D_array = [D_array D_k];
% Increase insolation until G=1
if (Sample > 20) & (G < 1)
G = G + .0003;
end
end
%Goto next sample
% Functions to plot
figure(1)
plot (Va_array, Pa_array, 'g')
% Overlay with P-V curves and MPP
Va = linspace (0, 45, 200);
hold on
for G=.2:.2:1
Ia = bp_sx150s1(Va, G, TaC);
Pa = Ia.*Va;
plot(Va, Pa)
[Pa_max, Imp, Vmp] = find_mpp(G, TaC);
plot(Vmp, Pa_max, 'r*')
end
title('(a) PV Power vs. Voltage')
xlabel('Module Voltage (V)')
ylabel('Module Output Power (W)')
axis([0 50 0 160])
hold off
figure(2)
plot (Va_array, Ia_array, 'g')
```

```
% Overlay with I-V curves and MPP
hold on
for G=.2:.2:1
Ia = bp_sx150s1(Va, G, TaC);
plot(Va, Ia)
[Pa_max, Imp, Vmp] = find_mpp(G, TaC);
plot(Vmp, Imp, 'r*')
end
title('(b) PV Current vs. Voltage')
xlabel('Module Voltage (V)')
ylabel('Module Current(A)')
axis([0 50 0 5])
hold off
figure(3)
hold on
plot (D_array, Po_array, 'b')
title('(c) Output Power vs. Duty Cycle')
xlabel('Duty Cycle')
ylabel('Output Power (W)')
axis([0 1 0 160])
hold off
figure(4)
plot (Vo_array, Io_array, 'g.')
hold on
Vo = linspace (0,90,200);
Io = Vo ./ Rload;
plot (Vo, Io)
title('(d) Output Current vs. Voltage')
xlabel('Output Voltage (V)')
```

```
ylabel('Output Current (A)')
axis([0 90 0 2])
hold off
```

A.1.7 MATLAB Script for MPPT Simulations with DC Pump Motor Load:

This MATLAB script is to test MPPT functionality with the DC pump motor as a load. It uses the output sensing direct control method with the P&O algorithm. It also calculates total energy output and total volume of water pump for a 12-hour period.

```
clear;
% Define constants
TaC = 25;
Rload =0.2;
deltaD = .0035;
G = 0.011;
D = 0.1;
D_k_1 = 0.1;
Va_k_1 = 0;
Pa_k_1 = 0;
Vo_k_1 = 0;
Io_k_1 = 0;
Po_k_1 = 0;
Volume = 0;
% Set up arrays storing data for plots
Va_array = [];
Ia_array = [];
Pa_array = [];
```

```
Vo_array = [];

Io_array = [];

Po_array = [];

D_array = [];

Rload_array = [];

Pmax_array =[];

Volume_array =[];

% Take43200samples

x=5.63:0.25:18.38;

y=[0.011 0.024 0.039 0.08 0.130 0.187 0.249 0.312 0.377 0.442 0.506 0.569 0.629 0.687
0.742 0.797 0.841 0.884 0.923 0.958 0.988 1.013 1.034 1.049 1.059 1.064 1.064 1.059 1.049
1.034 1.013 0.988 0.958 0.923 0.884 0.841 0.793 0.742 0.687 0.629 0.569 0.506 0.442 0.377
0.312 0.249 0.187 0.130 0.08 0.039 0.024 0.011];

xi=0:24/43199:24;

yi=interp1(x,y,xi,'cubic');

for Sample =1:43200

G = yi(Sample);

% Calculate input impedance of ideal buck boost converter (Rin)

Rin = (1-D_k)^2/D_k^2 * Rload;

% Locate the operating point of PV module and

% calculate its voltage, current, and power

f = @(x) x - Rin*bp_sx150s1(x,G,TaC);

Va_k = fzero (f, [0, 45]);

Ia_k = bp_sx150s1(Va_k,G,TaC);

Pa_k = Va_k * Ia_k;

% Measure the outputs for ideal buck-boost converter

Vo_k = D_k/(1-D_k) * Va_k;

Io_k = (1-D_k)/D_k * Ia_k;

% Calculate new Po and deltaPo

Po_k = Vo_k * Io_k;
```

```
deltaPo = Po_k - Po_k_1;
% Output voltage and current protection (30.6V/5.1A Max)
if (Vo_k >30.6) | (Io_k > 5.1) % '2%' margin added
if deltaPo >= 0
if D_k > D_k_1
D = D_k - deltaD; % Decrease duty cycle
else
D = D_k + deltaD; % Increase duty cycle
end
else
if D_k > D_k_1
D = D_k + deltaD; % Increase duty cycle
else
D_k = D_k - deltaD; % Decrease duty cycle
end
end
elseif (Vo_k > 30) | (Io_k >5)
D = D_k; % No change
elseif D_k < 0.1
D = 0.1; % Set minimum duty cycle
elseif D_k > 0.6
D = 0.6; % Set maximum duty cycle
else
% P&O Algorithm starts here
if deltaPo > 0
if D_k > D_k_1
  D = D_k + deltaD; % Increase duty cycle
  else
D = D_k - deltaD; % Decrease duty cycle
```

```
end
elseif deltaPo < 0
if D_k > D_k_1
D = D_k - deltaD; % Decrease duty cycle
else
D = D_k + deltaD; % Increase duty cycle
end
else
D = D_k; % No change
end
end
% Update history
Va_k_1 = Va_k;
Ia_k_1 = Ia_k;
Pa_k_1 = Pa_k;
Vo_k_1 = Vo_k;
Io_k_1 = Io_k;
Po_k_1 = Po_k;
D_k_1 = D_k;
% Calculate theoretical max
[Pa_max, Imp, Vmp] = find_mpp(G, TaC);
% Calculate volume water pumped (100 efficiency converter)
if Po_k > 35
Volume = 13/(60*150)*Po_k); % Volume of water pumped (L/sec)
else Volume =0;
end
% Store data in arrays for plots
Va_array = [Va_array Va_k];
Ia_array = [Ia_array Ia_k];
```

```
Pa_array = [Pa_array Pa_k];
Vo_array = [Vo_array Vo_k];
Io_array = [Io_array Io_k];
Po_array = [Po_array Po_k];
D_array = [D_array D_k];
Rload_array = [Rload_array Rload];
Pmax_array = [Pmax_array Pa_max];
Volume_array = [Volume_array Volume];
if (Sample > 160)
Rload = 9.5e-005*Vo_k^3 - 0.0087*Vo_k^2 + 0.37*Vo_k + 0.2;
end
end
% Total electric energy (Wh): theoretical and actual
Pth = sum(Pmax_array)/3600;
Pact = sum(Po_array)/3600;
% Volume of water pumped (L/day)
TotalVolume = sum(Volume_array);
figure(1)
plot (Va_array, Pa_array, 'g')
% Overlay with P-V curves and MPP
Va = linspace (0, 45, 200);
hold on
for G=.2:.2:1
Ia = bp_sx150s1(Va, G, TaC);
Pa = Ia.*Va;
plot(Va, Pa)
[Pa_max, Imp, Vmp] = find_mpp(G, TaC);
plot(Vmp, Pa_max, 'r*')
end
```

```
title('(a) PV Power vs. Voltage')
xlabel('Module Voltage (V)')
ylabel('Module Output Power (W)')
axis([0 50 0 160])
hold off
figure(2)
plot (Va_array, Ia_array, 'g')
% Overlay with I-V curves and MPP
hold on
for G=.2:.2:1
Ia = bp_sx150s1(Va, G, TaC);
plot(Va, Ia)
[Pa_max, Imp, Vmp] = find_mpp(G, TaC);
plot(Vmp, Imp, 'r*')
end
title('(b) PV Current vs. Voltage')
xlabel('Module Voltage (V)')
ylabel('Module Current(A)')
axis([0 50 0 5])
hold off
figure(3)
hold on
plot (D_array, Po_array, 'b')
title('(c) Output Power vs. Duty Cycle')
xlabel('Duty Cycle')
ylabel('Output Power (W)')
axis([0 1 0 160])
hold off
figure(4)
```

```
plot (Vo_array, Io_array, 'g.')
hold on
Vo = linspace (0,30,200);
Io = Vo ./ Rload;
plot (Vo, Io)
title('(d) Output Current vs. Voltage')
xlabel('Output Voltage (V)')
ylabel('Output Current (A)')
axis([0 30 0 6])
figure(5)
hold on
VolumeMin = Volume_array.*60;
sample = 1:43.2e+3;
Hour=sample./3600;
plot(Hour, VolumeMin)
xlabel('Hour')
ylabel('Flow Rate (L/min)')
axis([0 12 0 14])
```

A.1.8 MATLAB Script for MPPT Simulations with AC Pump Motor Load:

This MATLAB script is to test MPPT functionality with the AC pump motor as a load. It uses the output sensing direct control method with the P&O algorithm. It also calculates total developed output energy for a 12-hour period.

```
clear;
% Define constants
TaC = 25;
Z =67.66;
s =0.1226;
```

```
ws =1420;
Pg =0;
Rs = 4.85;
Rr = 3.805;
Xs = 2.513;
Xr = 2.513;
Xm = 81.05;
Rm = 500;
Va_k_1 = 0;
Pa_k_1 = 0;
Vo_k_1 = 0;
Io_k_1 = 0;
Po_k_1 = 0;
Pa_max = 0;
Pg_k_1 = 0;
pd_k_1 = 0;
s_k_1 = 0;
% Set up arrays storing data for plots
Va_array = [];
Ia_array = [];
Pa_array = [];
Vo_array = [];
Io_array = [];
Po_array = [];
%Pa_max_array =[];
Pg_array = [];
pd_array = [];
%s_array = [];
x=5.63:0.25:18.38;
```

```
y=[0.011 0.024 0.039 0.08 0.130 0.187 0.249 0.312 0.377 0.442 0.506 0.569 0.629 0.687
0.742 0.797 0.841 0.884 0.923 0.958 0.988 1.013 1.034 1.049 1.059 1.064 1.064 1.059 1.049
1.034 1.013 0.988 0.958 0.923 0.884 0.841 0.793 0.742 0.687 0.629 0.569 0.506 0.442 0.377
0.312 0.249 0.187 0.130 0.08 0.039 0.024 0.011];

xi=5.63:12.75/43199:18.38;

yi=interp1(x,y,xi,'cubic');

for Sample = 1:43200

G = yi(Sample);

% Calculate input impedance of ideal buck boost converter (Rin)

% Locate the operating point of PV module and

% calculate its voltage, current, and power

f = @(x) x - Z*bp_sx150s2(x,G,TaC);

Va_k = fzero (f, [0, 310]);

Ia_k = bp_sx150s2(Va_k,G,TaC);

Pa_k = Va_k * Ia_k;

Vo_k = Va_k;

Io_k = Ia_k;

Po_k = Pa_k;

Pg_k =(3/(3)^0.5)*((Io_k)^2)*(Rr/s);

pd_k = Pg_k*(1-s);

% Update history

Va_k_1 = Va_k;

Ia_k_1 = Ia_k;

Pa_k_1 = Pa_k;

Vo_k_1 = Vo_k;

Io_k_1 = Io_k;

Po_k_1 = Po_k;

Pg_k_1 = Pg_k;

pd_k_1 = pd_k;

%s_k_1 = s_k;
```

```
%[Pa_max, Imp, Vmp] = find_mpp1(G, TaC);
% Store data in arrays for plots
Va_array = [Va_array Va_k];
Ia_array = [Ia_array Ia_k];
Pa_array = [Pa_array Pa_k];
Vo_array = [Vo_array Vo_k];
Io_array = [Io_array Io_k];
Po_array = [Po_array Po_k];
Pg_array = [Pg_array Pg_k];
pd_array = [pd_array pd_k];
%s_array = [s_array s_k];
%Pa_max_array = [Pa_max_array Pa_max];
Z =67.66;
end
% Total electric energy (Wh): theoretical and actual
%Pth = sum(Pa_max_array)/3600;
Pact = sum(Po_array)/3600;
Pind = sum(pd_array)/3600;

% Functions to plot
%figure(1)
%plot (Va_array, Pa_array, 'g')
% Overlay with P-V curves and MPP
%Va = linspace (0, 300, 200);
%hold on
%for G=.2:.2:1
%Ia = bp_sx150s2(Va, G, TaC);
%Pa = Ia.*Va;
%plot(Va, Pa)
```

```
%[Pa_max, Imp, Vmp] = find_mpp1(G, TaC);
%plot(Vmp, Pa_max, 'r*')
%end
%title('(a) PV Power vs. Voltage')
%xlabel('Module Voltage (V)')
%ylabel('Module Output Power (W)')
%axis([0 300 0 2500])
%hold off
%figure(2)
%plot (Va_array, Ia_array, 'g')
% Overlay with I-V curves and MPP
%hold on
%for G=.2:.2:1
%Ia = bp_sx150s2(Va, G, TaC);
%plot(Va, Ia)
%[Pa_max, Imp, Vmp] = find_mpp1(G, TaC);
%plot(Vmp, Imp, 'r*')
%end
%title('(b) PV Current vs. Voltage')
%xlabel('Module Voltage (V)')
%ylabel('Module Current(A)')
%axis([0 300 0 10])
%hold off
%figure(3)
%hold on
%plot (D_array, Po_array, 'b')
%title('(c) Output Power vs. Duty Cycle')
%xlabel('Duty Cycle')
%ylabel('Output Power (W)')
```

```
%axis([0 1 0 2500])
%hold off
%figure(4)
%plot (Vo_array, Io_array, 'g.')
%hold on
%Vo = linspace (0,300,200);
%Io = Vo ./ Z;
%plot (Vo, Io)
%title('(d) Output Current vs. Voltage')
%xlabel('Output Voltage (V)')
%ylabel('Output Current (A)')
%axis([0 250 0 10])
%hold off
figure(1)
plot (Vo_array, pd_array, 'g')
hold on
title('(a)developed Power of induction motor vs. voltage without MPTT')
xlabel('Output Voltage (V)')
ylabel('developed Power (W)')
axis([0 400 0 2000])
hold off
figure (2)
hold on
sample = 1:43.2e+3;
Hour=sample./3600;
plot(Hour, pd_array)
xlabel('Hour')
ylabel('developed Power (W)')
axis([0 12 0 1600])
```